

THESIS ON NATURAL AND EXACT SCIENCES B238

**Optimised Signal Processing for Nonlinear
Ultrasonic Nondestructive Testing of
Complex Materials and Biological Tissues**

MARTIN LINTS



TALLINN UNIVERSITY OF TECHNOLOGY
School of Science
Department of Cybernetics

The dissertation was accepted for the defence of the degree of Doctor of Philosophy (Applied Mechanics) on 3 July 2017

Supervisors: Professor Andrus Salupere,
Department of Cybernetics, School of Science,
Tallinn University of Technology, Estonia

Associate Professor Serge Dos Santos, Hab. Dir. Rech.,
INSA Centre Val de Loire, Blois Campus,
U930 "Imagerie et Cerveau" Inserm–University of Tours,
Blois, France

Opponents: Professor Claes Hedberg,
Blekinge Institute of Technology,
Karlskrona, Sweden

Professor Patrick Marquié,
LE2I – FRE 2005 CNRS, Arts et Métiers,
Université Bourgogne Franche Comté, Dijon, France

Defence of the thesis: 29 August 2017

Declaration:

Hereby I declare that this doctoral thesis, my original investigation and achievement, submitted for the doctoral degree at Tallinn University of Technology and INSA Centre Val de Loire, has not been submitted for any academic degree elsewhere.

/Martin Lints/



European Union
European Social Fund



Investing
in your future

Copyright: Martin Lints, 2017

ISSN 1406-4723

ISBN 978-9949-83-139-5 (publication)

ISBN 978-9949-83-140-1 (PDF)

LOODUS- JA TÄPPISTEADUSED B238

**Optimeeritud signaalitöötlus mittelineaarsete
komplekssete materjalide ja bioloogiliste kudede
mittepurustavaks testimiseks ultraheliga**

MARTIN LINTS

THÈSE EN COTUTELLE
PRESENTÉE À L'UNIVERSITÉ DE TECHNOLOGIE DE TALLINN, Estonie
POUR OBTENIR LE GRADE DE DOCTEUR
DE L'UNIVERSITÉ DE TECHNOLOGIE DE TALLINN
ET DE L'INSA CENTRE VAL DE LOIRE

PAR
Martin LINTS

**Traitement du signal optimisé pour
l'évaluation non linéaire non destructive
des matériaux complexes
et des tissus biologiques**

ÉCOLE DOCTORALE
ÉNERGIE, MATÉRIAUX, SCIENCES DE LA TERRE ET DE L'UNIVERS
Discipline/ Spécialité : Sciences & Technologie Industrielle
soutenue le: **29 août 2017**

DIRECTEURS DE THÈSE:**Serge DOS SANTOS**Maître de Conférences HDR, INSA Centre Val de Loire –
Inserm U930-Université de Tours**Andrus SALUPERE**

Professeur, Université de Technologie de Tallinn, Estonie

JURY:**Jaana JANNO**

Professeur, Université de Technologie de Tallinn, Estonie

Aleksander KLAUSON

Professeur, Université de Technologie de Tallinn, Estonie

Rymantas KAZYS

Professeur, Université Technologique de Kaunas, Lituanie

Claes HEDBERG

Professeur, Institut de Technologie de Blekinge, Suède

Patrick MARQUIÉ

Professeur, Université Bourgogne Franche Comté, France

Julien BUSTILLO

Maître de Conférences, INSA Centre Val de Loire, France

RÉSUMÉ

Nous proposons l'innovation « TR-NEWS retardée » comme une extension des méthodes TR-NEWS, issues de la symbiose du retournement temporel (RT) et des méthodes de spectroscopie d'ondes élastiques non linéaires (NEWS), avec principales applications : le contrôle non destructif et l'imagerie ultrasonore médicale. Nous confirmons expérimentalement les bonnes performances des méthodes TR-NEWS pour : (i) des échantillons de composite CFRP aux propriétés dispersives ultrasonores, favorisant ainsi la réverbérabilité de la propagation acoustique ; (ii) des mesures de propriétés non classiques de la peau porcine par une instrumentation multi-échelles acousto-mécanique. Via les simulations numériques de propagations acoustiques non linéaires dans les CFRP, nous identifions et localisons les sources locales de défauts et de micro-endommagements. Elles valident l'identification d'un crack unique proche de la zone de focalisation. La nonlinéarité supposée de type contact acoustique, mesurée par « TR-NEWS retardée » et comparée aux techniques classiques d'inversion d'impulsion utilisées en imagerie médicale, permet une identification préservant la représentation temporelle de l'information. Ainsi, ce système d'instrumentation acousto-mécanique envisage la mesure de paramètres multi-échelles de nonlinéarité des tissus biologiques via les paramètres de Preisach–Mayergoz permettant de décrire leur vieillissement. Le chargement basse fréquence uniaxial synchronisé aux caractérisations ultrasonores haute fréquence (5 MHz) via « TR-NEWS retardée » suggère une nouvelle classe de dispositifs dotée d'une perspective de multimodalité dédiée à l'imagerie ultrasonore non invasive des propriétés biomécaniques des organismes vivants.

Mots-clés: ultrasons, traitement du signal, biomatériaux, CFRP, simulations numériques, Contrôle Non Destructif, TR-NEWS



Contents

List of Publications	10
List of Acronyms	12
Introduction	13
Acknowledgements	14
1 Background, motivation, and goals	15
1.1 Classical and nonclassical nonlinearity	16
1.2 Statement of the problem	17
Résumé	17
2 Time reversal signal processing methods	19
2.1 TR-NEWS signal processing	20
2.2 Delayed TR-NEWS signal processing	22
2.3 Summary	24
Résumé	25
3 Ultrasonic NDT of complex materials	26
3.1 Experimental setup	26
3.2 Numerical simulation model	27
3.3 Nonclassical nonlinearity for ultrasonic NDT of CFRP	28
3.4 Ultrasonic NDT optimisation by delayed TR-NEWS	29
3.4.1 Sidelobe reduction	30
3.4.2 Amplitude modulation	30
3.4.3 Analysis and modification of spectral content	32
3.4.4 Nonlinearity analysis	32
3.5 Analysis of damage in CFRP	32
3.5.1 Simulation model for damage	33
3.5.2 Results	34
3.6 Summary	37
Résumé	37
4 Multiscale characterisation of biological tissues	39
4.1 Acoustomechanical experiment setup	40
4.1.1 Digital Image Correlation	41
4.2 Porcine skin test results	41
4.3 Summary	44
Résumé	44

5 Conclusion	45
5.1 Perspectives	46
Résumé	47
Abstract	48
Kokkuvõte	49
Résumé de la thèse	50
References	52
Appendix A: Publications	59
Publication I	61
Publication II	71
Publication III	85
Publication IV	97
Publication V	107
Appendix B: CV	119
Curriculum Vitae	121
Elulookirjeldus	126

List of Figures

1	TR-NEWS virtual transducer concept	22
2	Delayed TR-NEWS steps	23
3	Carbon Fibre Reinforced Polymer (CFRP) block in the test configuration	27
4	Structure of the CFRP	27
5	Scheme of the side lobe reduction using delayed TR-NEWS	30
6	Delayed TR-NEWS focusing experiment with CFRP sample	31
7	Delayed TR-NEWS in CFRP for creating a specially shaped envelope at the focusing	31
8	Wave interaction caused by delayed TR-NEWS with a single delay focusing	32
9	Schematic of the simulation setup	33
10	PI nonlinearity depending on the receiving transducer position near 1 mm defect	35
11	Comparison of nonlinear signatures in displacement u_2 using PI and delayed TR-NEWS	36

12	Skin sample in loading machine with ultrasonic transducers attached by a hand clamp	40
13	Acoustomechanical test setup using mechanical and acoustic measurements	40
14	Synchronised mechanical data from skin sample extension, with TR-NEWS synchronisation points	42
15	Hysteresis based on DIC strain data	43
16	Delayed TR-NEWS nonlinearity measure in the acoustomechanical experiment with skin	43

List of Publications

- Publication I:** M. Lints, A. Salupere, and S. Dos Santos. Simulation of solitary wave propagation in carbon fibre reinforced polymer. *Proc. Estonian Acad. Sci.*, 64(3):297–303, 2015
- Publication II:** M. Lints, S. Dos Santos, and A. Salupere. Solitary Waves for Non-Destructive Testing Applications: Delayed Nonlinear Time Reversal Signal Processing Optimization. *Wave Motion*, 71:101–112, 2017.
<http://dx.doi.org/10.1016/j.wavemoti.2016.07.001>
- Publication III:** S. Dos Santos, M. Lints, N. Poirot, Z. Farová, A. Salupere, M. Caliez, and Z. Převorovský. Nonlinear Time Reversal for Non Destructive Testing of complex medium : a review based on multi-physics experiments and signal processing strategies. In P. Mazal, editor, *NDT in Progress 2015 - 8th International Workshop of NDT Experts, Proceedings*, pages 31–40. Brno University of Technology, October 2015
- Publication IV:** M. Lints, S. Dos Santos, C. Kožená, V. Kůs, and A. Salupere. Fully synchronized acoustomechanical testing of skin: biomechanical measurements of nonclassical nonlinear parameters. In *24th International Congress on Sound and Vibration, 23–27 July, 2017, London*, number 867. ICSV, International Institute of Acoustics and Vibrations, 2017
- Publication V:** M. Lints, A. Salupere, and S. Dos Santos. Simulation of detecting contact nonlinearity in carbon fibre polymer using ultrasonic nonlinear delayed time reversal. *Acta Acust. united Ac.*, 2017. (accepted)

Summary of the author’s contributions

- I** In Publication I, I was the main author, wrote the simulation program, carried out the simulations and the analysis of the results, prepared the figures, and wrote the manuscript.
- II** In Publication II, I was the main author, wrote the necessary scripts for the signal processing of the physical experiments, wrote the simulation programs, conducted the experiments and simulations, analysed the results, prepared the figures, and wrote the manuscript.
- III** In Publication III, I assembled the equipment for the experiment and conducted tentative measurements.
- IV** In Publication IV, I was the main author, assembled the experimental equipment, programmed the data communication protocol for the synchronised experiments and automation of the experiments. I analysed the experimental results, programmed and conducted the image processing and the extraction and

synchronisation of data from different sources, analysed the data, created the figures, and wrote the manuscript.

V In Publication V, I was the main author, wrote the simulation program, carried out all simulations and analysis of results, prepared all figures and the manuscript.

Approbation

I presented the results of the thesis at the following conferences:

1. **M. Lints**, A. Salupere, and S. Dos Santos. ‘Simulation of solitary wave propagation in carbon fibre reinforced polymer’, IUTAM Symposium on Complexity of Nonlinear Waves: 8–12 September 2014, Tallinn
2. **M. Lints**, A. Salupere, and S. Dos Santos. ‘Simulation of nonlinear time reversal wave propagation in carbon fibre reinforced polymer’, 11th European Conference on Non-Destructive Testing (ECNDT 2014), 6–10 October 2014, Prague, Czech Republic
3. **M. Lints**, S. Dos Santos, and A. Salupere. ‘Delayed time reversal for ultrasound focusing in non destructive testing’, Stochastic and Physical Monitoring Systems (SPMS), 22–27 June 2015, Drhleny, Czech Republic
4. S. Dos Santos, **M. Lints**, and A. Salupere. ‘Solitary waves for Non-Destructive Testing applications: Delayed nonlinear time reversal signal processing optimization’, Application of Mathematics in Technical and Natural Sciences (AMi-TaNS), 28 June–3 July 2015, Albena, Bulgaria, (S. Dos Santos invited paper)
5. **M. Lints**, A. Salupere, and S. Dos Santos. ‘Dispersion simulations in layered CFRP’, 28th Nordic Seminar on Computational Mechanics (NSCM 28), 22–23 October 2015, Tallinn, Estonia
6. **M. Lints**, S. Dos Santos, C. Kožená, V. Kůs, and A. Salupere. ‘Fully synchronized acoustomechanical testing of skin: biomechanical measurements of nonclassical nonlinear parameters’, 24th International Congress on Sound and Vibration (ICSV 24), 23–27 July 2017, London, United Kingdom

List of Acronyms

A.U.	Arbitrary Unit
CAN	Contact Acoustic Nonlinearity
CFRP	Carbon Fibre Reinforced Polymer
CPU	Central Processing Unit
DAQ	Data Acquisition
DIC	Digital Image Correlation
ESAM	Excitation Symmetry Analysis Method
FEM	Finite Element Method
NDT	Nondestructive Testing
NEWS	Nonlinear Elastic Wave Spectroscopy
PI	Pulse Inversion
PM	Preisach–Mayergoyz
SNR	Signal-to-Noise Ratio
TR	Time Reversal
TR-NEWS	Time Reversal – Nonlinear Elastic Wave Spectroscopy

Introduction

Ultrasonic Nondestructive Testing (NDT) and medical diagnostics are cost-effective analysis methods, where the most common applications are finding defects in industrial components and conducting imaging for medical diagnostics. In simplest applications, an ultrasonic wave is propagated in a medium and received from the same transducer to listen for echoes (pulse-echo technique). Alternatively it can be received by another transducer on the opposite side, listening for passed sound intensity and time of flight (pitch-catch technique) [38].

Recent developments have increased the signal processing capabilities of ultrasonic NDT equipment. Large effort has been devoted to increasing the imaging quality and developing user-friendly ways to get 2D and 3D images. The improved imaging often makes use of advanced transducer principles, such as phase-shifted arrays and laser vibrometers for measuring the ultrasonic wave in the test object. However, the NDT technology still largely uses the assumption of linear wave motion, because in ultrasonic measurements the energy levels are usually too low to measure nonlinearities. It is difficult to introduce waves of sufficiently large amplitude into a test material to ‘activate’ the nonlinear effects of wave propagation in order to make them strong enough to be measured. Additionally, as the mechanical properties of nonlinear materials are more difficult to characterise than those of linear materials, most applications in NDT and medical diagnostics still assume linear materials.

In linear measurements, there is a trade-off between the acquired resolution and the penetration depth of ultrasonic imaging. Analysis of nonlinear effects could allow detecting defects that are smaller than the wavelength of the ultrasound. Most industrial materials are stiff and linear when not damaged. For example, Carbon Fibre Reinforced Polymer (CFRP) is linear up to very high stresses and strains, unattainable by ultrasonic testing [50] and would require stresses of destructive testing magnitude for the nonlinearities to become apparent. However, the presence of micro-damage could be detected by considering its nonlinear effects on ultrasonic wave propagation. Biological tissues can also be nonlinear, hysteretic, and viscoelastic, so their ultrasonic investigation requires consideration of nonlinear effects [14, 48]. The same applies to many natural materials, for example rocks [27]. Often the damage is small-scale (less than ultrasonic wavelength) and distributed. Instead of relying on the more expensive X-ray tomography methods to detect these defects, the ultrasonic NDT could be extended to analyse the nonlinear effects of this kind of damage. Many types of defects in damaged materials can act as sources of nonlinearity for ultrasonic waves. Therefore the attention has recently shifted to using more advanced excitations and signal processing methods in ultrasonics in order to investigate damaged complex media, such as carbon fibre composites or biological tissues, for nonlinear effects.

For complex materials, various Nonlinear Elastic Wave Spectroscopy (NEWS) methods have been proposed [23, 58, 64, 65]. Time Reversal (TR) based methods

allow the use of long signal lengths and any number of transmitters to introduce a wave focusing into the medium [16, 19, 21, 22, 59], making it possible to create a signal with a higher power level and a better Signal-to-Noise Ratio (SNR) for investigating the nonlinearities in the material. Using TR with NEWS (TR-NEWS) helps to potentially amplify signal strength and increase the SNR in the location of damage or nonlinearities of the material [8, 24, 47, 63].

This thesis is organised as follows. Section 1 gives an overview of nonlinear ultrasonic testing. Section 2 introduces the main signal processing method used here—the delayed TR-NEWS—developed for the ultrasonic experiments and simulations of this thesis. Section 3 is devoted to the nonlinear ultrasonic NDT of complex materials by using as an example a CFRP block that could have delamination or microcracking damage creating nonlinear effects in the ultrasonic wave propagation. The ultrasonic characterisation of biological tissues is discussed in Section 4, using an example of an *ex vivo* porcine skin sample for the measurement of nonlinear mechanical parameters. Conclusions can be found in Section 5.

The main contribution of this thesis is the introduction of a novel delayed TR-NEWS signal processing method, that can be used in nonlinearity analysis of simulations and experiments of complex industrial materials and in medical diagnostics. The goal is to detect material damage and nonlinear effects.

Acknowledgements

My thanks go to my supervisor Andrus for always finding time to help and teach. I am grateful also to my co-supervisor Serge for teaching the experimental aspects of ultrasonics and introducing me to the French culture of work and leisure.

Many thanks to my friends in Blois for helpful discussions, advice, and support during my visits. My thanks go to Professor Mencik for inviting me to use the offices of LAMÉ laboratory during my multiple stays at INSA CVL.

And last but not least, I want to thank my wife Pille for her strong support and for sacrificing her time to allow me to pursue this interesting work and goals in conducting the research presented in this thesis. I want to thank my son Silver for reminding me each day that the world is large and full of interesting things.

The financial support from the Estonian Science Foundation, the Estonian Research Council and the national scholarship programmes Kristjan Jaak and DoRa, which are funded and managed by the Archimedes Foundation in collaboration with the Ministry of Education and Research, is appreciated. The support from PLET project of Région Centre-Val de Loire is acknowledged.

1 Background, motivation, and goals

In recent years there has been a considerable development of nonlinear ultrasonic NDT methods. It has been driven by the need for early defect detection in complex materials, which are usually difficult to analyse. A multitude of materials can be tested using ultrasonic NDT with many possible nonlinear description theories and mechanisms. Consequently, there cannot be a single universal *nonlinear* ultrasonic NDT method. This work studies materials with complex structure and uses two materials as examples for analysis: CFRP and skin. The developed methods could be applied to materials with the same type of structure and mechanical properties. For example, the methods developed for CFRP can be used for other fibre reinforced composites and laminates where comparable damage and defects can occur. Similarly, the hysteresis and nonlinearity measurement of skin could be used for other artificial and natural materials exhibiting the same type of multiscale elasticity properties.

Today CFRP is seeing increasing usage in industry. Having been in the past an expensive and high-tech material reserved for non-structural parts of aeronautical components, it is now also used for load-bearing purposes and also in automotive and civil engineering. Its advantage of low weight and high strength is often countered by its high cost and structural complexity, making ultrasonic NDT needed but difficult. Above all, NDT analysis is needed when CFRP is used in critical components, to decrease the probability of catastrophic failure due to one of its many complex failure mechanisms. These include microcracking and delamination.

The inhomogeneous composition of CFRP makes it difficult to conduct ultrasonic NDT. For example, the CFRP block used in the physical experiments of this thesis is composed of 144 layers of carbon fibre cloth, stacked in 45° alternating direction, glued with epoxy. The resulting block is lightweight and strong but difficult for the ultrasonic waves to penetrate. Even though the wavelength is larger than most of the inhomogeneities, the wave still ‘feels’ the underlying microstructure in terms of dispersion, dissipation, and complex propagation paths inside the test object. Complex propagation paths can be beneficial for TR signal processing method, which uses the internal reflections to create a spatio-temporal focusing of the ultrasonic wave in the NDT procedure, increasing the SNR [47, 63]. The delayed Time Reversal–Nonlinear Elastic Wave Spectroscopy (delayed TR-NEWS) is a further development of one of such procedures and is described in Section 2.

Another part of this thesis is related to the medical diagnostics and material characterisation of biological tissues, such as skin, teeth, and bones, which are nonlinearly elastic [20] even without defects. Traditionally in the ultrasonic medical diagnostics, the soft tissues are considered to be linearly elastic and homogeneous, which has given acceptable results for medical ultrasound. There are, however, many open problems concerning the determination of mechanical properties of the biological tissues that need to take nonlinearities into effect. Accurate characterisation of the

skin properties could be used in surgery simulations, medical ultrasonic diagnostics, disease diagnostics, research on skin ageing and damage, and many other problems in medicine and cosmetics.

All of the materials considered here have considerable microstructure and are complex, inhomogeneous, and anisotropic. Therefore they require sophisticated analysis methods to fully measure their multiscale properties. This complex task is at the moment an open problem, solved only partially, mostly by using phenomenological approaches. Nonlinear NDT methods have recently seen great advances and are becoming practical [32, 37]. The effects of nonlinearity usually considered for NDT uses are (i) harmonics (e.g. frequency shift, overtones) [62]; (ii) nonlinear dissipation [23]; (iii) scaled subtraction method [58] (also Pulse Inversion (PI)); (iv) symmetry analysis [13]; and (v) nonlinear resonance shift [64]. This thesis has added a new technique, which uses the breaking of the superposition principle to detect the nonlinear effects. It is described in Section 3.4.4.

1.1 Classical and nonclassical nonlinearity

Load-bearing materials usually act linearly in their working configuration and even more so in case of relatively small strains of ultrasonic testing. In biological tissues, nonlinear effects can exhibit themselves at smaller strains but are nevertheless difficult to detect in ultrasonic testing. It is unlikely to create a strain large enough to activate classical nonlinear elasticity (where the elastic energy is a quadratic and cubic function of strain [36]). In contrast, the nonclassical nonlinearity includes nonlinear effects from other causes [7, 56]: memory effects, interfaces, structural inhomogeneities, defects, etc. The nonclassical nonlinearity can also be only local.

Despite the complex microstructure and high levels of dispersion and dissipation, an undamaged CFRP block is still highly linear, when considering stress and strain levels possible with an ultrasonic wave. In Publication I we investigated the classical versus nonclassical nonlinearity in the layered 1D simulation of the CFRP at ultrasonic power levels. We showed that it is not realistic to detect the classical nonlinearity in CFRP using normal ultrasonic NDT power levels. However, a simple and small nonclassical nonlinearity of the mechanical diode type could be detected. It is known as ‘Contact Acoustic Nonlinearity’ (CAN) [7, 57]. Publication V uses a 2D linear layered Finite Element Method (FEM) model of CFRP that has a single CAN defect in order to detect its nonlinearity using different approaches.

A single CAN is relatively simple to simulate and analyse, but there is usually a distribution of defects with different sizes and angles, such as general microcracking of CFRP. Preisach–Mayergoyz (PM) hysteresis [1] is able to model this kind of distributed CAN damage [26, 34]. It includes losses and also enables introduction of the material nonlinearity [4, 22, 30]. The PM hysteresis model has been used for sandstone [28, 29] and later also for various other multiscale materials exhibiting

nonclassical nonlinearity [52, 54]: teeth, skin, etc. Hysteresis has several characteristic properties, such as congruency and wiping-out property, but it can mostly be described by the statistical distribution of hysteresis elements forming the PM space [45]. The distribution determines the hysteresis drawn by a loading path. Since the parameter space is large, advanced computational methods need to be used for materials characterisation from experimental data [35].

An acoustomechanical automated testing equipment has been built within the context of this thesis and is described in Section 4. It allows exciting the multi-scale hysteresis of a skin sample *ex vivo* by using automated routines and enables measuring the statistical properties of the test sample for future integration into the characterisation of the material.

1.2 Statement of the problem

Traditional linear ultrasonic NDT methods are well established and in active development in fields of transducer technology, beamforming, and signal processing. Nevertheless, they have several shortcomings for specialised applications. Complex test object geometry (size, contour, surface roughness, geometrical complexity, and discontinuities) and coarse internal structure (grain size, porosity, inclusions, or dispersed precipitates) can yield marginal or unsatisfactory results [2].

The main goals of this thesis are, using experimental and numerical methods, to investigate

- the feasibility of using nonlinear effects in NDT for the characterisation of complex materials such as composites and biological tissues;
- the novel delayed TR-NEWS signal processing method that enables detection of the nonlinear effects;
- CAN and hysteresis nonlinearities as possible defect models for complex materials, such as composites and biological tissues.

Résumé

Dans ce chapitre, nous décrivons les méthodes classiques de tests ultrasonores basés sur le principe de propagation acoustique non linéaire dans les milieux biologiques complexes ou les composites CFRP. Nous rappelons les hypothèses du comportement hystérétique des défauts et leurs propriétés multi-échelles comme étant à la base de l'origine de leur dégradation et/ou de leur vieillissement. Nous introduisons quelques propriétés des CFRP et décrivons l'importance de la prise en compte de la complexité des propriétés mécaniques des tissus biologiques. Après avoir décrit quelques méthodes de traitement du signal nécessaires à l'extraction des signatures

non linéaires, nous présentons dans la partie 1.1 les concepts de nonlinéarités classiques et non classiques. Dans la partie 1.2, les hypothèses fondamentales de l'étude sont argumentées et sont associées à la genèse de la mise en œuvre de la méthode TR-NEWS retardée.

2 Time reversal signal processing methods

Linear ultrasonic NDT methods are reliable and affordable in most industrial and medical applications, but for complex materials can yield poor results due to scattering, inhomogeneity, and nonlinearity of the material. This section describes a novel delayed TR-NEWS signal processing method, which improves the SNR and imaging quality, uses internal reflections of a complex material as an advantage, and allows analysis of nonlinear defects smaller than the ultrasonic wavelength. The development of this method was one of the main goals of this thesis.

The TR based methods create or improve the ultrasonic signal focusing and enhance the signal quality. They are modern techniques (in NDT) with applications also in communication, acoustics, and seismic imaging. In most applications TR works extremely well regardless of numerous mode conversions in reverberant media. A traditional and well-known TR method uses a Time Reversal Mirror using a 1D or 2D transducer array. A pulse is sent toward a defect from each transducer, and the time delay of the echo is recorded. Upon time reversing the echo delay, it is possible to focus on the echoing defect [19]. No a priori knowledge of the geometry of the test object is needed.

It is possible to use a single transducer instead of an array for TR focusing [16, 21]. A reverberant medium is excited by a short pulse (triangular, tone burst, etc.) from a single source at point A. The signal recorded at point B contains the initial arrival of the signal (main peak) and additionally the reverberation of the medium as the chaotic signal after the main pulse (coda). The coda contains information about the scatterers in the medium, since it has travelled through the object by various indirect propagation paths and reflections [18]. Time-reversing and re-sending the captured signal yields a focused wave at point B. Since the signal is sent from A to B for both passes, it is also called ‘reciprocal TR’ [63]. Therefore it is possible to use non-contact measurement equipment, such as a laser vibrometer, on point B. Its advantages include pointlike measurement, no coupling effects, flat and broadband response, and the possibility of automatically scanning the surface of the object [59]. The initial sent pulse should be a short excitation and the reception time window should be comparatively long to account for all of the reflections. This method amplifies the signal of the focused pulse because the arrivals of a long second excitation are compressed to a single focusing peak. The quality of the focusing, amplification, and SNR depends on the ergodicity of the material and on the length and bandwidth of the excitation.

In this thesis a further development of TR is used. The initial signal of single-channel TR can be optimised: a chirp (frequency sweep) signal can be used instead of the short pulse. The concept is similar to the pulse compression method known in the RADAR and SONAR technologies [17]. Because of the long duration of the excitation, the received signal must be cross-correlated with the excitation to reveal the true scattering information of the medium, which can then be time-reversed and retrans-

mitted to create the spatio-temporal focusing [6, 15]. The cross-correlation enables a wide range of broadband initial excitation signals to be used for TR, which can be optimised according to the equipment or material at hand. Its further development—delayed TR-NEWS—is the signal processing method used in this thesis to optimise the focusing and to detect nonlinearities and is one of the key results.

2.1 TR-NEWS signal processing

The TR-NEWS signal processing method solves two problems of ultrasonic NDT testing of complex materials (geometry, structure, etc.) that might have nonlinearities:

- Complex materials can exhibit scattering and multipath wave propagation, so receiving a clear ultrasonic image is difficult.
- Nonlinearities mostly require some minimum power level to activate. At sufficiently small strain levels, most materials act linearly, while with large strain they mostly act nonlinearly. Ultrasonic NDT testing equipment and medical diagnostics equipment are very limited in terms of transmitted wave power.

The TR-NEWS finds advantage in increased scattering of waves from the microstructure and heterogeneous inclusions of the material. This advantage is most prominent in materials with low attenuation [59].

For the signal focusing, the method uses two transmission passes and altogether four separate signal processing steps. Both transmissions are sent from the same transducer. The four signal processing steps can be summarised as follows:

Transmission of the broadband initial signal. This could be a short impulse, but in this thesis the linear chirp signal, which can have more power, is used:

$$c(t) = A \cdot \sin(\psi(t)). \quad (1)$$

Here the instantaneous phase is $\psi(t) = 2\pi \left(f_0 t + \frac{(f_1 - f_0)t^2}{2t_1} \right)$; the start and the end frequencies and the end time are respectively f_0 , f_1 , and $t_1 = T/2$; and T is the recording duration of the received signal (TR window length). The recorded signal (chirp-coded coda response [14]) can be written as

$$y(t) = h(t) * c(t) = \int_{\mathbb{R}} h(t - t') c(t') dt', \quad (2)$$

where $h(t)$ is regarded as the (unknown) impulse response (Green's function) of the medium.

Cross-correlation of the sent and received signals. In RADAR and SONAR signal processing, this step is known as *pulse compression* [17]. In an ideal transmission, the received signal is the same as the transmitted signal $y(t) = c(t)$. Since the autocorrelation of a chirp is an impulse signal $\Gamma_c(t) = c(t) * c(T - t) = \delta(t - T)$, then in case of reflectionless transmission, the cross-correlation gives an impulse signal at the time-of-flight time delay. In case of reflections, the corresponding additional delays and amplitudes are contained in the cross-correlation

$$\Gamma(t) = \int_{\Delta t} y(t - t')c(t')dt' \simeq h(t) * c(t) * c(T - t), \quad (3)$$

where Δt is the time window of the correlation. Therefore, in general the cross-correlation in TR-NEWS is proportional to the impulse response of the medium $\Gamma(t) \sim h(t)$.

Time-reversal of the correlation. Since Γ is proportional to the impulse response of the medium, it should contain information about the reflections and scattering of the wave propagation. Therefore propagating its time reversed version $\Gamma(T - t)$ should cancel out the delays between different propagation paths and scattering elements in the test object.

Transmission of the time-reversed correlation. The time-reversed cross-correlation is used as a new input for the second pass of the wave propagation. It is important that the test configuration (material properties, transducer placement, etc.) remains the same throughout all of these steps. The transmission of $\Gamma(T - t)$ creates the recognisable focused impulse signal with symmetrical sidelobes at the focal point of the receiver:

$$y_{\text{TR}}(t) = \Gamma(T - t) * h(t) \sim \delta(t - T/2), \quad (4)$$

where $y_{\text{TR}} \sim \delta(t - T/2)$ is the signal focused by TR under the receiving transducer.

These signal processing steps are illustrated in Fig. 1. Using these steps and initial broadband signal $c(t)$ results in a spatio-temporally focused impulse signal $y_{\text{TR}}(t)$ under the receiving transducer or vibrometer. The material or experiment configuration need not be known in advance, but must remain constant throughout both transmission passes. The resulting signal has an increased amplitude due to pulse compression from the broadband signal of length Δt to one sharp impulse focusing. Correspondingly, the SNR is also increased. Therefore this method is advantageous for activating and analysing material nonlinearities using various NEWS methods.

Various NEWS methods that can be used with TR exist. The power amplification property of the described TR method makes it possible to potentially activate the nonlinearities and defects that are otherwise hidden. Many methods have been developed

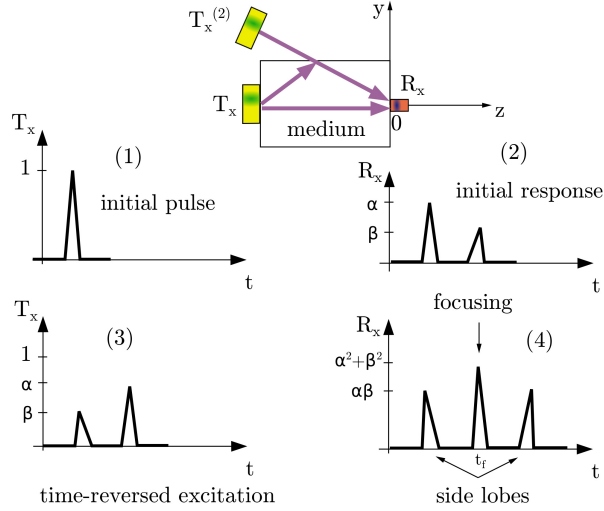


Figure 1 – TR-NEWS virtual transducer concept: (1) the initial broadband excitation $T_x(t)$ propagates in a medium; (2) additional echoes from interfaces and scatterers as new virtual sources $T_x^{(2)}$; (3) time reversal; (4) response $y_{TR}(t)$ with a spatio-temporal focusing at $z = 0$; $y = 0$; $t = t_f$ and symmetric sidelobes with respect to the focusing. Figure from [42].

for nonlinearity detection, which can also be used with this signal processing method. The broadband excitation of the chirp signal provides an opportunity to analyse the spectral content of the resulting focusing for the generation of additional harmonics from the possibly sub-wavelength defects [65]. It is possible to use the scaling subtraction method [5, 55], Pulse Inversion (PI) [14] and its modified form Excitation Symmetry Analysis Method (ESAM) [13] among many others [60].

2.2 Delayed TR-NEWS signal processing

The *delayed TR-NEWS* signal processing [15] is a further development of TR-NEWS, which allows the manipulation of the focused wave shape. Its first experimental and simulation results in CFRP were presented in Publication II, where various signal optimisation possibilities were demonstrated. The delayed TR-NEWS optimisation relies on the single impulse signal focusing of the TR-NEWS, which is used as a new basis for generating an arbitrary wave envelope by scaling and overlaying several focused signals with some temporal offset. As delayed TR-NEWS is able to create an arbitrary arrival and interaction of the focused impulse signals, new applications, described in this Section, become possible.

The concept of delayed TR-NEWS is the following: if transmitting one time reversed cross-correlation $\Gamma(T - t)$ results in a single focused peak $y_{TR}(t)$, then

transmitting a superposition of several scaled (a_i) and delayed (τ_i) cross-correlations should generate a collection of focused peaks with the same scaling and delay values ($a_i \cdot y_{TR}(t - \tau_i)$), if linear superposition holds. The superposition of scaled and delayed cross-correlations can be described as

$$\Gamma_s(T - t) = \sum_{i=0}^n a_i \Gamma(T - t + \tau_i) = \sum_{i=0}^n a_i \Gamma(T - t + i\Delta\tau), \quad (5)$$

where a_i is the i -th amplitude coefficient and τ_i is the i -th time delay. In case of uniform time delay, $\Delta\tau$ is the time delay between samples. Upon propagating this $\Gamma_s(T - t)$ through a medium according to the last step of TR-NEWS, a delayed scaled shape of the signal at the focusing point can be created. As an example, creating a superposition of two cross-correlations, where the second one is scaled and delayed, and its resulting focusings are illustrated in Fig. 2.

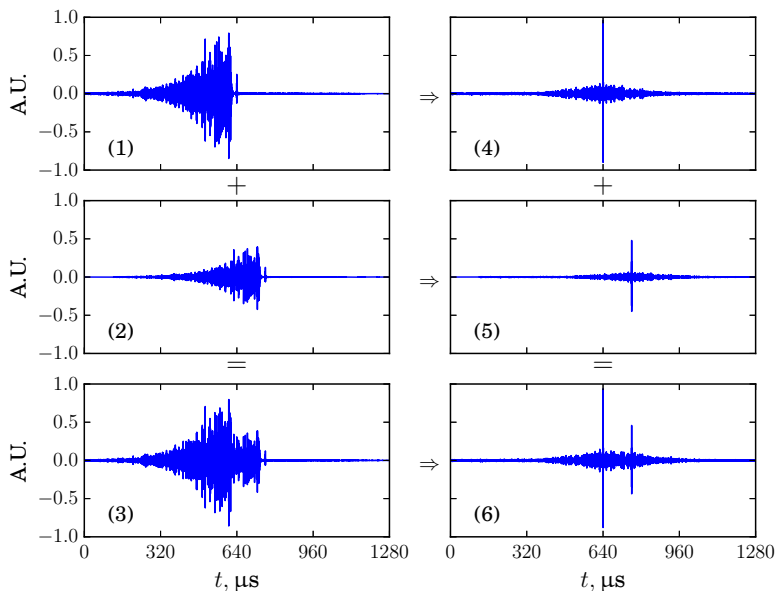


Figure 2 – Delayed TR-NEWS steps. Left column: superposition of cross-correlations. Right column: superposition of focused waves. (1) Cross-correlation (Eq. (3)); (2) delayed and scaled cross-correlation; (3) linear superposition of two cross-correlations (Eq. (5)), which becomes the new excitation; (4) focusing (Eq. (4)); (5) delayed and scaled focusing; (6) linear superposition of the two focusing peaks (Eq. (6)).

It is possible to predict the value of the delayed TR-NEWS focusing in linear, undamaged material by the linear superposition of single focusing. The corresponding delays τ_i and amplitudes a_i are applied for superpositioning the scaled and delayed

versions of a single TR-NEWS focused signal (Fig. 2 right column):

$$\begin{aligned}
 y_{\text{dTR}}(t) &= \left[\sum_i a_i \Gamma_c(T-t+\tau_i) \right] * h(t) \quad \underline{\underline{\text{linearity}}} \\
 &= \sum_i a_i \Gamma_c(T-t+\tau_i) * h(t) = \sum_i a_i y_{\text{TR}}(t-\tau_i). \quad (6)
 \end{aligned}$$

This prediction y_{dTR} allows finding the optimal delay and amplification parameters for delayed TR-NEWS before transmitting the ultrasound for the measurement pass. In experiments with undamaged CFRP (Publication II), the prediction was accurate up to the noise level. Furthermore, since the prediction relies on linear superposition, it should only work in undamaged material. Therefore the difference between the prediction and the actual measured result of the delayed TR-NEWS could indicate the presence of a nonlinearity, for example damage or a defect. This is discussed further in Section 3.4.4.

In conclusion, the delayed TR-NEWS measurement usually requires three wave propagation passes. The first two passes are for the full TR-NEWS measurement, yielding the correlation and focused wave signals. Then the single focusing can be used for the prediction and fine-tuning of the delay τ_i and amplitude a_i values in Eq. (6), which are then applied to delay and scale the correlation data in Eq. (5). The third pass is the propagation of the delayed and scaled superposition of correlations, yielding the delayed TR-NEWS measurement, which can be compared to the prediction to see if the linear superposition holds. The second pass of the TR-NEWS can be skipped if the prediction Eq. (6) is not used.

2.3 Summary

TR-NEWS is a signal processing method that enables the use of a single channel transducer system to create a spatio-temporal focusing in the test medium by taking advantage of its complex internal structure, scattering and internal reflections. The focused wave has more power and a better SNR, making it possible to potentially activate local nonlinearities in the test object and to detect them using various NEWS methods.

A novel signal processing method—delayed TR-NEWS—has been developed based on the known TR-NEWS method. Delayed TR-NEWS opens new possibilities in the focused signal modification for various goals: sidelobe reduction, focusing optimisation (arbitrary wave envelope), spectral content modification and analysis. Due to its accurate prediction in linear, undamaged materials, this method can be also used as a nonlinearity detection measure, where baseline measurements are not needed.

Résumé

Ce chapitre présente l'historique du développement des outils de traitement du signal qui ont été nécessaires à l'élaboration de la méthode de renversement temporel non linéaire. L'importance de la prise en compte de la complexité du milieu à imager, de la présence de conversion de modes complexes, et des multiples échos est considéré comme une plus-value pour l'efficacité des méthodes de retournement temporel et constitue un avantage pour la focalisation des ondes et de l'activation des nonlinéarités. Dans la partie 2.1, le traitement du signal est décrit mettant en exergue les avantages de la compression d'impulsion associée l'inversion d'impulsion. La partie 2.2 est, quant à elle, dédiée à la méthode TR-NEWS retardée développée dans le cadre de cette thèse.

3 Ultrasonic NDT of complex materials

Industrial materials are generally designed to work in the linear and small deformation regime, making the measurement of classical nonlinearity difficult. However, nonclassical nonlinearity can arise in damaged materials that are otherwise linear [3]. Publication I shows by simulations that it is unlikely to measure the classical nonlinearity of undamaged CFRP, but nonclassical nonlinearity arising from defects could be detected even with the small strains of ultrasonic NDT. The TR-NEWS based methods are used for analysis of complex materials, as they gain advantage from the internal reflections and microstructure for the wave focusing. In the previous section a novel signal processing method, delayed TR-NEWS, was introduced. It was analysed by experiments and simulations for undamaged, linear CFRP.

The following simulations and experiments were conducted to study nonlinear ultrasonic NDT:

1. 1D Chebyshev pseudospectral simulation in periodic bi-layered CFRP, for understanding which nonlinearities could be detected with the usual ultrasonic test power levels (Section 3.3);
2. Experiments and 2D FEM simulations of CFRP for validating the delayed TR-NEWS signal optimisation methods for various effects in linear and undamaged material (Section 3.4);
3. 2D FEM simulations in CFRP with absorbing boundary conditions and a CAN type defect, for validating the nonlinearity analysis of delayed TR-NEWS (Section 3.5).

The simulations and experiments were conducted using single channel TR-NEWS as described in Section 2. Bi-layered aluminium, CFRP sample blocks, and porcine skin were used as the test media for the validation of the signal processing methods, damage detection, and material elasticity characterisation developed in this thesis.

This section explains the course of simulations and experiments in developing the ultrasonic NDT of complex materials in the presence of nonclassical nonlinearities. It is shown that the delayed TR-NEWS helps to create different optimisations of the TR-NEWS focusing. Moreover, it offers a new method for detecting nonlinear effects in NDT.

3.1 Experimental setup

The simplest TR-NEWS ultrasonic NDT setup uses one receiving and one transmitting transducer, like used here, shown in Fig. 3. The test equipment consisted of

Preamplifier: Juvitek TRA-02 (0.02–5 MHz) connected to a computer;

Amplifier: ENI model A150 (55 dB at 0.3-35 MHz);

Shear wave transducer: Technisonic ABFP-0202-70 (2.25 MHz);

Longitudinal wave transducer: Panametrics V155 (5 MHz).

The special software for driving TRA-02 allowed us to choose excitations and to correlate, time reverse, and analyse the signals using a graphical interface computer program. Additional signal processing was done by one-off computer scripts and programs.



Figure 3 – CFRP block in the test configuration with the transmitting transducer at the side and the receiving transducer on top. Figure from Publication II.

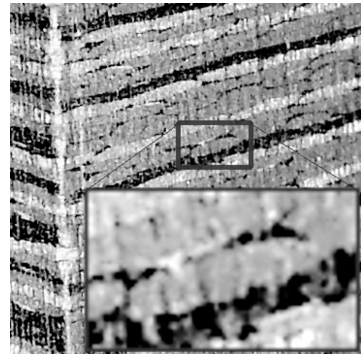


Figure 4 – Structure of the CFRP with the fabric yarns in tight packing and epoxy filling the voids. Figure from Publication II.

3.2 Numerical simulation model

The structure of CFRP polymer is complex and hierarchical: it is composed of layers of carbon fibre cloth, which are woven from yarns, which in turn are composed of individual fibres. Epoxy is between the fibres and has different mechanical properties (Fig. 4).

A laminate model was used in the simulations because it is less complex than the actual structure of CFRP. The epoxy and carbon fibre layers alternate and the anisotropic carbon fibre layers have different directionality of weave. The layers of the model are homogeneous, but the discontinuity of elasticity properties can introduce dispersion. The laminate model is still simpler for meshing and simulation than the fully described material. Here the 1D simulation uses fixed thickness layers and 2D simulations use layers of stochastic thicknesses.

The statistical distribution of the yarn sizes was calculated from a close-up image of the actual composite block. The thicknesses of the layers are proportional to the

dimensions calculated from the stochastic value function according to the distribution, so they are proportional to the structure size of the CFRP. The layered model should therefore describe the stochastic structure of the CFRP better than of a simple laminate with uniform layer thicknesses. The computation of the thicknesses is described in [42]. The model consists of three different types of materials with the following mechanical properties:

- pure epoxy layer as isotropic material: $E = 3.7$ GPa, $\nu = 0.4$, $\rho = 1200$ kg/m³;
- composite with fabric at 0/90° direction as transversely isotropic material: $E_1 = E_2 = 70$ GPa, $G_{12} = 5$ GPa, $\nu_{12} = 0.1$, $\rho = 1600$ kg/m³;
- composite with fabric at 45°/45° direction as transversely isotropic material: $E_1 = E_2 = 20$ GPa, $G_{12} = 30$ GPa, $\nu_{12} = 0.74$, $\rho = 1600$ kg/m³.

In simulations, all deformations are assumed to be small $\epsilon_{kl} = \frac{1}{2}(u_{k,l} + u_{l,k})$. The equations of motion in each piecewise continuous layer are

$$\begin{cases} \sigma_{kl,k} + \rho \ddot{u}_l = 0, \\ \sigma_{kl} = \sigma_{lk}, \end{cases} \quad (7)$$

where u_l is displacement, σ_{kl} is stress tensor, ρ is density, dot notation is used for differentiation, and usual tensor notation and Cartesian coordinates are used.

3.3 Nonclassical nonlinearity for ultrasonic NDT of CFRP

In Publication I, the simulations are conducted on a 1D layered model of 43 mm thick CFRP composite block, which has classical and nonclassical nonlinearities. The constitutive equation for the 1D wave propagation is

$$\sigma = \alpha E (\epsilon - \beta \epsilon^2), \quad \begin{cases} \alpha \leq 1 & \text{if } \epsilon \geq 0, \\ \alpha = 1 & \text{if } \epsilon < 0. \end{cases} \quad (8)$$

Here α describes nonclassical nonlinearity, which is similar to a mechanical diode: the material is weaker in tension than in compression [57], and β describes classical nonlinearity. In the simulation it is assumed that $\beta = -15$ and $\alpha = 97\%$ (for $\epsilon \geq 0$) could be realistic values for CFRP [25].

The 1D simulations of wave motion in CFRP use the Chebyshev collocation method for computation. The solution is approximated at gridpoints by a polynomial, which is easily differentiated. Unlike the finite difference and finite element methods, the collocation method is global: all the points contribute to the derivatives of each point. The main advantages of this method are (i) smaller computational cost due to the smaller number of required gridpoints, and (ii) simplicity of programming

for nonlinear problems and in case of high spatial derivatives. The Chebyshev polynomial is a good choice for boundary value problems. The clustering of gridpoints toward the ends of the computational region helps to avoid Runge's phenomenon, which causes oscillations in interpolation in case of equispaced interpolation points. Each layer of the laminate model is treated by a separate polynomial. The polynomials are required to satisfy continuity of the boundary conditions between them.

Publication I investigates the possibility of having a detectable nonlinearity in CFRP. The effect of the two different types of nonlinearity are analysed. The simulations confirm that when realistic values for the classical nonlinearity β are used, the nonlinear effect on the wave propagation is negligible. In contrast, even a slight nonclassical nonlinearity has an immediate effect on the propagation of an elastic wave, because it is zero-centred, in terms of strain, and is activated at any ultrasonic power level. The excitation length is also modified to study the effect of the dispersion due to the periodically alternating material layers. If the half-cosine spans 15 pairs of carbon fibre–epoxy layer pairs, the effect of the layered model will be unnoticeable, but when it is decreased to 3 pairs, the wave will 'feel' the microstructure and cause dispersion. In case of the half-cosine pulse, the nonclassical nonlinearity can visibly interact with the dispersion, similarly to the balance of dispersion and nonlinearity in a solitary wave. The propagation length of the simulated ultrasonic waves was quite long, as it travelled twice through the 43 mm thickness of the computational model.

In CFRP, which is mechanically highly linear, the nonclassical nonlinear effects could be caused by microdamage or delamination and be in the form of asymmetrical stiffness. The nonclassical nonlinearities could probably be detected in real composite materials at ultrasonic power levels whereas classical nonlinearities are too small to be activated.

3.4 Ultrasonic NDT optimisation by delayed TR-NEWS

In Publication II the physical experiments and FEM simulations of a CFRP block were used to analyse the applicability of delayed TR-NEWS optimisation for ultrasonic NDT problems. The 2D simulations used a linear, undamaged material model, programmed using FEniCS [44] package, applying the implicit Newmark's timestepping algorithm and Dirichlet boundary conditions. Nonlinearities were not introduced, since the CFRP block in these experiments was undamaged, so the simulation was for linear material, for comparison between the experiments and simulations.

The delayed TR-NEWS allows several different optimisation procedures to fine-tune the wave focused by TR in order to either (i) modify the focused wave shape; (ii) amplify the available signal and activate the nonlinearities; (iii) increase the SNR; or (iv) detect the presence of nonlinear effects (considered in Section 3.4.4).

3.4.1 Sidelobe reduction

A typical TR-NEWS focusing contains sidelobes, in addition to the focused signal peak, which in linear and undamaged material should be symmetrical [61]. The sidelobes will always be present due to multiple reflections passing over the signal injection point after the end of the initial signal [16]. The decrease of the sidelobes could allow for increased SNR in applications where just the single delta-peak is needed. This optimisation is based on overlaying the sidelobes of the original TR-NEWS focused signal by the delayed and advanced copies of the signal with matching negative amplitudes to the sidelobe amplitude. This works well, since the frequency of the sidelobe usually matches quite well the main peak. The principle of this operation is illustrated in Fig. 5.

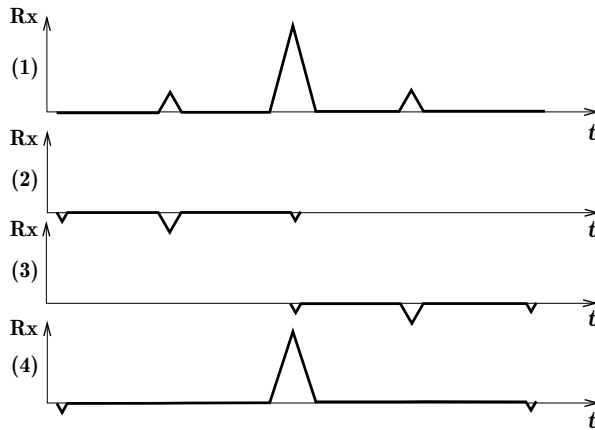


Figure 5 – Scheme of the sidelobe reduction using delayed TR-NEWS: (1) initial y_{TR} focusing with sidelobes (Eq. (4)); (2) and (3) scaled and shifted focusing for eliminating sidelobes; (4) resulting y_{dTR} of adding together signals (1)–(3) with reduced sidelobes and slightly reduced main peak. Figure from Publication II.

A prototype automatic algorithm for finding the necessary amplitude and delay values to decrease the sidelobes of TR-NEWS using this scheme was programmed. Eventually the original and optimised focused signals would look quite the same aside from the decrease of the sidelobes relative to the main peak (Fig. 6).

3.4.2 Amplitude modulation

The most direct application of the delayed TR-NEWS is the use of the impulse signal of the TR-NEWS focused signal as a new basis for amplitude modulation. The time delays τ_i and amplitudes a_i of Eq. (5) can be chosen to create a focused wave with an arbitrary envelope. In Publication II it was shown in experiments (and simulations) that this works well and can be potentially used to modify the focused pulse shape according to the problem or material under testing. Figure 7 shows the creation of sech^2 and \sin envelope pulses.

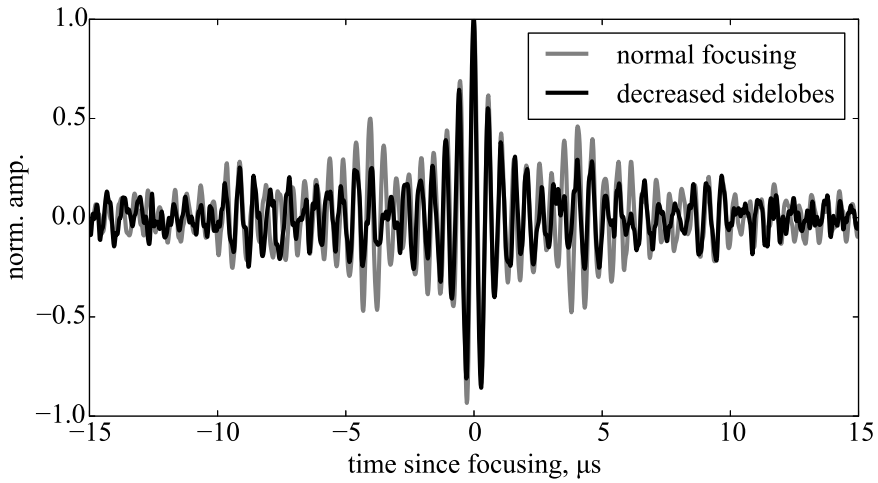


Figure 6 – Delayed TR-NEWS focusing experiment with a CFRP sample. By superpositioning two time-delayed and scaled copies of the focused pulse on the sidelobes, the relative size of the sidelobes can be decreased. Figure from Publication II.

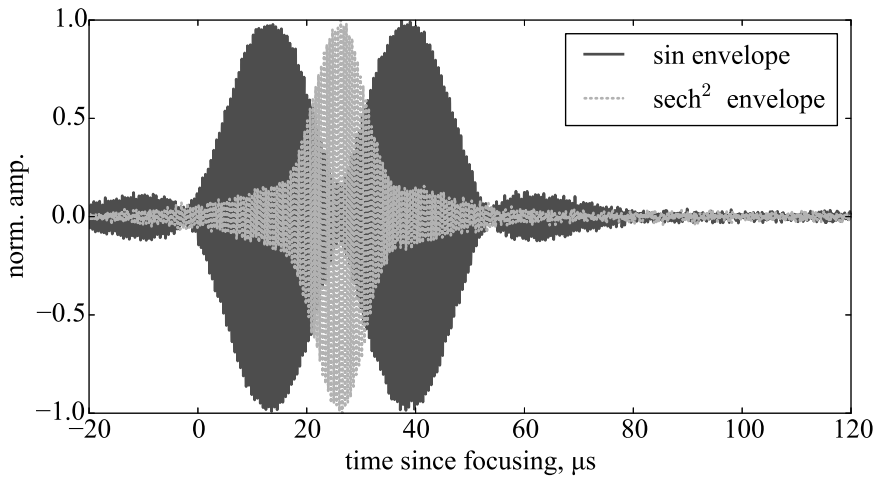


Figure 7 – Delayed TR-NEWS in CFRP for creating a specially shaped envelope at the focusing. Figure from Publication II.

3.4.3 Analysis and modification of spectral content

The spectrum of the TR-NEWS focused signal has been brought into attention from the beginning of this signal processing method, enabling to potentially detect wave mixing in an ergodic medium. The delayed TR-NEWS allows taking a step further in spectral analysis by enabling the introduction of other frequencies into the focusing. Since the focusing can be manipulated directly by the delay values, it is possible to introduce any frequency, limited by transducer, into the focusing region; therefore helping to potentially enhance the wave mixing and its analysis.

3.4.4 Nonlinearity analysis

One of the key findings of this thesis is the possibility of using delayed TR-NEWS to create a wave interaction in the focusing area, which makes it possible to analyse if their interaction follows the linear superposition principle. In Publication II it was found that a slight temporal offset of delayed TR-NEWS focused waves can create an interaction in the spatial focusing region (Fig. 8), which can be compared to its linear superposition prediction (Eq. (6)).

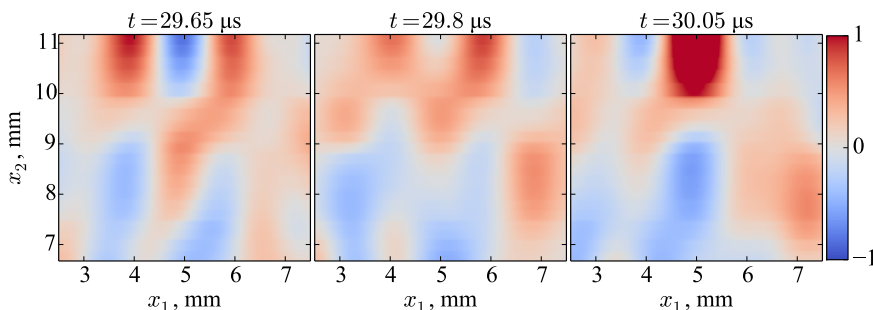


Figure 8 – Wave interaction caused by delayed TR-NEWS with a single delay focusing. Coordinates are denoted by x_1 and x_2 , focusing takes place at $t = 30 \mu\text{s}$. Figure from Publication II.

As a delamination defect, CAN, or some other type of nonlinearity breaks the superposition principle, the defects could be detected by the breakdown of linear superposition. The experiments in Publication II show that in case of an intact material the linear superposition holds surprisingly accurately. However, in case of a nonclassical nonlinearity, the superposition indeed breaks down, as shown in Publication V. This means that the interaction of two focused waves does not equal the sum of these waves.

3.5 Analysis of damage in CFRP

One of the goals of this thesis was to develop a method for detecting defects as sources of nonlinearities in complex materials. It was ascertained that the contact

defect could be detected at ultrasonic power levels. It was proposed in Publication II that delayed TR-NEWS could be used for detecting the nonlinear effects of a defect by creating a wave interaction in the focusing region and then comparing the actual measured results with the prediction relying on linear superposition. This idea was tested in Publication V by simulation, because no CFRP sample having a known and suitable damage was available. The simulations validate the possibility of using delayed TR-NEWS to detect delamination damage and estimate the type and extent of damage. Such damage needs to be introduced in real material for testing by physical experiments.

3.5.1 Simulation model for damage

The simulation model is similar to the one described in Section 3.4. The differences include absorbing boundary conditions on the lower and left sides, so the simulation is in a quarter-infinite space, and a contact crack just under the surface near the TR-NEWS focusing region (Fig. 9). The signal processing utilises two measures of nonlinearity: the established PI method and the novel delayed TR-NEWS (Eq. (5)). The simulation time window is 60 μ s.

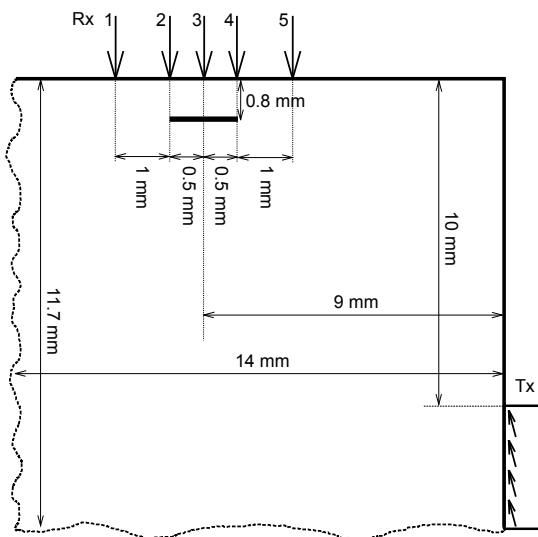


Figure 9 – Schematic of the simulation setup (not to scale) with the transmitting transducer (Tx) position on lower right, receiving transducer (Rx) positions (1–5) on top and the defect just below the Rx position. Figure from Publication V.

A new 2D FEM simulation program was created, written in Fortran and Python using SciPy [33] and F2PY [49] packages. This is a contact problem and therefore has local nonclassical nonlinearity in the form of asymmetric stiffness. Otherwise the material is linear. Contact gap treatment uses penalty plus Lagrange multiplier method for normal contact, with Coulomb friction introduced by the penalty method

for the tangential contact [42, 46]. Due to the sensitivity of contact problems to timestep length, the solution is computed by explicit timestepping method [51, 67].

3.5.2 Results

The delayed TR-NEWS and the established PI methods were compared for their abilities of detecting the nonlinear effect signature. Neither of these methods require a baseline measurement. Firstly, the effect of the recording transducer placement relative to the 1 mm defect was analysed. Secondly, the defect size was incrementally decreased and again comparisons were made between the two methods. In all these measurements, the defect size was sub-wavelength.

The TR-NEWS procedure, used for the PI analysis, creates a spatio-temporal focusing near the receiving transducer. Firstly, the PI nonlinearity detection simulation was conducted for various receiving positions near the 1 mm defect to understand the effect of the distance between the transducer and the defect on the measured nonlinearity. This simulates a nonlinear NDT procedure for finding a near-surface defect by scanning the surface of the object by measuring from several places (positions 1–5 in Fig. 9). Figure 10 shows the corresponding PI results along with the found nonlinearity measure. Position 3 is nearest to the defect, so it contains the strongest PI nonlinearity signal. The nonlinearity is still visible for measurement points near the gap ends (positions 2 and 4). The defect is not detectable by the PI measure on farther points (1 and 5). It must be noted, however, that even for focusing points 1 and 5, the focusing still has asymmetrical sidelobes (in case of undamaged material, the signal is always symmetrical). This symmetry has been in the past used as an indication of damage or nonlinearity [9, 14, 61].

Next, the effect of the defect size on the received signal is analysed. For these simulations the receiving transducer is in the ideal position (position 3), and the crack size is incrementally decreased from 1 mm to 0.034 mm. Figure 11 shows the comparison of the nonlinearity measures. The delay parameters are $a_1 = 1$ and $\tau_1 = 1 \mu\text{s}$ in Eq. (5). Although the delayed TR-NEWS nonlinearity has a larger maximum in case of a 1 mm defect, the advantage disappears as the defect size decreases. They are still relatively comparable. The important difference is that in case of PI, the nonlinearity is mostly in the sidelobe region; conversely, the nonlinearity shown by delayed TR-NEWS is mostly contained in the focusing time region (around $t = 30 \mu\text{s}$), which could make it easier to detect in automated applications. On the other hand, delayed TR-NEWS requires additional input values for the delay time τ_i and amplitude a_i , making PI easier to apply.

The PI and delayed TR-NEWS methods have different measuring durations: PI requires four wave transmissions (two full TR-NEWS measurements), but delayed TR-NEWS only three wave transmissions. Therefore the latter is faster in case of time-sensitive measurement applications.

In Publication V, the main idea that delayed TR-NEWS is able to detect the presence of nonlinear contact gap defect was confirmed. Its nonlinear signature is at

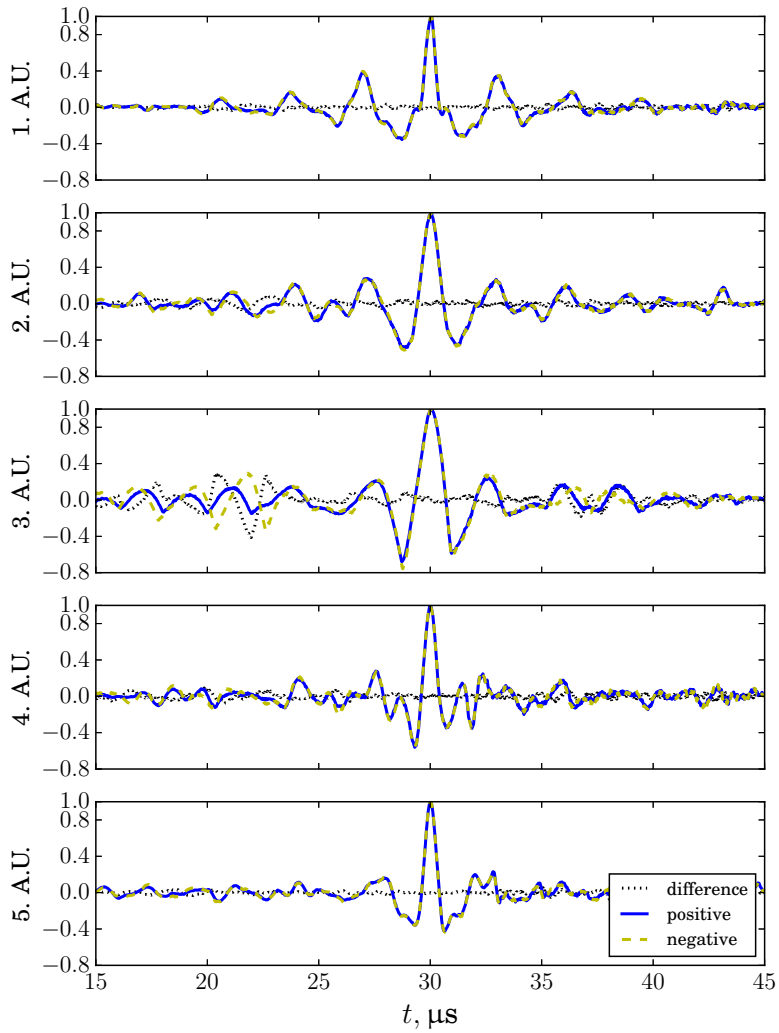


Figure 10 – PI nonlinearity depending on the receiving transducer position near 1 mm defect (A.U. - amplitude units). Figure from Publication V.

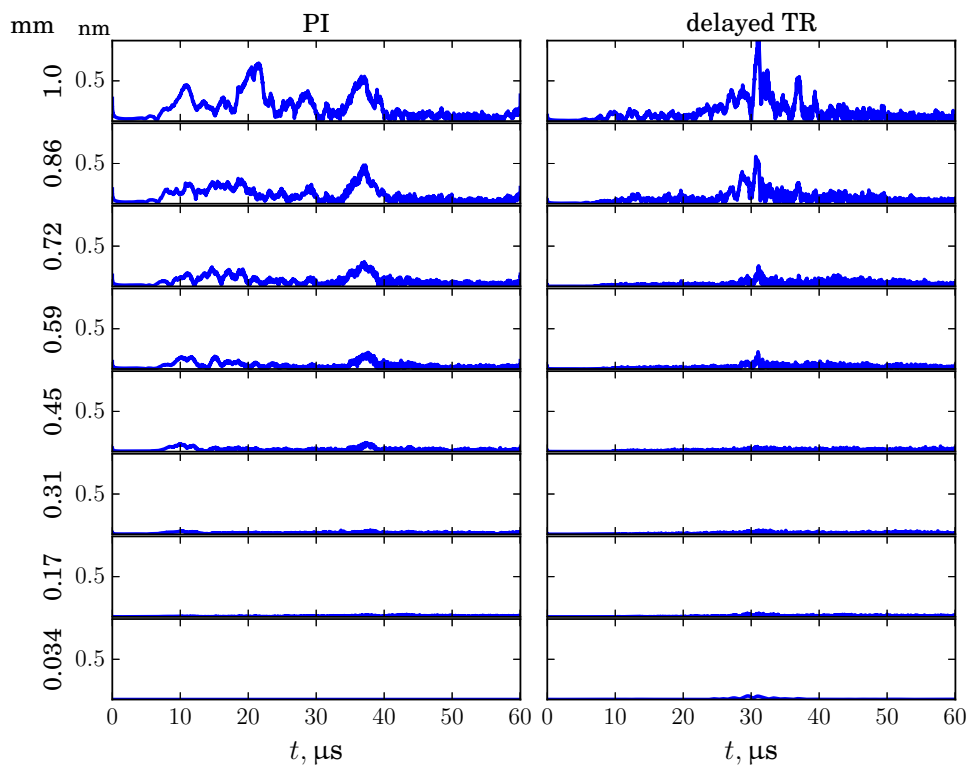


Figure 11 – Comparison of nonlinear signature envelopes in displacement u_2 using PI and delayed TR-NEWS for defect size from 1 mm to 0.034 mm. Figure from Publication V.

least as strong as that from the established PI method. In case of decreasing defect sizes, their ability to detect the damage remained roughly equal. However, there are notable differences between the two methods:

- PI nonlinearity measure appears in the sidelobe region of the focused wave, that of the delayed TR-NEWS near the focusing region;
- PI is robust and does not require any additional parameters, but the delayed TR-NEWS can be optimised and potentially used to excite the defect itself by its resonance frequency;
- PI requires four full transmissions (two transmissions per one TR-NEWS measurement), the delayed TR-NEWS only three full transmissions, which decreases the required total measurement time in time-critical applications, such as measuring viscoelastic materials (skin and other biological tissues) in acoustomechanical testing.

3.6 Summary

It was confirmed by simulations in Publication I that for CFRP it is difficult to characterise the classical nonlinearity in ultrasonic experiments due to too small strain attainable at common ultrasonic power levels, but it might be possible to detect small defects, such as contact gap delaminations, by their nonclassical nonlinear effects. In the course of this work, we arrived at one completely new measure of nonlinear effect, which comes from the delayed TR-NEWS. Simulations and experiments show that for CFRP and possibly other complex materials, this signal processing method can be used for creating a focused signal, enabling introduction of more power into the probed region, increasing SNR, allowing optimisation of the focused wave shape or creation of a close interaction of waves. Additional simulations with a single defect near the focusing region confirm that sub-wavelength defects in fibre reinforced composites and laminate materials can be detected by using delayed TR-NEWS nonlinearity detection. It relies on the possibility of creating an interaction of waves at the TR-NEWS focusing. Since the delayed TR-NEWS has a precise prediction in a linear material, deviation from this linear prediction could be considered as a nonlinear effect.

Résumé

Ce chapitre décrit explicitement la démarche expérimentale et numérique conduite pour améliorer l'imagerie ultrasonore des milieux complexes par une amélioration du principe de retournement temporel non linéaire spécifiquement appliqué au milieu endommagé décrit à partir de nonlinéarités non classiques. Le dispositif expérimental TR-NEWS et les modifications qui ont été apportées dans cette thèse sont renseignés

dans la partie 3.1. Les parties 3.2 et 3.3 sont dédiées aux simulations numériques, et à la description de la nonlinéarité non classique dans les CFRP, respectivement. Ensuite, le cœur du travail de thèse est décrit dans la partie 3.4 au sein de laquelle les avantages de l'excitation TR-NEWS retardée est présentée pour : (i) la réduction des lobes latéraux issus de cette focalisation TR-NEWS ; (ii) la possibilité de modulation d'amplitude du signal focalisé ; (iii) les perspectives d'une optimisation dynamique en temps réel de l'excitation en vue d'une génération d'impulsions solitoniques. Enfin, l'analyse des modifications spectrales induites par la présence de nonlinéarités non classiques est étudiée dans les CFRP d'un point de vue numérique. Il est à nouveau démontré que le principe TR-NEWS permet, via une optimisation d'excitation adaptée, l'extraction de la signature non linéaire de la dégradation locale du milieu à imager.

4 Multiscale characterisation of biological tissues

Ultrasonic medical diagnostics is a large industry, which still uses mostly linear wave propagation principles. Biological tissues are typically viscoelastic, complex, nonlinear, and have memory effects and microstructure [20]. There are many possible benefits in accurate characterisation of the nonlinear properties, such as surgery simulation, disease diagnostics, and research on skin and ageing. The purpose of the acoustomechanical experiments is to measure the multiscale nonlinear mechanical properties of complex biological tissues, for example skin.

The universality of the PM hysteresis for complex materials is discussed in Publication III. The PM hysteresis model [45] is a good choice for modelling complex, nonclassical nonlinear materials, such as skin [11]. Unfortunately, as the model is complex, it is difficult to find parameters for it. Therefore an acoustomechanical setup is needed to fully excite the measured medium and enable exploration of the complete parameter space of the hysteresis model. The PM model requires the material to have self-similarity as a multiscale property and can model nonlinear and viscoelastic properties of the material. The described setup couples the mechanical and acoustic testing by using a mechanical load frame extension and simultaneously conducting ultrasonic delayed TR-NEWS NDT experiments on the test object (skin). The TR-NEWS signal processing method has been previously successfully applied to tooth ageing characterisation and skin sample analysis [14]. In skin, the complete setup with PM space characterisation and TR-NEWS experiments could be used to characterise skin elasticity and ageing [10].

In this section the improvements of measurement equipment and analysis of skin are described in experiments of *ex vivo* porcine skin tissue sample, as described in Publication IV. The test setup must be able to excite the test object in all excitations that the model has to characterise. The tests are synchronised and semi-automated to scan the parameter space of the biological tissue sample. The mechanical and acoustic excitations of the skin make it possible to measure the nonlinear multiscale elastic properties of the skin tissue. The automation allows further optimisation of the parameter search for the elasticity model and consideration of more nonlinear effects (relaxation, viscoelasticity, memory, ageing) than just a single load frame or acoustic test. Statistical distribution of the mechanical properties can be measured.

The constructed acoustomechanical test setup is able to excite the skin sample mechanically, using arbitrary loading, while conducting the delayed TR-NEWS and PI measurements at specified times. The resulting data is sufficient for the characterisation of the PM space and nonlinear effects of the material. Future applications can include developing equipment for *in vivo* skin analysis for the measurement of human skin ageing by measuring its PM space parameters. Moreover, these principles can also be used to analyse other types of materials, as PM hysteresis is universal in multiscale characterisation of complex materials, as shown in Publication III.

4.1 Acoustomechanical experiment setup

In this thesis, the relevant work concerns building and conducting initial tests on synchronised acoustomechanical test setup, suitable for nonlinear property characterisation of ex vivo skin (Fig. 12). The composition of the used ultrasonic test equipment is listed in Section 3.1. The mechanical extension and synchronisation equipment includes

Camera: IDS:

- 1:2.8 50 mm \varnothing 30.5 TAMRON lens, or
- 1:2.8 100 mm Canon macro lens EF USM;

Electromechanical load frame: MTS Criterion model C43;

Load cell: MTS model LPB.502, max 500 N, sensitivity 2.055 mV/V;

Synchronisation pulse extender: GPG-8018G pulse generator;

Synchronisation indicator: LED lamp.

The focus of the work was on creating a prototype test setup, complete with full synchronisation between the mechanical loading and ultrasonic test equipment. The principle of synchronisation is shown in Fig. 13. The actual prototype diverges somewhat from the schematic due to time and equipment constraints, but fulfils the main goal of synchronised automatic multiscale testing of materials.



Figure 12 – Skin sample in the loading machine with ultrasonic transducers attached by a hand clamp. Figure from Publication IV.

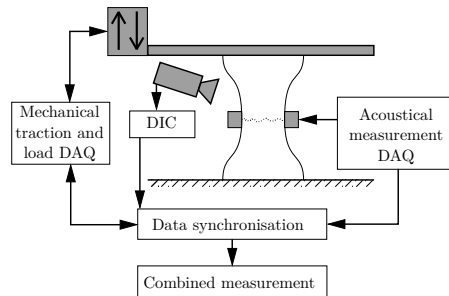


Figure 13 – Acoustomechanical test setup using mechanical and acoustic measurements (DAQ–Data Acquisition, DIC–Digital Image Correlation). Figure from Publication IV.

Because of the constraints of the equipment, the test setup prototype uses a single one-way synchronisation signal from the computer controlling the TR-NEWS equipment to the load frame, read by its independently running computer. The synchronisation is conducted by timestamps, saved in TR-NEWS experiment data file names,

and simultaneously in the data file created by the computer controlling the load frame. The load frame automatically stops the extension movement during the duration of the TR-NEWS test due to the synchronisation signal, because this ultrasonic signal processing requires constant state during the measurement. The synchronisation signal also turns on a LED lamp which is in the view of the camera recording the video for the Digital Image Correlation (DIC) [31], where it can be detected later in video post-processing. The end result is that (i) the extension is stopped for the duration of the TR-NEWS measurement and (ii) the TR-NEWS measurements, load frame data, and extension data from DIC can be fully synchronised.

4.1.1 Digital Image Correlation

Although the load frame can very precisely measure and save the load frame extension and load data, the extension may be insufficient for testing a porcine skin sample. The problem is that, firstly, the skin may be inhomogeneous and therefore the strain field is not necessarily uniform and, secondly, the skin sample might be damaged or slip out of the load frame clamps, in which case the elongation of the test sample does not coincide with the extension of the load frame. Therefore the DIC procedure is used to measure the actual strain field data from the skin test object.

The DIC procedure consists of preparing the material surface with a visible texture that can be used for image correlation, and then recording the video of the material extension. The DIC procedure extracts the strain of the material from the video frame by dividing the region of interest of the image into sections (rectangles) on which image correlation extracts the displacement from the image of the previous frame. In our implementation, the LED indicator lamp signal is also captured by image processing to synchronise the DIC data with the load frame and ultrasonic testing.

Commercial and open-source solutions exist for DIC; however, for flexibility reasons our own DIC procedure was programmed in Python using scikit-image [66] and SciPy [33] packages. The resulting 2D extension data can be highly accurate and also show the relaxation effect of a viscoelastic material, which would remain undetected when only analysing the load frame extension data. The main goal of the accurate strain data is to have precise data for hysteresis. The area of the hysteresis loop describes the energy lost in the extension process and is used for PM space characterisation. Using the DIC strain synchronised with the load data from the load frame results in precise hysteresis data, based on which the material PM space parameter measurement can be conducted.

4.2 Porcine skin test results

The experiments were conducted using the delayed TR-NEWS to detect nonlinearities during the extension and relaxation of the skin sample. A sinusoidal load path with an increasing amplitude and base value was used for mechanical excitation. The

video recording was processed using DIC to reveal the true strain near the ultrasonic measurement area and synchronised using the measurement timestamps and the LED indicator lamp wired to the signal line, visible in the video. Figure 14 shows the test results with the strain from DIC, load frame, and the loading and the synchronisation points. The PM space characterisation is often done based on the hysteresis data, shown in Fig. 15. Synchronisation was conducted during each TR-NEWS measurement. This synchronisation procedure is also required for acquiring accurate hysteresis data loops because of the complex deformation of the skin sample in the load frame and the fluctuating data acquisition rate of the load frame equipment and video camera.

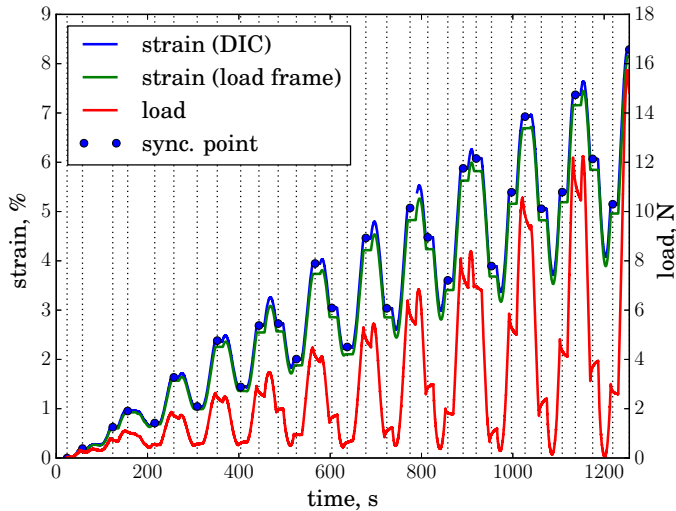


Figure 14 – Synchronised mechanical data from skin sample extension, with TR-NEWS synchronisation points

The skin sample that was used in this test was 200×40 mm rectangle with an average thickness of 3.4 mm and 172 mm initial distance between the clamps. The ultrasonic input chirp excitation was 0–5 MHz. A $0.44 \mu\text{s}$ delay was introduced between the two TR-NEWS peaks to detect the nonlinear effects by the breakdown of the linear superposition prediction.

The delayed TR-NEWS experimental data shows the evolution of nonlinear effects during the loading and relaxing cycles of the skin sample (Fig. 16). The nonlinear effects seem to be on the left side of the focusing ($t = 640 \mu\text{s}$), located near the nulls of the sidelobes of all tests. There is a noticeable and monotonic evolution of lines in the bottom plot of Fig. 16, not dependent on the cyclical movement of the load frame (Fig. 14). This might indicate damage or ageing of the skin sample. This nonlinearity is also noticeably above the noise floor (noise can be seen to the right of the focusing in Fig. 16).

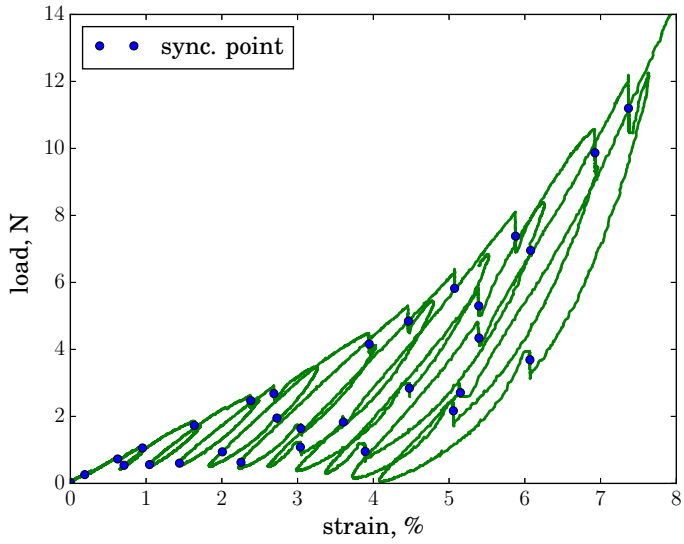


Figure 15 – Hysteresis based on DIC strain data

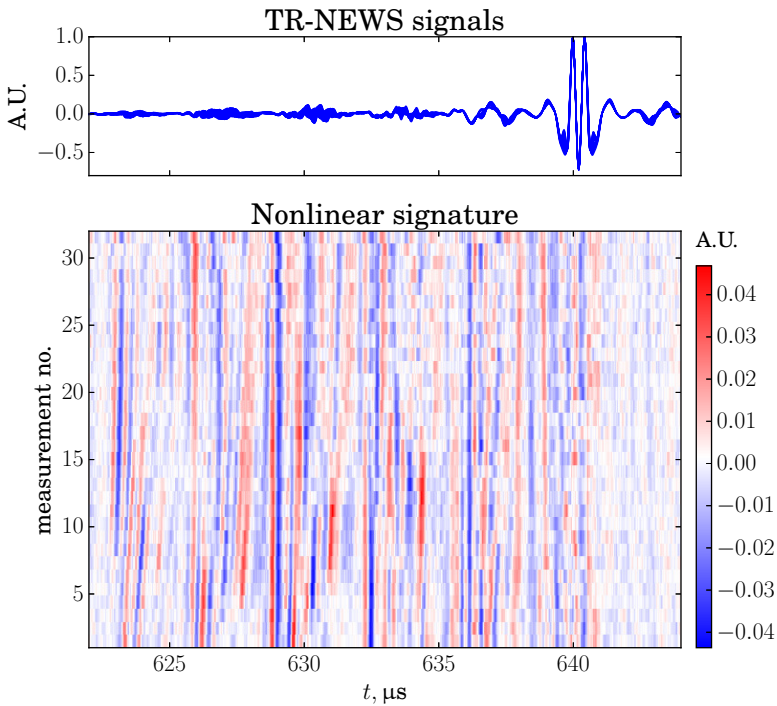


Figure 16 – Top: 32 delayed TR-NEWS signals with two generated peaks. Bottom: the difference between the predicted and measured delayed TR-NEWS wave interaction (nonlinearity). Time $t = 640 \mu\text{s}$ is the initial TR-NEWS focusing time.

4.3 Summary

A specialised test equipment prototype was built, which allows automated multiscale testing of complex, multiscale sheet material, for example ex vivo porcine skin. In our application, the hysteresis of the skin is activated by the quasicyclic quasistatic mechanical extension. At the same time, the ultrasonic delayed TR-NEWS testing is conducted on the material in a crossing plane, which can measure the linear as well as nonlinear effects. Nonlinear effects in the skin sample can come from the memory effects, ageing, or damage of the skin. Further analysis can be conducted by fitting the hysteresis curve data to the PM space model.

- Up to now, the test equipment is a prototype. Given more time, a more user-friendly synchronisation could be developed.
- The delayed TR-NEWS and PI nonlinearity measures for the skin sample are phenomenological. Their cause and applicability to PM space mathematical model and some complex physical models need to be confirmed in additional tests.
- The test equipment could be more specialised, to conserve the CPU workload. At the moment, the data acquisition of the load frame and simultaneous video recording seem to be CPU-intensive, causing fluctuations in load data sampling frequency and video frame rate. This problem is alleviated in post-processing by the precise synchronisation points.

Résumé

Le dernier chapitre traite de la finalité de ce travail dans le domaine de l'imagerie harmonique ultrasonore multi-échelles. Le milieu biologique étudié est la peau porcine et l'objectif est de proposer une caractérisation multi-échelles des propriétés acousto-mécaniques non classiques de la peau humaine. Le dispositif développé dans le cadre du projet régional PLET est présenté en partie 4.1 et les résultats sont interprétés en partie 4.2 et 4.3.

5 Conclusion

This thesis investigates if and how the nonlinear effects of material elasticity can be measured in ultrasonic NDT of complex materials and medical diagnostics of biological tissues. The goal was to find how to detect the nonlinear effects that could indicate material damage and ageing or be used in the characterisation of nonlinear mechanical parameters. The ultrasonic NDT procedures relying on linear wave propagation work well in most materials. However, it can be difficult to apply these procedures in complex materials, such as modern composites or biological tissues, where the material is not necessarily continuous, homogeneous or linearly elastic. Delaminations or microcracking can occur in composite materials; ageing and memory effects in biological tissues. The mechanisms of this type of damage are inherently nonlinear and require nonlinearity analysis.

The analysis of complex industrial and biological materials can be difficult due to the internal structure interfering with the ultrasonic wave motion in the material. One solution to this problem is the reciprocal Time Reversal, as utilised in the TR-NEWS signal processing method. It is highly suitable for complex materials, since it uses the internal reflections of the material as new sources of excitation for creating a focused signal. It enables increasing the SNR by creating a spatio-temporally focused signal pulse in the material.

One of the main results of this thesis was the development of delayed TR-NEWS signal processing method and its validation by simulations and experiments. This new signal processing method has several possible uses in analysis of complex materials and the nonlinear effects on ultrasonic wave propagation:

- creating an interaction of waves at the focusing point,
- detection of nonlinear effects in the focusing region,
- creating a focused signal of an arbitrary envelope,
- sidelobe reduction,
- spectral analysis of the focused signal.

The main results can be summarised as follows:

- The TR-NEWS and delayed TR-NEWS procedures make it possible to analyse the nonlinear effects in various types of complex materials, potentially including teeth, skin, stone, metal, composites, etc. These procedures are particularly suited for complex materials because they can amplify the received signal and improve the SNR.
- In the presence of nonlinear damage, the ultrasonic NDT wavelength can be an order of magnitude larger than the scale of the microstructure and the nonlinear effects will still show the presence of damage.

- For CFRP, any realistic classical material nonlinearity will probably not be detectable at ultrasonic power levels. However, nonclassical nonlinearity (such as that arising from damage and ageing) could potentially be detected even at small power levels of ultrasonics, depending on the type of damage.
- A novel acoustomechanical test setup was created. It can be used to characterise the mechanical properties of various materials that exhibit multiscale properties (such as skin).
- The new signal processing method that was developed in this thesis, the delayed TR-NEWS, can be used for detecting and analysing delamination defects in carbon fibre composites and nonlinearities in biological tissues by the resulting nonlinear effects.

5.1 Perspectives

Application of the results published in this thesis is in the prototype phase and many future improvements are possible. These cover both principal (signal processing, validation, calibration) and procedural (equipment, methods) aspects of the work.

- The results of skin tests will be analysed for fitting with the PM hysteresis model.
- The simulation model could be advanced further. A collection of defects with random angles and sizes could be introduced, or local or global hysteresis nonlinearity could be introduced.
- The (delayed) TR-NEWS experimental setup could be developed further to include several transmitters to increase the available power level at the focusing. A vibrometer could be used instead of the piezoelectric transducer for better broadband response and lack of coupling effects.
- Physical experiments with the delayed TR-NEWS nonlinearity detection should be performed on a CFRP test object with some known damage.
- The acoustomechanical test setup could be improved and optimised to simplify its use and decrease the experiment time.
- The nonlinearity measures should be validated against the defect size of complex media and age of biological tissues.
- New applications using delayed TR-NEWS focusing optimisation can be developed.

Résumé

Les principaux résultats numériques et expérimentaux concernant l'amélioration de la focalisation TR-NEWS est décrite dans la conclusion. Sont mises en exergue les principales avancées ayant conduit à publications dans des revues :

- la possibilité de réduction des lobes latéraux intrinsèques à TR-NEWS,
- la possibilité de création d'une focalisation à enveloppe de forme arbitraire (solitonique, etc.) et contrôlable,
- la possibilité de création d'une interaction d'ondes au point de focalisation via une excitation de type balayage de fréquence compressée,
- la détection localisée d'une signature non linéaire de type non classique dans une région d'étude déterminée (imagerie ultrasonore).

De nombreuses perspectives sont enfin décrites en dernière partie de la conclusion en ouvrant ainsi les nombreuses applications industrielles et médicales potentielles de ce travail de thèse numérique et expérimental.

Abstract

In this thesis the possibility of nonlinear ultrasonic NDT is investigated for complex materials and biological tissues. The delayed TR-NEWS signal processing method is developed, which is based on the TR-NEWS method. TR-NEWS is a method well-suited for materials with complex structure: it allows spatio-temporal focusing of a long ultrasonic chirp signal to the region near the receiving transducer, forming an impulse pulse. The received signal power and SNR are increased as a result. Delayed TR-NEWS allows the use of this focused wave pulse as a new basis for either the signal optimisation or, alternatively, for the detection of nonlinearity by the breakdown of linear superposition. This method is used in physical experiments and simulations. The physical experiments are made on an undamaged CFRP block and a porcine skin sample. The skin is tested in a synchronised acoustomechanical setup specially designed in the course of this thesis.

In 1D pseudospectral simulations for CFRP, it is determined that while classical nonlinearity cannot probably be detected in ultrasonic NDT, it could be possible to detect nonclassical nonlinear effects such as those from cracks and microdamage. Physical experiments and 2D FEM simulations of linear, undamaged CFRP are compared for studying the delayed TR-NEWS method, its applicability in optimising the focused wave, and also for creating an interaction of waves at the focusing region with a linear superposition prediction. This suggests the possibility of detecting nonlinearities by comparing the actual signal from interaction to the linear prediction. Finally, more 2D simulations are conducted for CFRP with a single contact gap nonlinearity near the focusing region. The nonlinearity is measured by PI and delayed TR-NEWS. It is determined that delayed TR-NEWS is able to detect the defect at least as well as the PI method. It is ascertained that the PM hysteresis model could describe the nonclassical nonlinearity of damaged materials and biological tissues. A synchronised acoustomechanical test setup is created to test such multiscale nonlinearity. The simultaneous mechanical load test and ultrasonic delayed TR-NEWS test can be used to measure the mechanical properties of skin.

Kokkuvõte

Selles töös uuritakse ultrahelil põhinevat mittepurustavat testimist komplekssete materjalide ja bioloogiliste kudede jaoks. Välja on arendatud hilistunud ajalisel ümberpöördel põhinev mittelineaarse elastsuslaine spektroskoopia (*delayed TR-NEWS*). Senituntud ajaline ümberpööre koos mittelineaarse elastsuslaine spektroskoopiaga on sobilik keeruka struktuuriga materjalide testimiseks, kuna kasutab pikka algset signaali, mis ajalise ümberpöörde ja signaali kokkusurumise abil fokuseeritakse vastuvõtva sensori lähedusse, tekitades ajas ja ruumis fokuseeritud pulsi. Selle tulemuseks suureneb signaali võimsus ja signaali-müra suhe. Hilistunud ajaline ümberpööre kasutab seda fokuseeritud pulssi uue baasina, et optimeerida fokuseeritud laine kuhu või tuvastada mittelineaarseid efekte (lineaarse superpositsiooni nurjumise näol). Seda signaalitöötlust kasutatakse füüsikalistes eksperimentides ja simulatsioonides. Füüsikalised eksperimendid on tehtud süsinikkiudkomposiidiga ja seanahaga. Naha katsete jaoks on koostatud sünkroniseeritud akustomehaaniline katseseade.

1D pseudospektraalsed simulatsioonid süsinikkiudkomposiidis näitavad, et kui klassikaline mittelineaarsus jääb tõenäoliselt tuvastamatuks, siis mitteklassikaline mittelineaarsus, näiteks tulenevalt pragudest ja mikrokahjustustest, võiks olla tuvastatav ka ultrahelil põhinevas mittepurustavas testimises. Võrreldakse eksperimente ja 2D lõplike elementide meetodi simulatsioone lineaarses ja kahjustamata süsinikkiudkomposiidis, tuvastamaks hilistunud ajalise ümberpöörde kasutusvõimalusi fokuseeritud signaali optimeerimiseks ja mittelineaarsuste tuvastamiseks koos lineaarse prognoosiga. Tulemused näitavad, et mittelineaarsusi võiks tuvastada võrreldes tegelike mõõtmistulemusi lineaarse superpositsiooni prognoosiga. Lõpuks analüüsitakse 2D simulatsioone materjalil, kus on üks kontaktiga pragu, mis on mittelineaarsuse allikaks. Mittelineaarsust mõõdetakse pulsi inversiooniga ja hilistunud ajalise ümberpöördega. Tuvastatakse, et need meetodid annavad võrreldava tugevusega mittelineaarse signaali. On kindlaks tehtud, et Preisach–Mayergoyzi hüstereesi mudel on sobilik mitteklassikalise mittelineaarsuse modelleerimiseks kahjustunud materjalides ja bioloogilistes kudedes. Sünkroniseeritud akustomehaanilist katseseadet kasutatakse sellise mitmemastaapse mittelineaarsuse testimiseks. Seanahaga tehtud katses tekitatakse üheaegselt suuri deformatsioone mehaanilise tõmbemasinaga ja väikseid deformatsioone ultraheli mittepurustava testimise seadmega. See võimaldab mõõta naha mehaanilisi omadusi, sealhulgas mittelineaarsust, hüstereesi, vananemist ja mälu efekte.

Résumé de la thèse

Dans ce travail de thèse, une innovation est présentée et validée dans le domaine du contrôle non destructif (CND) des matériaux complexes et des tissus biologiques. L'innovation TR-NEWS retardée est ici définie comme une extension de la méthode TR-NEWS, issue de la symbiose entre le retournement temporel (RT) et les méthodes de spectroscopie d'ondes élastiques non linéaires (NEWS). Dans un premier temps, nous confirmons les très bonnes performances des méthodes TR-NEWS pour la caractérisation des matériaux dotés de structures complexes : elles permettent en outre de focaliser un signal ultrasonore codé par balayage de fréquence (étendu spatio-temporellement) sur une région proche du transducteur ultrasonore de réception, formant ainsi une impulsion aux propriétés de symétrie exploitables, et aux performances remarquables en terme de puissance acoustique et de rapport signal sur bruit (SNR). L'ajout d'un protocole d'excitation induisant le concept de "TR-NEWS retardée" permet de constituer une nouvelle base de signaux propres aux propriétés acoustiques focalisées. En utilisant la brisure de symétrie introduite par la non vérification du principe de superposition induite par la nonlinéarité locale, cette optimisation de l'excitation permet une détection et une extraction de la signature non linéaire, validée par des simulations numériques et de nombreuses expérimentations. Les validations expérimentales ont été conduites conformément au projet initial ; valider l'approche dans les deux domaines du CND et de l'imagerie médicale ultrasonore. Les tests ont été conduits sur des échantillons de composite CFRP dotés de propriétés dispersives ultrasonores, favorisant ainsi la réverbérabilité de la propagation acoustique. La deuxième validation a été conduite dans le cadre du projet PLET (Propriétés Locales Visco-Elastiques de la peau par TR-NEWS) financé par la Région Centre Val de Loire dont le but était de proposer une instrumentation multi-échelles acousto-mécanique de mesures de propriétés non classiques de la peau porcine en extension uniaxiale, spécifiquement réalisée dans le cadre de cette thèse.

Via les simulations numériques 1D pseudospectrales de propagations acoustiques non linéaires dans les CFRP, et même si il est vérifié que la nonlinéarité classique globale ne peut être détectée par CND non linéaires, il est néanmoins possible d'identifier et de localiser les sources locales de défauts et de micro-endommagement. Les expérimentations physiques et les simulations 2D par méthodes d'éléments finis (FEM) ont été conduites pour valider le concept TR-NEWS retardé, son applicabilité pour optimiser la focalisation acoustique et son potentiel quant à la possibilité de créer une interaction d'ondes localisée dans la zone de focalisation. Cette innovation suggère la possibilité de détecter des signatures non linéaires par comparaison entre la réponse réelle du milieu exploré par l'expérience et la prédiction théorique sous hypothèse d'un comportement linéaire. Finalement, pour les CFRP, de nombreuses simulations valident l'identification d'un crack unique proche de la zone de focalisation. La nonlinéarité supposée de type contact acoustique (CAN) est mesurée par TR-NEWS retardée et comparée aux techniques classiques d'inversion d'impulsion utilisée en

imagerie médicale.

Il est ainsi démontré que la méthode “TR-NEWS retardée” permet une identification au moins aussi performante que l’inversion d’impulsion, aussi rapide et préservant la représentation dans le domaine temporel. Pour ce qui concerne la validation sur tissus biologiques, le système de synchronisation acousto-mécanique développé permet d’envisager la mesure de paramètres multi-échelles de nonlinéarité des tissus biologiques au travers de paramètres de Preisach–Mayergoyz (espaces PM) permettant ainsi de décrire le vieillissement des tissus biologiques. Le chargement basse fréquence uniaxial effectué simultanément aux investigations ultrasonores haute fréquence via TR-NEWS retardé suggère d’envisager une nouvelle classe de dispositifs avec une perspective de multimodalité dédiée à l’imagerie ultrasonore non invasive des propriétés biomécaniques des organismes vivants.

References

- [1] V. Aleshin and K. Van Den Abeele. Micro-potential model for acoustical hysteresis. In *Proceedings of the 18th International Congress on Acoustics*, volume 3, pages 1859–1862, 2004.
- [2] A. S. Birks, R. E. Green, and P. McIntire. *Nondestructive Testing Handbook*. American Society for Nondestructive Testing, 1991.
- [3] P. Blanloeuil, L. R. F. Rose, J. A. Guinto, M. Veidt, and C. H. Wang. Closed crack imaging using time reversal method based on fundamental and second harmonic scattering. *Wave Motion*, 66:156–176, 2016.
- [4] D. Broda, W. J. Staszewski, A. Martowicz, T. Uhl, and V. V. Silberschmidt. Modelling of nonlinear crack-wave interactions for damage detection based on ultrasound – A review. *J. Sound Vibration*, 333:1097–1118, 2014.
- [5] C. Bruno, A. Gliozzi, M. Scalerandi, and P. Antonaci. Analysis of elastic nonlinearity using the scaling subtraction method. *Phys. Rev. B*, 79(6):064108, 2009.
- [6] F. Ciampa and M. Meo. Nonlinear elastic imaging using reciprocal time reversal and third order symmetry analysis. *J. Acoust. Soc. Am.*, 131(6):4316–4323, 2012.
- [7] P. P. Delsanto, editor. *Universality of Nonclassical Nonlinearity: Applications to Non-Destructive Evaluations and Ultrasonics*. Springer, 2006.
- [8] S. Dos Santos, S. Amami, Š. Vejvodová, and Z. Převorovský. Symmetry analysis signal processing for local nonlinear scatterers signature of complex materials structural integrity. In *Proceedings of the 10th ECNDT*, Moscow, 2010.
- [9] S. Dos Santos, B. Choi, A. Sutin, and A. Sarvazyan. Nonlinear imaging based on time reversal acoustic focusing. In *Proc. of the 8ème Congrès Français d’Acoustique*, pages 359–362, 2006.
- [10] S. Dos Santos, Z. Dvořáková, M. Caliez, and Z. Převorovský. Nonlinear time reversal signal processing techniques applied to acousto-mechanical imaging of complex materials. *J. Acoust. Soc. Am.*, 138(3):1835–1835, 2015.
- [11] S. Dos Santos, V. Kůs, D. Remache, J. Pittet, M. Gratton, and M. Caliez. Memory effects in the biomechanical behavior of ex vivo skin under acoustomechanical testings: a multiscale Preisach modeling of aging. In *Proceedings of the 23rd International Congress on Sound & Vibration*, 2016.

- [12] S. Dos Santos, M. Lints, N. Poirot, Z. Farová, A. Salupere, M. Caliez, and Z. Převorovský. Nonlinear Time Reversal for Non Destructive Testing of complex medium : a review based on multi-physics experiments and signal processing strategies. In P. Mazal, editor, *NDT in Progress 2015 - 8th International Workshop of NDT Experts, Proceedings*, pages 31–40. Brno University of Technology, October 2015.
- [13] S. Dos Santos and C. Plag. Excitation symmetry analysis method (ESAM) for calculation of higher order non-linearities. *Int. J. Non-Linear. Mech.*, 43:164 – 169, 2008.
- [14] S. Dos Santos and Z. Převorovský. Imaging of human tooth using ultrasound based chirp-coded nonlinear time reversal acoustics. *Ultrasonics*, 51(6):667–674, 2011.
- [15] S. Dos Santos, S. Vejvodová, and Z. Převorovský. Nonlinear signal processing for ultrasonic imaging of material complexity. *Proc. Estonian Acad. Sci.*, 59(2):108–117, 2010.
- [16] C. Draeger and M. Fink. One-Channel Time Reversal of Elastic Waves in a Chaotic 2D-Silicon Cavity. *Phys. Rev. Lett.*, 79:407–410, Jul 1997.
- [17] E. C. Farnett and G. H. Stevens. Pulse Compression Radar. In M. I. Skolnik, editor, *Radar handbook*, volume 2. McGraw-Hill, 1990.
- [18] M. Fehler and H. Sato. Coda. *Pure Appl. Geophys.*, 160(3):541–554, 2003.
- [19] M. Fink. Time Reversal of Ultrasonic Fields - Part I: Basic Principles. *IEEE Trans. Ultrason., Ferroelect., Freq. Control*, 39(5):555–566, 1992.
- [20] Y. C. Fung. *Biomechanics: Mechanical Properties of Living Tissues*. Springer-Verlag, 1993.
- [21] D. Givoli. Time Reversal as a Computational Tool in Acoustics and Elastodynamics. *J. Comput. Acoust.*, 22(03):1430001, Sept. 2014.
- [22] T. Goursolle, S. Dos Santos, O. Bou Matar, and S. Callé. Non-linear based time reversal acoustic applied to crack detection: Simulations and experiments. *Int. J. Non-Linear. Mech.*, 43(3):170 – 177, 2008. 11th International Workshop on Nonlinear Elasticity in Materials.
- [23] A. Granato and K. Lücker. Theory of mechanical damping due to dislocations. *J. Appl. Phys.*, 27:583–593, 1956.
- [24] M. Griffa, B. E. Anderson, R. A. Guyer, T. J. Ulrich, and P. A. Johnson. Investigation of the robustness of time reversal acoustics in solid media through

- the reconstruction of temporally symmetric sources. *J. Phys. D: Appl. Phys.*, 41(8):085415, 2008.
- [25] P.-Y. Guerder, S. Giordano, O. Bou Matar, and J. O. Vasseur. Tuning the elastic nonlinearities in composite nanomaterials. *J. Phys. Condens. Matter*, 27(14):145304, 2015.
- [26] X. Guo, D. Zhang, and J. Zhang. Detection of fatigue-induced micro-cracks in a pipe by using time-reversed nonlinear guided waves: A three-dimensional model study. *Ultrasonics*, 52(7):912–919, 2012.
- [27] R. A. Guyer and P. A. Johnson. *Nonlinear Mesoscopic Elasticity: The Complex Behaviour of Granular Media including Rocks and Soil*. WILEY-VCH, 2009.
- [28] R. A. Guyer, K. R. McCall, and G. N. Boitnott. Hysteresis, Discrete Memory, and Nonlinear Wave Propagation in Rock: A New Paradigm. *Phys. Rev. Lett.*, 74:3491–3494, 1995.
- [29] R. A. Guyer, K. R. McCall, G. N. Boitnott, L. B. Hilbert, and T. J. Plona. Quantitative implementation of Preisach-Mayergoyz space to find static and dynamic elastic moduli in rock. *J. Geophys. Res. Solid Earth*, 102(B3):5281–5293, 1997.
- [30] K. Helbig and P. N. J. Rasolofosaon. A Theoretical Paradigm for Describing Hysteresis and Nonlinear Elasticity in Arbitrary Anisotropic Rocks. In *Anisotropy 2000*, pages 383–398. Society of Exploration Geophysicists, 2001.
- [31] F. Hild and S. Roux. Digital Image Correlation: from Displacement Measurement to Identification of Elastic Properties – a Review. *Strain*, 42(2):69–80, 2006.
- [32] K.-Y. Jhang. Nonlinear ultrasonic techniques for nondestructive assessment of micro damage in material: A review. *Int. J. Precis. Eng. Manuf.*, 10(1):123–135, Jan 2009.
- [33] E. Jones, T. Oliphant, P. Peterson, et al. SciPy: Open source scientific tools for Python, 2001–.
- [34] J. Kober and Z. Převorovský. Theoretical investigation of nonlinear ultrasonic wave modulation spectroscopy at crack interface. *NDT & E International*, 61:10–15, 2014.
- [35] C. Kožená, V. Kůs, and S. Dos Santos. Hysteresis and memory effects in skin aging using PM space density identification. In *2016 15th Biennial Baltic Electronics Conference (BEC)*, pages 179–182, 2016.

- [36] L. D. Landau and E. M. Lifshitz. *Theory of Elasticity*, volume 7 of Course of Theoretical Physics. Pergamon Press, second revised and enlarged edition, 1970.
- [37] T. H. Lee and K. Y. Jhang. Experimental investigation of nonlinear acoustic effect at crack. *NDT&E International*, 42:757–764, 2009.
- [38] M. Levy, H. E. Bass, and R. Stern, editors. *Modern Acoustical Techniques for the Measurement of Mechanical Properties*. Academic Press, 2001.
- [39] M. Lints, S. Dos Santos, C. Kožená, V. Kůs, and A. Salupere. Fully synchronized acoustomechanical testing of skin: biomechanical measurements of non-classical nonlinear parameters. In *24th International Congress on Sound and Vibration, 23–27 July, 2017, London*, number 867. ICSV, International Institute of Acoustics and Vibrations, 2017.
- [40] M. Lints, S. Dos Santos, and A. Salupere. Solitary Waves for Non-Destructive Testing Applications: Delayed Nonlinear Time Reversal Signal Processing Optimization. *Wave Motion*, 71:101–112, 2017.
<http://dx.doi.org/10.1016/j.wavemoti.2016.07.001>.
- [41] M. Lints, A. Salupere, and S. Dos Santos. Simulation of solitary wave propagation in carbon fibre reinforced polymer. *Proc. Estonian Acad. Sci.*, 64(3):297–303, 2015.
- [42] M. Lints, A. Salupere, and S. Dos Santos. Simulation of defects in CFRP and delayed TR-NEWS analysis. Research Report Mech 320/17, Tallinn University of Technology, Department of Cybernetics, 2017.
- [43] M. Lints, A. Salupere, and S. Dos Santos. Simulation of detecting contact nonlinearity in carbon fibre polymer using ultrasonic nonlinear delayed time reversal. *Acta Acust. united Ac.*, 2017. (accepted).
- [44] A. Logg, K.-A. Mardal, and G. Wells, editors. *Automated Solution of Differential Equations by the Finite Element Method: The FEniCS Book (Lecture Notes in Computational Science and Engineering)*. Springer, 2012.
- [45] I. D. Mayergoyz. *Mathematical Models of Hysteresis and Their Applications*. Elsevier, 2003.
- [46] A. R. Mijar and J. S. Arora. An augmented Lagrangian optimization method for contact analysis problems, 1: formulation and algorithm. *Struct. Multidisc. Optim.*, 28:99–112, 2004.
- [47] M. Miniaci, A. S. Gliozzi, B. Morvan, A. Krushynska, F. Bosia, M. Scalerandi, and N. M. Pugno. Proof of Concept for an Ultrasensitive Technique to Detect

- and Localize Sources of Elastic Nonlinearity Using Phononic Crystals. *Phys. Rev. Lett.*, 118:214301, 2017.
- [48] L. Pan, L. Zan, and F. Foster. Ultrasonic and viscoelastic properties of skin under transverse mechanical stress in vitro. *Ultrasound Med. Biol.*, 24(7):995–1007, 1998.
- [49] P. Peterson. F2PY: a tool for connecting Fortran and Python programs. *Int. J. Comp. Sci. Eng.*, 4(4), 2009.
- [50] W. H. Prosser. Ultrasonic Characterization of the Nonlinear Elastic Properties of Unidirectional Graphite/Epoxy Composites. Technical report, NASA, 1987.
- [51] J. N. Reddy. *An Introduction to the Finite Element Method*. McGraw-Hill, 2006.
- [52] J. Riviere, S. Hauptert, P. Laugier, T. Ulrich, P.-Y. Le Bas, and P. A. Johnson. Time reversed elastic nonlinearity diagnostic applied to mock osseointegration monitoring applying two experimental models. *J. Acoust. Soc. Am.*, 131(3):1922–1927, 2012.
- [53] A. Salupere, M. Lints, and J. Engelbrecht. On solitons in media modelled by the hierarchical KdV equation. *Arch. Appl. Mech.*, 84:1583–1593, 2014.
- [54] M. Scalerandi, V. Agostini, P. P. Delsanto, K. Van Den Abeele, and P. A. Johnson. Local interaction simulation approach to modelling nonclassical, nonlinear elastic behavior in solids. *J. Acoust. Soc. Am.*, 113(6):3049–3059, 2003.
- [55] M. Scalerandi, A. S. Gliozzi, C. L. Bruno, and K. Van Den Abeele. Nonlinear acoustic time reversal imaging using the scaling subtraction method. *J. Phys. D: Appl. Phys.*, 41(21):215404, 2008.
- [56] I. Y. Solodov and B. A. Korshak. Instability, Chaos, and “Memory” in Acoustic-Wave–Crack Interaction. *Phys. Rev. Lett.*, 88(1), 2001.
- [57] I. Y. Solodov, N. Krohn, and G. Busse. CAN: an example of nonclassical acoustic nonlinearity in solids. *Ultrasonics*, 40(1):621–625, 2002.
- [58] A. Sutin, P. Johnson, and J. TenCate. Development of nonlinear time reversed acoustics (NLTRA) for applications to crack detection in solids. In *Proc. of the World Congress of Ultrasonics*, pages 121–124, Sept. 2003.
- [59] A. M. Sutin, J. A. TenCate, and P. A. Johnson. Single-channel time reversal in elastic solids. *J. Acoust. Soc. Am.*, 116(5):2779–2784, 2004.
- [60] M. Tanter, J. L. Thomas, F. Coulouvrat, and M. Fink. Breaking of time reversal invariance in nonlinear acoustics. *Phys. Rev. E*, 64(016602), 2001.

- [61] T. Ulrich, M. Griffa, and B. Anderson. Symmetry-based imaging condition in time reversed acoustics. *J. Appl. Phys.*, 104(6):064912, 2008.
- [62] T. J. Ulrich, P. A. Johnson, and A. Sutin. Imaging nonlinear scatterers applying the time reversal mirror. *J. Acoust. Soc. Am.*, 119(3):1514–1518, 2006.
- [63] T. J. Ulrich, A. M. Sutin, R. A. Guyer, and P. A. Johnson. Time reversal and non-linear elastic wave spectroscopy (TR NEWS) techniques. *Int. J. Non-Linear Mech.*, 43(3):209–216, 2008.
- [64] K. E.-A. Van Den Abeele, J. Carmeliet, J. A. TenCate, and P. A. Johnson. Nonlinear Elastic Wave Spectroscopy (NEWS) Techniques to Discern Material Damage, Part II: Single-Mode Nonlinear Resonance Acoustic Spectroscopy. *Res. Nondestr. Eval.*, 12:31–42, 2000.
- [65] K. E.-A. Van Den Abeele, P. A. Johnson, and A. Sutin. Nonlinear Elastic Wave Spectroscopy (NEWS) Techniques to Discern Material Damage, Part I: Nonlinear Wave Modulation Spectroscopy (NWMS). *Res. Nondestr. Eval.*, 12:17–30, 2000.
- [66] S. van der Walt, J. L. Schönberger, J. Nunez-Iglesias, F. Boulogne, J. D. Warner, N. Yager, E. Guillard, T. Yu, and the scikit-image contributors. scikit-image: image processing in Python. *PeerJ*, 2:e453, 6 2014.
- [67] D. Xu and K. D. Hjelmstad. A New Node-to-Node Approach to Contact/Impact Problems for Two-Dimensional Elastic Solids Subject to Finite Deformation. Technical report, Newmark Structural Engineering Laboratory of Department of Civil and Environmental Engineering at the University of Illinois at Urbana-Champaign, May 2008.

Appendix A: Publications

Publication I

M. Lints, A. Salupere, and S. Dos Santos. Simulation of solitary wave propagation in carbon fibre reinforced polymer. *Proc. Estonian Acad. Sci.*, 64(3):297–303, 2015



Simulation of solitary wave propagation in carbon fibre reinforced polymer

Martin Lints^{a,b*}, Andrus Salupere^a, and Serge Dos Santos^b

^a CENS, Institute of Cybernetics at Tallinn University of Technology, Akadeemia tee 21, 12618 Tallinn, Estonia

^b INSA Centre Val de Loire, Blois Campus, 3 Rue de la Chocolaterie, CS 23410, F-41034 Blois Cedex, France

Received 17 December 2014, accepted 29 July 2015, available online 20 August 2015

Abstract. The emergence and propagation of solitary waves is investigated for carbon fibre reinforced polymer using numerical simulations for Non-Destructive Testing (NDT) purposes. The simulations are done with the Chebyshev collocation method. The simplest laminate model is used for the periodical structure of the material from which dispersion will arise. Classical and nonclassical nonlinearities are introduced in the constitutive equation. The balance of the dispersion and nonlinearity is analysed by studying the shape-changing effects of the medium on the initial input pulse and the possibility of solitary wave propagation is considered. Future applications of solitary waves for nonlinear medical imaging and NDT of materials are discussed.

Key words: CFRP, solitary waves, Non-Destructive Testing, TR–NEWS, nonlinearity, dispersion.

1. INTRODUCTION

The recent ten years have seen considerable development of optimized signal processing methods for improving nonlinear Non-Destructive Testing (NDT) methods derived from Nonlinear Elastic Wave Spectroscopy (NEWS) and supplemented by symmetry invariance and Time Reversal (TR). The emerging TR–NEWS method is a useful tool for microcracks detection of various complex samples [1], but also recently for the localization of nonlinear scatterers in a wide sense [2]. TR–NEWS signal processing is performed with symmetrization of coded excitation using cross-correlation, pulse-inversion [3], or chirp-coded schemes, which are promising alternatives to frequency coding. The response to positive and negative excitations enables to extract the nonlinear signature of the tested sample.

In materials with nonlinear and dispersive properties, solitary waves could be used for NDT [4,5]. They are stable in propagation and have elastic interactions due to the balance between the nonlinearity and dispersion. This robustness could improve the monitoring capabilities of layered, granular, or functionally graded materials. It is well known that in such a medium, dispersion and nonlinearity could be combined in a way that solitonic

propagation could be observed. The dispersion can be caused by the material microstructure [6] or layers [7,8], and the nonlinearity by the microdamage or soft inclusions [9]. Using solitonic excitation, a medium with these properties could be analysed. The solitary waves can experience a phenomenon called ‘selection’ where the amplitude and velocity of a solitary wave tend to finite values, which depend on the nonlinearity and dispersion [10–12]. In some microstructured models, the solitary wave propagation can also be sensitive to the ratio of macro- and microstructural dispersions and a general ‘shape’ of the initial profile [13], which could likewise be used for diagnostic purposes.

Carbon Fibre Reinforced Polymers (CFRPs) are being increasingly used for applications requiring both a high strength to weight ratio and reliability, for example in aerospace, automotive, and naval industries. Therefore demand for the robustness of NDT of layered composites is rising. The material is geometrically complex and has several micro-scales: firstly, the scale of individual carbon fibres that make up a single yarn; secondly, the scale of individual yarns from which the fabric is woven; and finally in 2D or 3D cases, the scale of individual layers (carbon fabric and polymer). This makes the use of conventional NDT techniques difficult, which is why

* Corresponding author, martin.lints@cens.ioc.ee

this work analyses the potential use of solitary waves for testing a material with nonclassical nonlinearities at multiscale level. In this work the plies of the composite are regarded as homogeneous orthotropic materials. This multiscale complexity also justifies the use of methods such as TR-NEWS because they have shown extreme efficiency in complex media, such as composites and biological tissues.

The numerical simulations are done by the Chebyshev collocation method with Chebyshev polynomials used for approximating physical quantities and finding the spatial derivatives. The simulations take into account the layered character of the material and are performed for a 144 layered CFRP test sample. In addition to the dispersion arising from the layered configuration, the material is assumed to be weakly nonlinear. The goal is to determine the influence of nonlinearity on the character of the propagating waves. The main attention is paid to the formation of solitary waves. The conditions for the emergence of a solitary wave and its propagating characteristics are analysed for future use in physical experiments.

This paper is presented as follows. Firstly, the model of the CFRP material is described, the classical and nonclassical nonlinearities are introduced into the governing equations, and the key points about the numerical method are described. Secondly, the simulation results are presented and then analysed for the effect of a small but global nonclassical nonlinearity.

2. MODEL

The modelled material is a CFRP block with a thickness of 43 mm, consisting of 144 layers (Fig. 1). It is composed of fabric woven from yarns of fibre and impregnated with epoxy. The cross-section of the yarns is of elliptical shape (Fig. 2) and the material has inclusions of pure epoxy, so a wave propagating through the material will encounter yarns (fibres with epoxy) and areas of pure epoxy. The simplest material model for the test object is the laminate model (Fig. 3) in which (i) the

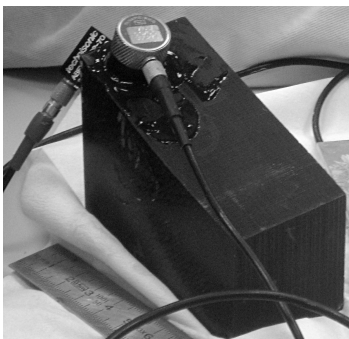


Fig. 1. Carbon Fibre Reinforced Polymer (CFRP) block of 144 layers tested with ultrasonic of NDT.

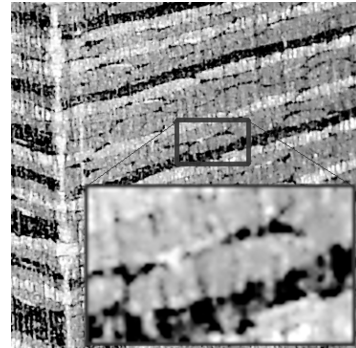


Fig. 2. Close-up image of the structure of the test object.

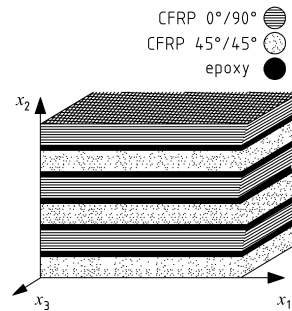


Fig. 3. Material model of the CFRP block.

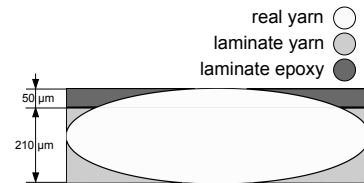


Fig. 4. The material is modelled as a laminate, with the thickness of individual laminae proportional to the cross-sectional area of the material.

material consists of homogeneous layers, (ii) each layer has its own elasticity properties, and (iii) dispersion arises due to the periodical discontinuity of the properties. The widths of the layers are proportional to the area of the cross-section of the yarn (Fig. 4) and are here modelled as laminates of constant thickness (thickness $h_e = 50 \mu\text{m}$ for the epoxy layer and $h_{\text{CFRP}} = 210 \mu\text{m}$ for the pure CFRP layer). The longitudinal wave modulus for the epoxy layer $E_e = 6.5 \text{ GPa}$ and for the CFRP layer $E_{\text{CFRP}} = 13.6 \text{ GPa}$.

2.1. Mathematical model

The deformations are assumed to be small: $\epsilon_{kl} = \frac{1}{2} (u_{k,l} + u_{l,k})$. The Cauchy’s equations governing the

wave motion in each piecewise continuous layer are

$$\begin{cases} \sigma_{kl,k} + \rho \ddot{u}_l = 0, \\ \sigma_{kl} = \sigma_{lk}. \end{cases} \quad (1)$$

The constitutive equation is

$$\sigma = \alpha E (\varepsilon - \beta \varepsilon^2). \quad (2)$$

In the above equations σ denotes stress, ε denotes strain, u denotes displacement, ρ is the density of the material, and E is the modulus of elasticity. The Einstein's summation convention is used. An index after a comma denotes a derivative in that direction. Weak classical nonlinearity is given by β and nonclassical nonlinearity by α . Here the nonclassical nonlinearity means that the material can have an abrupt change in the elasticity modulus (in this work on $\varepsilon = 0$). This permits strong nonlinear effects in cases of small strain. Nonclassical nonlinearity parameter α allows the material to be weaker in tension than in compression [14]: $\alpha \leq 1$ if $\varepsilon \geq 0$ and $\alpha = 1$ always if $\varepsilon < 0$. There is no nonclassical nonlinearity if $\alpha = 1$ for all ε . In order to use the pulse-inversion method [3], dynamic boundary conditions with both positive and negative polarities and with temporal extent τ were used.

$$\sigma(0,t) = \begin{cases} \pm 35 \cdot 10^3 \left(1 + \cos \left(\pi \frac{t-\tau/2}{\tau/2} \right) \right), & \text{if } t \leq \tau, \\ 0, & \text{if } t > \tau. \end{cases} \quad (3)$$

2.2. Numerical method

The numerical simulations use the Chebyshev collocation method where the solution is approximated at gridpoints by a polynomial that is easy to differentiate. Unlike the finite difference methods, it is a global method where all the points contribute to the derivatives at each point. Its main advantage is lower computational cost due to the smaller number of points needed to describe the problem and simplicity of use in case of nonlinearities and a high order of spatial derivatives. For the Chebyshev collocation method the variables are stored at the Chebyshev extrema points, allowing the interpolation scheme to avoid the Runge's phenomenon (Fig. 5), which would arise in case of equidistant distribution of collocation points (Fig. 6) [15]. The spatial differentiation uses one Chebyshev differentiation matrix [16], and the integration in time is carried out using a `vode` solver [17] in the SciPy package [18].

The spatial differentiation and calculations are initially done on each layer separately. Thereafter the layers are interconnected by carrying over the stress and the particle velocity as shown in Fig. 7, allowing the energy to propagate both ways. The boundary conditions of stress $\sigma = 0$ or particle velocity $v = 0$ can be specified according to the problem.

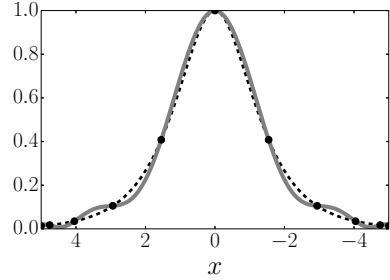


Fig. 5. Interpolation in the case of Chebyshev points.

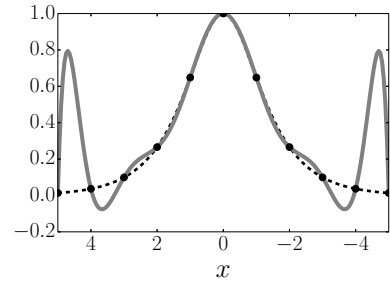


Fig. 6. Interpolation in the case of equi-spaced points.

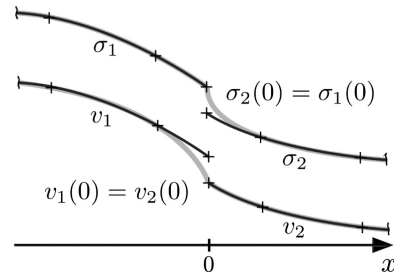
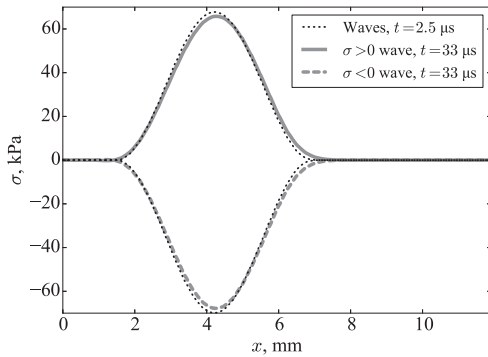


Fig. 7. Matching between the layers during the timestep.

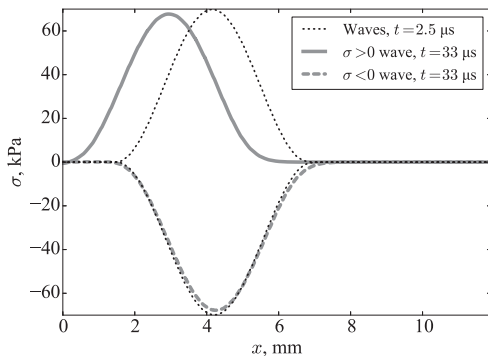
3. SIMULATIONS

Dynamic boundary conditions (Eq. (3)) were used to excite the wave in the medium. The simulation scheme was verified by doubling the number of spatial grid points, running the simulation again, and comparing the results. In case of little or no change in results, the scheme is suitable. For some material parameters, Eq. (1) with purely classical nonlinearity ($\alpha = 1$ in Eq. (2)) has been proven to sustain solitonic waves [19]. The simulations in this work are done to suggest the possibility of the existence of solitary waves in case of CFRP material parameters when introducing classical and nonclassical nonlinearities.

Firstly, a wide pulse half-cosine stress wave of Eq. (3), where $\tau = 2 \mu\text{s}$, was inserted into a 43-mm thick material. The pulse is allowed to reflect from the rear wall, return, and reflect from the front wall. The nearly initial pulse and twice-reflected pulse are compared. The reflections are, for the simplicity of analysis, from fixed ends. This means that the sign of the pulse is not changed by the reflections. The ‘wavelength’ corresponds to about 15 pairs of CFRP–epoxy layers. Figure 8 illustrates comparison between two cases: Fig. 8a where there is only classical nonlinearity $\beta = -15$ and $\alpha = 1$ for all ε ; and Fig. 8b where there are both classical and nonclassical nonlinearities $\beta = -15$ and $\alpha = 97\%$ if $\varepsilon \geq 0$. The results do not exhibit an oscillatory tail behind the pulse (toward $x = 0$). In Fig. 8a the classical nonlinearity of $\beta = -15$ does not change



(a) Only classical nonlinearity: $\beta = -15$, $\alpha = 1$.

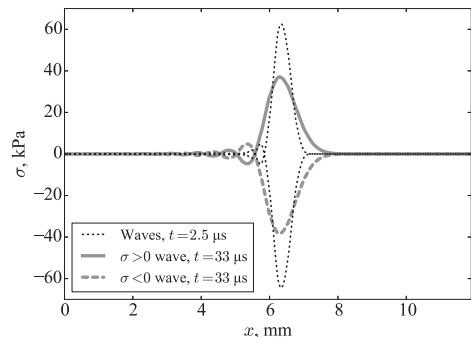


(b) Both nonlinearities: $\beta = -15$, $\alpha = 97\%$.

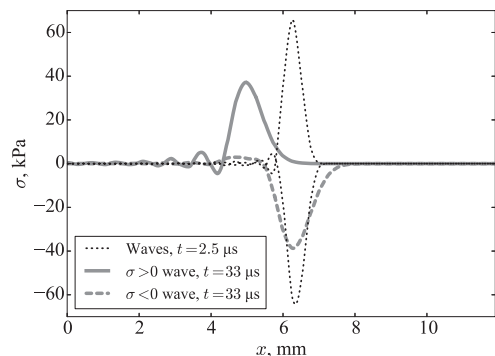
Fig. 8. Propagation of a half-cosine pulse with the width of $\tau = 2 \mu\text{s}$. The black dotted lines show the wave profile near the beginning of the propagation. Bold grey lines show wave profiles of positive and negative polarities after propagating and reflecting twice in the 43 mm wide medium. The spatial coordinate is denoted by x .

the propagation characteristics in any noticeable way. In Fig. 8b the addition of nonclassical nonlinearity $\alpha = 97\%$ decreases the velocity of the positive pulse.

Secondly, the initial pulse width was shortened to $\tau = 0.4 \mu\text{s}$, corresponding to about three pairs of epoxy–CFRP simulated laminate. The shorter wavelength ‘feels’ the microstructure and introduces oscillations due to the dispersion. The results are shown in Fig. 9. The case of $\beta = -15$ and $\alpha = 1$ for all ε is shown in Fig. 9a, and for $\beta = -15$ and $\alpha = 97\%$ if $\varepsilon \geq 0$ in Fig. 9b. Obviously the velocity of the positive σ pulse is again lower than for the negative pulse. Additionally, the effect of the inhomogeneous medium is immediately recognizable by an oscillatory tail of the pulses. Furthermore, in case of nonclassical nonlinearity in Fig. 9b, both positive and negative pulses change shape in the propagation. For the positive pulse the oscillatory tail has increased slightly. For the negative pulse the oscillatory tail decreases and smoothens.



(a) Only classical nonlinearity: $\beta = -15$, $\alpha = 1$.



(b) Both nonlinearities: $\beta = -15$, $\alpha = 97\%$.

Fig. 9. Propagation of a half-cosine $\tau = 0.4 \mu\text{s}$ pulse. The black dotted lines show the wave profile near the beginning of the propagation. Bold grey lines show wave profiles of positive and negative polarities after propagating and reflecting twice in the 43 mm wide medium. The spatial coordinate is denoted by x .

4. DISCUSSION

In the case of long-wavelength pulse $\tau = 2 \mu\text{s}$ in Fig. 8, there is no noticeable wave steepening effect, which is normally found in nonlinear wave propagation. Since the pulses stay either purely positive or purely negative, the only nonlinearity affecting the *shapes* of the pulses is classical nonlinearity β , while the nonclassical nonlinearity α only affects the velocities of the pulses.

The situation changes when the pulse length is shortened to $\tau = 0.4 \mu\text{s}$, because it will become affected by the layered material, causing dispersion. The dispersion generates an oscillatory tail behind the main pulse for all results in Fig. 9. The purely classical nonlinearity with $\beta = -15$ (and $\alpha = 1$) is not strong enough to affect the wave propagation noticeably (Fig. 9a), only the dispersion decreases the amplitude of the main peak. However, the situation is different with small nonclassical nonlinearity of $\alpha = 97\%$ (Fig. 9b), as both positive and negative pulses change shape. The oscillatory tail decreases for the negative pulse and increases for the positive pulse, resembling the behaviour of a solitary wave. Figure 9b furthermore shows that at the beginning of the propagation the shape of the positive pulse is slightly more gradual than the shape of the negative pulse. It resembles the wave-steepening effect commonly seen in nonlinear wave propagation, suggesting that the negative pulse behaves in a solitary wave-like manner. Its speed of propagation is greater than that of the positive pulse and it is more stable thanks to the nonclassical nonlinearity counteracting the dispersion by affecting the positive parts of the oscillatory tail.

In these simulations the nonclassical nonlinearity $\alpha = 97\%$ affects the solution far more than the classical nonlinearity $\beta = -15$. The material parameters should be measured with nonlinear NDT techniques [20] in order to ascertain reasonable magnitudes for nonlinearities. For measuring the nonclassical nonlinearity, a sinusoidal pulse could be propagated in this material. The pulse would have its negative part travelling faster than its positive. If the sinusoidal pulse was short (close to a single period), it would become compressed in propagation if the dynamic boundary condition was $\sigma(0,t) \sim +\sin$ and stretched if $\sigma(0,t) \sim -\sin$. The amount of distortion could indicate the magnitude of the nonclassical nonlinearity α in the constitutive Eq. (2).

5. CONCLUSIONS

It has been shown that in the case of large-wavelength pulses with the pulse width of 15 epoxy-CFRP pairs, the dispersion is not noticeably strong. Moreover, the classical nonlinearity of $\beta = -15$ with CFRP elasticity parameters is not strong enough to induce a noticeable change in wave shape. Introduction of nonclassical nonlinearity in addition to classical nonlinearity will bring about a speed difference between positive and

negative pulses. The speed difference of positive and negative parts of a sinusoidal pulse here could indicate the magnitude of the nonlinearity.

However, a pulse with a length corresponding to 3–4 epoxy-CFRP layers will ‘feel’ the layered configuration of the material, so it will have an oscillatory tail due to the dispersion. Introducing a small *nonclassical* nonlinearity of the magnitude $\alpha = 97\%$ (in addition to classical nonlinearity $\beta = -15$) will change the shape of the pulse in different ways depending on the sign of the wave amplitude. Essentially, the oscillatory tail of the positive σ pulse will be increased and the tail of the negative σ pulse will be decreased. This resembles the propagation of a solitary wave by having (i) an effect resembling wave steepening, (ii) balancing between dispersion and nonlinearity, and (iii) a larger speed of a negative σ pulse compared to a positive pulse.

We found in this study that the nonclassical nonlinearity would produce favourable effects for solitary wave propagation in the case of CFRP material, which could be used for the nonlinearity characterization and microdamage detection of the material. The nonclassical nonlinearity is zero-centred in this work and produces changes of velocity between the positive and negative parts of a wave even for small stress wave propagation. The material parameters, the type, and the magnitude of the nonlinearities need to be verified.

The Chebyshev collocation method was found suitable for 1D simulations of discontinuous media. The future work will include 2D simulations and analysis of wave propagation in complex nonlinear media. This should model potential materials better for solitary wave characterization and enable to take into account other complexities that surely affect the nonlinear acoustics of the material. As the results of this work show, it is necessary to consider additional sources of nonlinearity, other than the classical nonlinear parameter β , at different scales to see solitary wave-like evolution of waves.

Advances of imaging complex layered media by new signal processing schemes, involving solitonic coding, would improve the methods used today in medical imaging and NDT. Some biological complex layered media, such as the human skin, could benefit from such new coding schemes. Solitonic coding signal processing with using the orthogonality properties needed in classical nonlinear imaging potentially allows the use of elastic properties of soliton–soliton interactions in order to conduct fast nonlinear imaging.

ACKNOWLEDGEMENTS

This research was supported by the EU through the European Regional Development Fund (project TK124 (CENS)), by the Estonian Science Foundation (grant No. 8658), and national scholarship programmes Kristjan Jaak and DoRa (funded by the Archimedes Foundation in collaboration with the Estonian Ministry of Education

and Research), and by the Région Centre-Val de Loire within the PLET APP financial grant No. 2013-00083147.

REFERENCES

1. Dos Santos, S. and Prevorovsky, Z. Imaging of human tooth using ultrasound based chirp-coded nonlinear time reversal acoustics. *Ultrasonics*, 2011, **51**, 667–674.
2. Frazier, M., Taddese, B., Antonsen, T., and Anlage, S. M. Nonlinear time reversal in a wave chaotic system. *Phys. Rev. Lett.*, 2013, **110**, 063902.
3. Dos Santos, S., and Plag, C. Excitation symmetry analysis method (ESAM) for calculation of higher order nonlinearities. *Int. J. Nonlinear. Mech.*, 2008, **43**, 164–169.
4. Ilison, L., Salupere, A., and Peterson, P. On the propagation of localized perturbations in media with microstructure. *Proc. Estonian Acad. Sci. Phys. Math.*, 2007, **56**, 84–92.
5. Lomonosov, A. M., Kozhushko, V. V., and Hess, P. Laser-based nonlinear surface acoustic waves: from solitary to bondbreaking shock waves. In *Proc. 18th ISNA. AIP*, 2008, **1022**, 481–490.
6. Engelbrecht, J., Berezovski, A., Pastrone, F., and Braun, M. Waves in microstructured materials and dispersion. *Philos. Mag.*, 2005, **85**, 4127–4141.
7. LeVeque, R. J. Finite-volume methods for non-linear elasticity in heterogenous media. *Int. J. Numer. Meth. Fl.*, 2002, **40**, 93–104.
8. Berezovski, A., Berezovski, M., and Engelbrecht, J. Numerical simulation of nonlinear elastic wave propagation in piecewise homogeneous media. *Mat. Sci. Eng.*, 2006, **418**, 364–369.
9. Hauptert, S., Renaud, G., Rivière, J., Talmant, M., Johnson, P. A., and Laugier, P. High-accuracy acoustic detection of nonclassical component of material nonlinearity. *J. Acoust. Soc. Am.*, 2011, **130**, 2654–2661.
10. Vallikivi, M., Salupere, A., and Dai, H.-H. Numerical simulation of propagation of solitary deformation waves in a compressible hyperelastic rod. *Math. Comput. Simulat.*, 2012, **82**, 1348–1362.
11. Porubov, A. *Amplification of Nonlinear Strain Waves in Solids*. Series on Stability, Vibration, and Control of Systems. World Scientific, 2003.
12. Kliakhandler, I. L., Porubov, A. V., and Velarde, M. G. Localized finite-amplitude disturbances and selection of solitary waves. *Phys. Rev. E*, 2000, **62**, 4959–4962.
13. Salupere, A., Lints, M., and Engelbrecht, J. On solitons in media modelled by the hierarchical KdV equation. *Arch Appl. Mech.*, 2014, **84**, 1583–1593.
14. Solodov, I. Y., Krohn, N., and Busse, G. CAN: an example of nonclassical acoustic nonlinearity in solids. *Ultrasonics*, 2002, **40**, 621–625.
15. Gil, A., Segura, J., and Temme, N. *Numerical Methods for Special Functions*. Society for Industrial Mathematics, 2007.
16. Trefethen, L. N. *Spectral Methods in MATLAB*. SIAM, 2000.
17. Brown, P. N., Byrne, G. D., and Hindmarsh, A. C. VODE: A variable-coefficient ode solver. *SIAM J. Sci. Stat. Comp.*, 1989, **10**, 1038–1051.
18. Jones, E., Oliphant, T., Peterson, P., et al. SciPy: open source scientific tools for Python, 2001. <http://www.scipy.org> (accessed 12.08.2014).
19. LeVeque, R. J. and Yong, D. H. Solitary waves in layered nonlinear media. *SIAM J. Appl. Math.*, 2003, **63**, 1539–1560.
20. Dos Santos, S., Vejevodova, S., and Prevorovsky, Z. Nonlinear signal processing for ultrasonic imaging of material complexity. *Proc. Estonian Acad. Sci.*, 2010, **59**, 108–117.

Üksiklainete leviku numbrilised simulatsioonid süsinikkiudkomposiitmaterjalis

Martin Lints, Andrus Salupere ja Serge Dos Santos

Üksiklaineteks nimetatakse dispersiivses ja mittelineaarses keskkonnas levivaid stabiilse kujuga lokaliseeritud laineid. Juhul kui üksiklained interakteeruvad omavahel elastselt, nimetatakse neid solitonideks. Üksiklained võivad mittepurustavas testimises osutada kasulikeks tänu nende suurele stabiilsusele ja kuju sõltuvusele materjali omadustest. Nende rakendamine võib lubada keerulise geomeetria või keerulise sisestruktuuriga materjalide (mikrostruktuur-või granulaarsed materjalid) detailsemat või kiiremat uurimist.

Antud töös on uuritud süsinikkiudkomposiiti kui materjali, millel võivad olla nii klassikalised kui ka (mikro-kahestustest tulenevalt) mitteklassikalised mittelineaarsused. Dispersiooni tekitab keskkonna perioodiline kihilisus. Modelleeritav materjal on 144-kihiline süsinikkiudkomposiit. Antud töös oli kasutusel lihtne laminaatmudel tükati pidevatest keskkondadest. Matemaatiline mudel baseerub Cauchy liikumisvõrranditel ja mittelineaarsel olekuvõrrandil, kus materjali jäikus võib sõltuda nii deformatsiooni suuruselt kui ka selle märgist. Numbrilised eksperimendid on tehtud Chebyshevi pseudospektraalmeetodiga.

Simulatsioonide tulemused näitavad, et kuigi klassikaline mittelineaarsus võib olla liiga väike, tasakaalustamaks dispersiooni simuleeritud komposiidis, siis seevastu üsna väike mitteklassikaline mittelineaarsus muudab lainelevikut olulisel määral. Sealjuures on sellisel mittelineaarsusel suuremate lainepikkuste korral ilmne efekt positiivse ja negatiivse pingelaine leviku kiiruses. Väiksemate lainepikkuste juures, kus dispersioon avaldub tugevamalt, on positiivse ja negatiivse amplituudiga lainetel lisaks liikumiskiiruse erinevusele ka oluline erinevus laine kuju ning selle "sabas" olevate ostsillatsioonide suurus. Selline negatiivne pingelaine on suhteliselt stabiilne ja selle omadused sarnanevad üksiklaine omadustele, mis viitab mitteklassikalise mittelineaarsuse soodsale mõjule üksiklainete tekitamisel kihelistes materjalides.

Publication II

M. Lints, S. Dos Santos, and A. Salupere. Solitary Waves for Non-Destructive Testing Applications: Delayed Nonlinear Time Reversal Signal Processing Optimization. *Wave Motion*, 71:101–112, 2017.
<http://dx.doi.org/10.1016/j.wavemoti.2016.07.001>



Solitary waves for Non-Destructive Testing applications: Delayed nonlinear time reversal signal processing optimization



M. Lints^{a,b,*}, S. Dos Santos^a, A. Salupere^b

^a INSA Centre Val de Loire, Blois Campus, 3 Rue de la Chocolaterie CS 23410, F-41034 Blois Cedex, France

^b Institute of Cybernetics at Tallinn University of Technology, Akadeemia tee 21, 12618 Tallinn, Estonia

HIGHLIGHTS

- Delayed TR-NEWS signal is proposed for NDT of complex materials.
- FEM simulation and experiments of CFRP are matched to study wave propagation.
- Wave focusing in complex medium is improved by decreasing the signal side lobes.
- The received wave at the focusing can be modified to have an arbitrary envelope.
- Method could be used in the future to study nonlinear wave interaction.

ARTICLE INFO

Article history:

Received 1 March 2016
Received in revised form 24 June 2016
Accepted 2 July 2016
Available online 14 July 2016

Keywords:

Delayed Time Reversal-Nonlinear Elastic
Wave Spectroscopy
Carbon Fibre Reinforced Polymer
Solitary waves
Non Destructive Testing
Finite Element Method

ABSTRACT

An original signal processing method called delayed Time Reversal-Nonlinear Elastic Wave Spectroscopy is introduced in the present paper. The method could be used to amplify signal in certain regions of the material under Non Destructive Testing. It allows to optimize and change the shape of the received focused wave in the material, either by making the focusing sharper by decreasing the side lobes or making it wider by modifying the actual focusing peak. It is also possible to use the focused signal as a delta-basis to construct a signal with arbitrary envelope or reduce the side lobes of the focused signal. These concepts are shown to work well in the simulations and the physical experiments. This signal processing method is particularly promising for nonlinear and solitary wave analysis, since it allows to create an interaction of sharp and solitary wave peaks just underneath the receiving transducer. Due to simple and accurate linear prediction of the received interaction signal, any differences of measurements and predictions could indicate the presence of nonlinearities.

© 2016 Elsevier B.V. All rights reserved.

1. Introduction

The objective of the paper is to present the concept of delayed Time Reversal-Nonlinear Elastic Wave Spectroscopy (delayed TR-NEWS) [1]. It is an original method based on TR-NEWS method, used to obtain and modify focusing or convergence of ultrasonic waves in complex media.

Original TR-NEWS signal processing procedure can be used to focus the wave energy under the receiving transducer or vibrometer of an ultrasonic Non-Destructive Testing (NDT) setup. TR-NEWS is a promising method for evaluation of complex,

* Corresponding author at: Institute of Cybernetics at Tallinn University of Technology, Akadeemia tee 21, 12618 Tallinn, Estonia.
E-mail addresses: martin.lints@cens.ioc.ee (M. Lints), serge.dossantos@insa-cvl.fr (S. Dos Santos), salupere@ioc.ee (A. Salupere).

dispersive and nonlinear media because it relies on the internal reflections as virtual transducers [1] to focus the wave energy into a specific spot in a certain time, therefore taking advantage of the complex internal structure of the material [2]. Such focused wave has an improved signal-to-noise ratio, making it suitable for investigating dispersive, chaotic or highly attenuating media [3,4].

During the last ten years there has been an increase of interest in using symmetry and similarity properties in the signal processing of nonlinear acoustics [5–7]. New signal processing methods have been developed and validated for NDT and harmonic imaging. Pulse Inversion (PI) techniques [8,9], have been extended and generalized using Symmetry Analysis [10]. Coded excitations (for example a chirp signal) and signal processing are now considered as efficient ways for imaging the complexity in bio-materials. These methods improve the determination of nonlinear properties by using optimized excitations [11].

Recently there has been a considerable development of TR based NEWS methods using invariance with respect to TR and reciprocity, both in numerical and experimental aspects. These methods have been experimentally elaborated as the well-known TR-NEWS methods [12–16]. TR-NEWS fundamental experimental demonstrations [17] have been conducted with applications in the improvement of nonlinear scatterers identification using symbiosis of symmetry analysis (TR, reciprocity, chirp-coded PI, etc.) and NEWS methods. TR-NEWS based imaging continues to be developed, with new systems being designed to obtain better focusing and optimal images. New excitations are now under study in order to give to TR-NEWS methods the practicability needed for both the NDT and the medical imaging community [18].

A new direction in NDT is the use of solitary waves, as their important properties differ from linear waves and they are overall well-studied phenomenon [19]. Nonlinear effects depend mostly on the signal power and wave shape. This shape could then be analysed and compared to linear cases to detect the presence of nonlinearities.

In this paper the delayed TR-NEWS is numerically and experimentally validated for allowing to manipulate the focused wave shape of the ordinary TR-NEWS. It is a promising method for studying the nonlinear properties of materials in nonlinear acoustics and NDT of complex materials and composites. The paper will demonstrate the signal optimization potential of the delayed TR-NEWS method for NDT purposes using experiments in bi-layered aluminium and Carbon Fibre Reinforced Polymer (CFRP) and simulations in CFRP. It will be shown that the wave focused under the receiving transducer can be manipulated to have a different shape. The method will be shown to be useful for changing the extent of the material affected by focused ultrasonic wave, side lobe reduction and introduction of low-frequency signal into the medium by amplitude modulation. It is also possible to introduce a low-frequency wave by high frequency input by using delayed TR-NEWS as amplitude modulation of the low frequency signal. Additionally, it will be shown that the method is highly predictable in linear materials, and could be used to analyse nonlinear effects as deviations from the linear prediction.

Physical experiments were carried out on a bi-layered aluminium and a CFRP sample. The findings were studied further using Finite Element Method (FEM) simulations on a linearly elastic laminate model of CFRP block with stochastic layer thicknesses to examine the signal propagation and focusing inside a complex material. It is well known that layered periodical materials can be dispersive and therefore solitary waves can emerge in the presence of nonlinearities in such materials [20,21].

The goal of this paper is to show that the delayed TR-NEWS procedure gives good results in numerical and physical experiments for examining complex materials. In Section 2 the test object and the experimental setup are described and the computational model is introduced. In Section 3 the signal processing steps of TR-NEWS and delayed TR-NEWS methods are explained. In Section 4 the results of numerical and physical experiments are presented. In Section 5 the conclusions and the possible practical uses of delayed TR-NEWS procedure are given.

2. Materials and methods

The delayed TR-NEWS signal processing method was initially validated in a bi-layered aluminium sample [22]. In the present paper the method was used to optimize the signal in a complex CFRP sample and the wave motion inside the CFRP was further studied using a FEM model. Having an agreement between the FEM model and physical experiments, it is possible to study the wave motion in more detail. While physical experiments give the actual measured values on the surface of the test object, the simulations allow to investigate the internal wave field in the object.

The simulations and experiments must agree qualitatively. The quantitative agreement is less important because: (i) We are studying how waves behave at the focusing; (ii) Simulations are in 2D due to computational constraints while the real world is in 3D and this always produces differences in quantitative results; (iii) The developed signal optimization must be robust enough to account for some variations in signal power; (iv) In this work the simulation and experimental material is considered linearly elastic, rendering amplitude analysis unnecessary.

2.1. Experiment configuration

The tests were conducted with TR-NEWS ultrasonic testing equipment which focuses the wave energy near the surface of the material under the receiving transducer. The initial validation was conducted on a bi-layered aluminium sample [22]. Thereafter the tests were performed on a CFRP block (composed of 144 layers of carbon fibre fabric). It was excited from its side with 70° shear wave transducer. The signal was received with a plane wave transducer on the top of the block (Fig. 1).

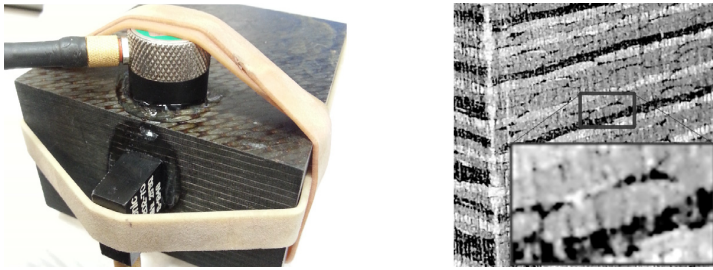


Fig. 1. Carbon Fibre Reinforced Polymer (CFRP) block (left) and its structure (right). This test configuration was chosen arbitrarily in order to verify the practical feasibility of the method in an NDT test.

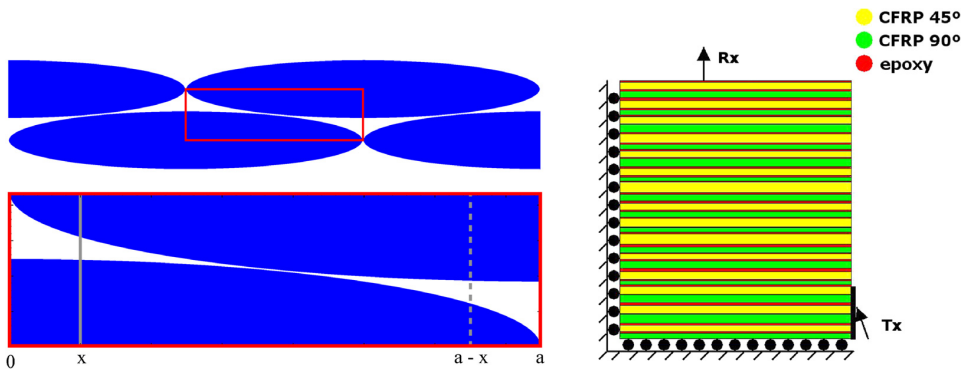


Fig. 2. The material consisting of elliptic yarns in tight packing (left) is modelled as a laminate with stochastic thicknesses of layers (right) due to different possible wave paths encountering different thicknesses of CFRP yarn and epoxy.

The roles of the transducers are not changed during the experiment as the focusing of an ultrasonic wave relies on the signal processing of TR-NEWS. This is a two-pass method where the receiving and transmitting transducers do not change their roles. In this sense the “Time Reversal” denotes the signal processing method which accounts for internal reflections of the material as virtual transducers in the material to use for focusing the wave in the second pass of the wave transmission. The placement of the transducers is otherwise not important: they could be placed arbitrarily in NDT investigation, they do not have to be in line with each other, but the configuration must remain fixed during the TR-NEWS procedure.

The test equipment consisted of:

Preamplifier Juvitek TRA-02 (0.02–5 MHz) connected to a computer,
 Amplifier ENI model A150 (55 dB at 0.3–35 MHz),
 Shear wave transducer Technisonic ABFP-0202-70 (2.25 MHz),
 Longitudinal wave transducer Panametrics V155 (5 MHz).

2.2. Finite element model

CFRP is composed of fabric woven from yarns of fibre impregnated with epoxy. The cross-section of the yarns has elliptical shape (Fig. 1) and the material has inclusions of pure epoxy between yarns, so a wave propagating through the material would encounter yarns (fibres with epoxy) and areas of pure epoxy. A simple laminate model was used for FEM: the material was considered to be homogeneous, generally anisotropic, but linearly elastic where each layer had its own elasticity properties according to the carbon fibre cloth orientation. The thicknesses of the individual layers were acquired from a function of random variables according to the probability of the wave encountering these thicknesses in packed ellipse configuration of the real material (Figs. 1 and 2). Dispersion could be expected to arise due to the discontinuity of the material properties. In this way the layered model, which is often used in studying of nonlinear waves in complex materials [20,21], is extended by making the layers have stochastic thicknesses. The stochastic thicknesses take into account the normal distribution of the ellipse sizes and the uniform distribution of geometric probability which describes where along the ellipse width the wave passes through the ellipse (Fig. 2).

The material in the simulation was modelled as laminate model of three different kinds of layers with different mechanical properties [23]:

- pure epoxy layer as an isotropic material: $E = 3.7$ GPa, $\nu = 0.4$, $\rho = 1200$ kg/m³,
- composite with fabric at 0/90° orientation as transversely isotropic material: $E_1 = E_2 = 70$ GPa, $G_{12} = 5$ GPa, $\nu_{12} = 0.1$, $\rho = 1600$ kg/m³,
- composite with fabric at 45°/45° orientation as transversely isotropic material: $E_1 = E_2 = 20$ GPa, $G_{12} = 30$ GPa, $\nu_{12} = 0.74$, $\rho = 1600$ kg/m³.

The thickness of each separate composite yarn layer was found with

$$f_C(x) = \frac{b}{a} \left(\sqrt{a^2 - x^2} + \sqrt{2ax - x^2} \right), \quad (1)$$

and the thickness of its corresponding pure epoxy layer with

$$f_E(x) = \sqrt{3}b - f_C(x) \quad (2)$$

where $a = \mathcal{N}(\mu_a, \sigma_a^2)$ and $b = \mathcal{N}(\mu_b, \sigma_b^2)$ are normal random variables for the semi-axes of the ellipses found from the distribution of carbon fibre ellipses in the real material (Fig. 1). Therefore the computational model reflects the actual material due to the randomness of the layer thicknesses being in accordance with the carbon fibre ellipses in actual CFRP block. Uniform random variable $x = \mathcal{U}(0, a)$ is a function of geometric probability which describes where along the ellipse semi-major axis the wave passes through the ellipse (in the direction of its minor axis) (Fig. 2). The laminate model was constructed by finding the semi-major axis length a (where mean $\mu_a = 0.750$ mm, dispersion $\sigma_a = 0.130$ mm) and semi-minor axis length b (where mean $\mu_b = 0.130$ mm, dispersion $\sigma_b = 0.025$ mm) and wave traversing location x which is a random variable for a pair of layers (composite and epoxy). The composite fabric orientation (90° or 45°) alternated for each pair (Fig. 2). The model consisted of 50 such pairs which were generated and stacked together. The thicknesses of composite fabric and epoxy layers were found from Eqs. (1) and (2). As a practical aspect, the thickness of an epoxy layer f_E could not be too small or it prohibited the generation of a good FEM mesh.

2.2.1. Equations

The material in the simulation was assumed to be linearly elastic. The following variational problem was solved [24]:

$$\int_V \rho \ddot{u} \delta u dV + \int_V \sigma_{ij} \delta \varepsilon_{ij} dV - \int_\Gamma f \cdot \delta u dS = 0, \quad (3)$$

where u is displacement, ρ is material density, σ_{ij} is stress, ε_{ij} is strain and f is traction on surface. Newmark's method was used for time stepping (time step $\Delta t_s = 5 \cdot 10^{-8}$ s). The constant average acceleration variant of the Newmark's scheme has following relations

$$\begin{cases} \dot{u}_{s+1} = \dot{u}_s + \Delta t_s \frac{\ddot{u}_s + \ddot{u}_{s+1}}{2}, \\ u_{s+1} = u_s + \Delta t_s \dot{u}_s + (\Delta t_s)^2 \frac{\ddot{u}_s + \ddot{u}_{s+1}}{4}. \end{cases}$$

From these equations one can express acceleration

$$\ddot{u}_{s+1} = \frac{4}{(\Delta t_s)^2} u_{s+1} - \ddot{u}_s - \frac{4}{\Delta t_s} \dot{u}_s - \frac{4}{(\Delta t_s)^2} u_s,$$

and substitute $\ddot{u} = \ddot{u}_{s+1}$ into Eq. (3). After that the equation for solving the wave motion problem in a layer becomes as follows:

$$\int_V \left[\rho \left(\frac{4}{(\Delta t_s)^2} u_{s+1} - \ddot{u}_s - \frac{4}{\Delta t_s} \dot{u}_s - \frac{4}{(\Delta t_s)^2} u_s \right) \delta u + \sigma_{ij} \delta \varepsilon_{ij} \right] dV = \int_\Gamma t \cdot \delta u dS.$$

This FEM variational model was solved using FEniCS libraries [25].

2.2.2. Boundary conditions

The following boundary conditions (Fig. 2, right) were used in the FEM simulation:

- Excitation signal was introduced by Dirichlet boundary condition on the right hand side of bottom 7 pairs of layers. The excitation was introduced in 70° angle upwards and lasted for 60 μ s.
- Dirichlet boundary condition of zero displacement $u_1 = 0$ on left and $u_2 = 0$ on bottom boundary.

In physical experiments the displacement component u_2 was recorded at the top of the sample, at $x_1 = 5$ mm from the left side of the material (Fig. 2) (equivalent for the receiver placement in the experiment, 9 mm from the free right hand side in Fig. 1). Since the displacement component u_2 was used for signal processing, it was also the component exhibiting TR-NEWS focusing and the only component shown in the results.

The signal input and output correspond to the physical experiment shown in Fig. 1. There were some differences between the simulations and the experiments due to computational considerations. Notable differences were that the simulations considered only the material between and near the transducers, not the whole CFRP object, so the wave field had less space to travel and reverberate from. Also the simulations did not include losses. The simulations used 60 μ s signal length while the physical experiments had 1280 μ s signal length. Obviously, the simulations were in 2D, unlike the physical experiments.

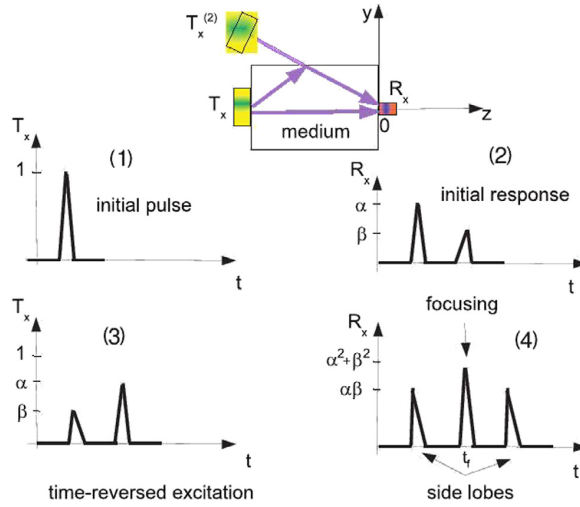


Fig. 3. Schematic process of TR-NEWS with the virtual transducer concept. (1) The initial broadband excitation $T_x(t)$ propagates in a medium. (2) Additional echoes coming from interfaces and scatterers in its response R_x could be associated to a virtual source $T_x^{(2)}$. (3) Applying reciprocity and TR process to R_x . (4) The time reversed new excitation $T_x = R_x(-t)$ produces a new response R_x (the TR-NEWS coda $y_{TR}(t)$) with a spatio-temporal focusing at $z = 0; y = 0; t = t_f$ and symmetric side lobes with respect to the focusing.

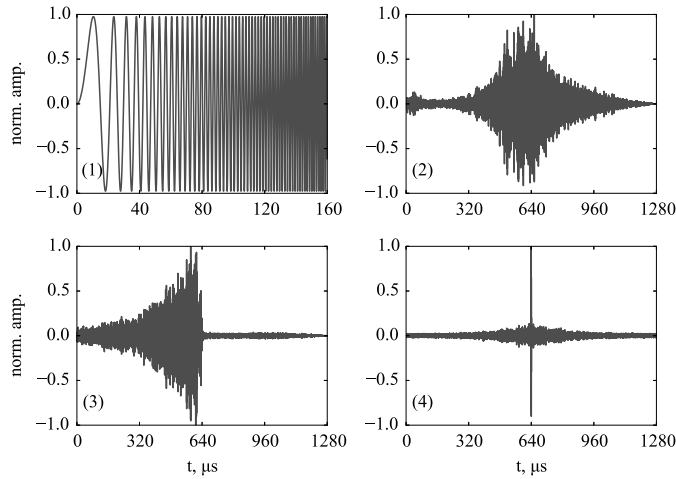


Fig. 4. Chirp-coded TR-NEWS signal processing steps in bi-layered aluminium experiment: (1) chirp excitation; (2) output recorded at Rx; (3) cross-correlation between input and output; (4) focusing resulting from transmitting the time-reversed cross-correlation as a new ultrasonic input.

3. Delayed TR-NEWS signal processing

This section describes the signal processing steps of the delayed TR-NEWS method used identically in simulations and physical experiments. Both the delayed and the original TR-NEWS methods are two-pass techniques for use in NDT experiments. The first pass is used to gather information about internal reflections (virtual transducers) in material. The second pass transmits an optimized excitation which uses these internal reflections to focus the wave under receiving transducer. Both passes are conducted in the same direction without replacing the transmitting and receiving transducers with each other. The first steps of the delayed TR-NEWS method coincide with the known TR-NEWS procedure consists of the following steps [1] (outlined in Figs. 3 and 4):

1. The first transmission pass involves transmitting a chirp-coded excitation $c(t)$ through the medium

$$c(t) = A \sin(\psi(t)),$$

where $\psi(t)$ is linearly changing instantaneous phase. In this work, a sweep from 0 to 2 MHz was used.

2. Simultaneously the chirp-coded coda response $y(t)$ with a time duration T is recorded

$$y(t, T) = h(t) * c(t) = \int_{\mathbb{R}} h(t - t', T)c(t')dt',$$

where $h(t - t', T)$ is regarded as impulse response of the medium. Here the asterisk denotes convolution and $y(t, T)$ the direct response from the receiving transducer when transmitting the chirp excitation $c(t)$ through the medium.

3. Next the information about the internal reflections $\Gamma(t)$ is found by cross-correlating the received response $y(t, T)$ with the sent chirp-coded excitation $c(t)$. This is computed for some time period Δt ,

$$\Gamma(t) = \int_{\Delta t} y(t - t', T)c(t')dt' \simeq h(t) * c(t) * c(T - t, T). \quad (4)$$

Here $h(t) * c(t) * c(T - t, T)$ is a pseudo-impulse response. It is proportional to the impulse response $h(t)$ if using linear chirp excitation for $c(t)$ because then $\Gamma_c(t) = c(t) * c(T - t) = \delta(t - T)$. Therefore the actual correlation $\Gamma(t) \sim h(t)$ contains information about the wave propagation paths in complex media. Time reversing the correlation $\Gamma(t)$ from the previous step results in $\Gamma(T - t)$ used as a new input signal. This time-reversed $\Gamma(T - t)$ is shown in Figs. 3(3) and 4(3).

4. The second pass of the transmission involves re-propagating the new excitation $\Gamma(T - t)$ in the same configuration as the initial chirp, yielding the received signal

$$y_{TR}(t, T) = \Gamma(T - t) * h(t) \sim \delta(t - T), \quad (5)$$

where $y_{TR} \sim \delta(t - T)$ is now the focused signal under receiving transducer where the focusing takes place at time T . This is because $\Gamma(t)$ contains information about the internal reflections of the complex media. Transmitting its time reversed version $\Gamma(T - t)$ eliminates these reflection delays by the time signal reaches the receiver, resulting in the focused signal y_{TR} (Eq. (5)).

The test configuration must remain constant during all of these steps, otherwise the focusing is lost. The roles of the transmitting and the receiving transducers are never exchanged. Time reversal in this sense is conducted purely in the signal processing: it will use the internal reflections to create focusing under the receiving transducer in the second pass of the ultrasonic transmission. This concludes the signal processing steps for the TR-NEWS procedure which are known and published [1,3].

The subject of this paper is the delayed TR-NEWS signal processing method, which is based on the TR-NEWS, so it uses the same initial steps. Its added value over the TR-NEWS is the possibility of changing the focused wave by considering a single focused y_{TR} signal as a new basis which can be used to build arbitrary wave shapes at the focusing. This is done by time-delaying and superimposing n time-reversed correlation $\Gamma(T - t)$ signals [1] (Fig. 5 left column)

$$\Gamma_s(T - t) = \sum_{i=0}^n a_i \Gamma(T - t + \tau_i) = \sum_{i=0}^n a_i \Gamma(T - t + i\Delta\tau), \quad (6)$$

where a_i is the i th amplitude coefficient and τ_i the i th time delay. In case of a uniform time delay the $\Delta\tau$ is the time delay between the samples. Upon propagating this $\Gamma_s(t - T)$ through the media according to the last step of TR-NEWS, a delayed scaled shape of signal at the focusing point can be created (Fig. 5 right column). Various optimizations are possible using the delayed TR-NEWS scheme, for example amplitude modulation, signal improvement and side lobe reduction. It is possible to counteract the side lobes of a single focusing pulse by its time-delayed and scaled versions, according to the scheme in Fig. 6.

It is possible to predict the result of the delayed TR-NEWS focusing in a linear material (Fig. 5 right column):

$$\begin{aligned} y_{dTR}(t) &= \left[\sum_i a_i \Gamma_c(T - t + \tau_i) \right] * h(t) \stackrel{\text{linearity}}{=} \\ &= \sum_i a_i \Gamma_c(T - t + \tau_i) * h(t) = \sum_i a_i y_{TR}(t - \tau_i). \end{aligned} \quad (7)$$

The purpose of the linear prediction of the delayed TR-NEWS result is twofold. Firstly it can be used to find optimal delay and scaling values for the delayed TR-NEWS experiment, using the original focusing peak y_{TR} . Secondly it could be possible to analyse the differences between the predicted and actual measured delayed TR-NEWS result. The difference could indicate the magnitude of nonlinear effects, because the prediction relies on the applicability of linear superposition and is found to be quite accurate in experiments with linear material.

4. Results and discussion

The physical experiments were carried out on bi-layered aluminium and CFRP samples, the simulations only on layered FEM model of CFRP. Firstly the CFRP simulation and experiment results are compared to establish a link between them. Due to computational considerations, the signal length of the simulation is 60 μ s and in experiment it is 1280 μ s. The TR-NEWS

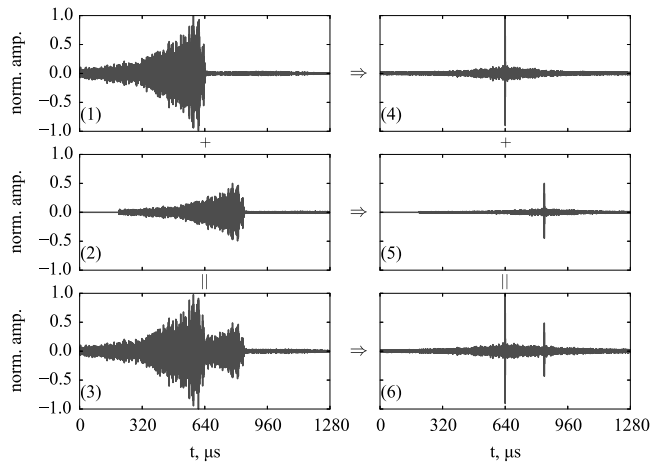


Fig. 5. Delayed TR-NEWS signal processing steps conducted in bi-layered aluminium, starting from the cross-correlation step (left column) and prediction of linear superposition of waves (right column): (1) cross-correlation (Eq. (4)); (2) delayed and scaled cross-correlation; (3) linear superposition of two cross-correlations which becomes the new excitation; (4) focusing (Eq. (5)); (5) delayed and scaled focusing; (6) Linear superposition of the two focusing peaks.

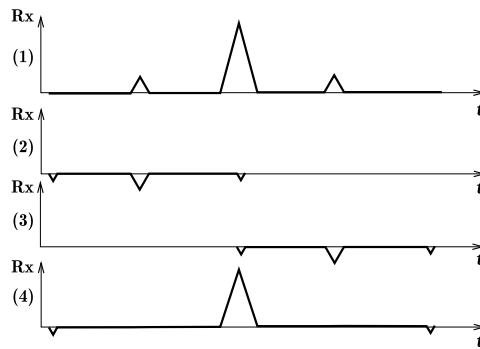


Fig. 6. Scheme of the side lobe reduction using delayed TR-NEWS: (1) initial y_{TR} focusing with side lobes (Eq. (5)); (2) and (3) scaled and shifted focusing for eliminating side lobes; (4) resulting y_{dTR} from adding together signals (1)–(3) has reduced side lobes but slightly reduced main peak.

focusing y_{TR} produces the focusing peak in the middle of the signal, therefore this midpoint is taken as point of reference as “time since focusing” to compare the simulation and experiment results. The amplitudes are normalized to the maximum value of absolute values in line plots. Both the simulations and the experiments use the same chirp $c(t)$ frequency range from 0 to 2 MHz. As much as possible, all simulations and experiment parameters are taken to be identical. Particularly the time delay values are the same when comparing delayed TR-NEWS simulation with experiment.

4.1. Validation of simulations for delayed TR-NEWS

Firstly, the simulations are compared to the experiments for CFRP for single TR-NEWS focusing peak y_{TR} . The close-up of the peak is shown in Fig. 7. A good agreement between the period of the focusing peak in simulation and experiment can be seen. Also, the approximate levels of noise in simulation and experiment are similar.

Secondly, the simulation and the experiment are compared in case of delayed TR-NEWS signal processing where five delays are taken with relative amplitudes $a_i = \{0.1, 0.2, 0.3, 0.4, 0.5\}$, and a delay $\Delta\tau = 1 \mu\text{s}$ between them (Eq. (6)). The results of the corresponding simulation and experiment are shown in Fig. 8. Again, there is a qualitative correspondence between the simulation and the experiment.

4.2. Optimization of the focusing peak

Having just one additional delayed focusing peak in delayed TR-NEWS ($a_i = \{1, 1\}$ and $\Delta\tau = 0.25 \mu\text{s}$ in Eq. (6)), the width of the focusing is modified and the side lobes decreased. The preliminary verification has been performed on

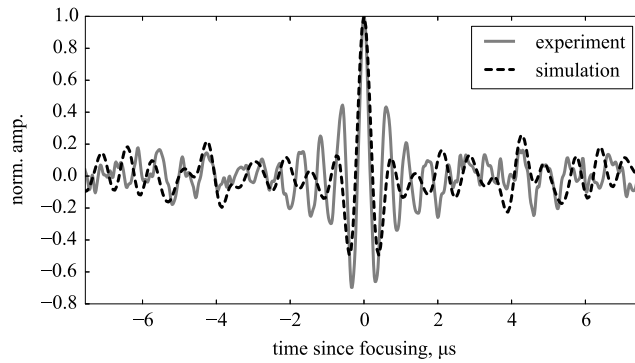


Fig. 7. TR-NEWS wave focusing in CFRP, comparison of the TR-NEWS simulation with the physical experiment.

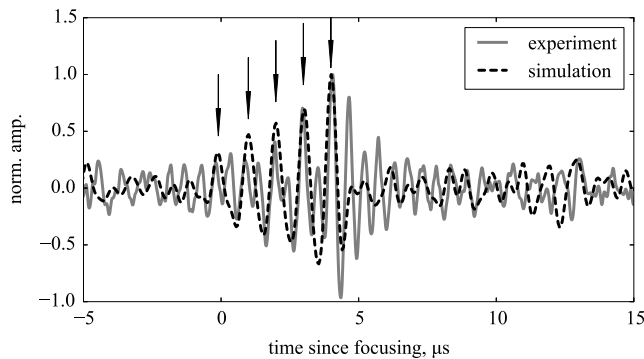


Fig. 8. Comparison of the delayed TR-NEWS CFRP physical experiment and simulation. The five peaks are delayed with intervals $\Delta\tau = 1\mu\text{s}$ and have relative amplitudes $a_i = \{0.1, 0.2, 0.3, 0.4, 0.5\}$.

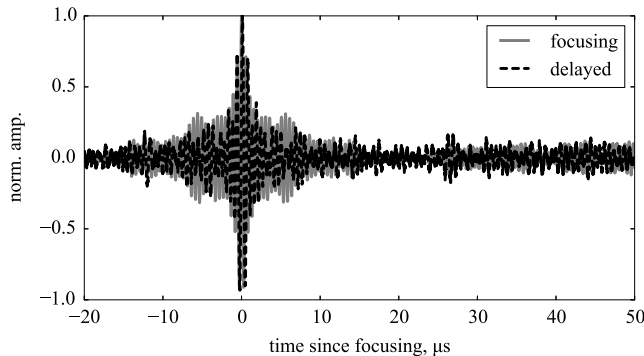


Fig. 9. Improvement of focusing in bi-layered aluminium due to delayed TR-NEWS experiment with delay $\Delta\tau = 0.25\mu\text{s}$ and $a_i = \{1, 1\}$.

bi-layered aluminium sample, and later also in CFRP sample and simulations. The effect of such delay (compared to the original TR-NEWS focusing) on the side lobes of the bi-layered aluminium can be seen in Fig. 9. Much of the side lobe has been decreased at the expense of some added noise outside the focusing region. The same experiment and simulation have been conducted in CFRP, using coincidentally the same value $\Delta\tau = 0.25\mu\text{s}$. In CFRP experiment and simulation (Fig. 10), the improvement is not as pronounced as in case of bi-layered aluminium: the decrease of oscillations adjacent to main focusing peak is smaller.

In CFRP such $0.25\mu\text{s}$ delay mainly modifies the width of the focusing peak itself, making it wider, as can be seen from experiments and simulations in CFRP in Fig. 10. This property could be used to modify the spatial extent of the higher amplitude focusing. In these experiments this increase of the width of focused wave is small (Fig. 11) but different frequencies in different materials could yield better results in widening the area affected by high-amplitude focusing. The

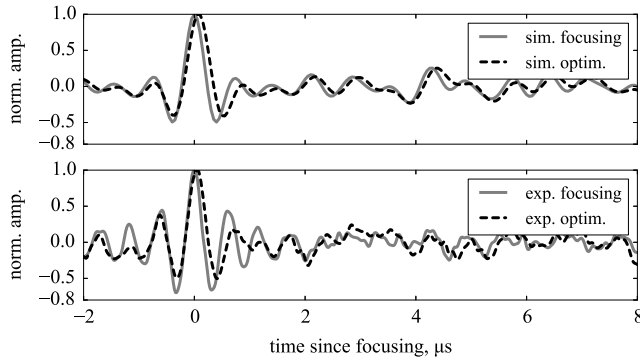


Fig. 10. Comparison of delayed TR-NEWS in simulation (upper subfigure) and experiment (lower subfigure) with $0.25 \mu\text{s}$ delay, comparing the widening of the pulse.

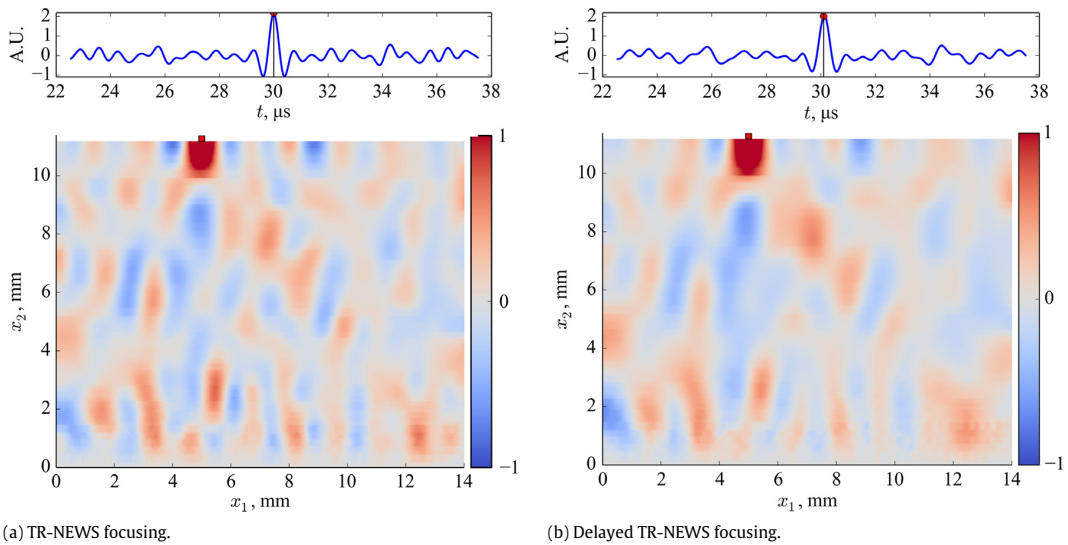


Fig. 11. Extent of the material affected by high amplitude ($A_{\text{max}} > 1$) focused wave in case of TR-NEWS focusing and delayed TR-NEWS focusing for $\Delta\tau = 0.25 \mu\text{s}$, $a_i = \{1, 1\}$. Unnormalized results are shown with focusing maximum amplitude $A_{\text{max}} > 2.0$. Additional video files are available in the supplementary materials (see [Appendix A](#)).

reduction of the side lobe, while noticeable, is small. In the CFRP simulation the focusing amplitude is also lowered from $A_{\text{max}} = 2.27$ to $A_{\text{max}} = 2.07$ due to the delayed TR-NEWS widening of the focusing. The maximum amplitude of the input excitation was always $A = 1$.

In all of these experiments and simulations, the delayed TR-NEWS results have been in good accordance with their linear superposition predictions (Eq. (7)), allowing to fine-tune the delay parameters before conducting the experiment. The small difference between the prediction and the experiment in bi-layered aluminium with $a_i = \{1, 1\}$, $\Delta\tau = 0.25 \mu\text{s}$ can be seen in [Fig. 12](#). It is clear that the difference between the prediction and the experiment is close to zero at the crests and troughs of the signal and it has extremal values between them due to slight phase differences between the prediction and the actual measurement.

4.3. Wave interaction at the focusing point

The simulations are important because they show what happens inside the material. It could be possible to use the delayed TR-NEWS for examining of nonlinear materials supporting solitary waves and to create an interaction of high amplitude waves right at the receiving transducer. The simulation results confirm that the focusing under the receiver is indeed a constructive interaction of several waves and not just a passing of one wave ([Fig. 13](#)). The proposed nonlinear analysis method would rely on delayed TR-NEWS to pump the medium full of energy to be focused near the receiver and

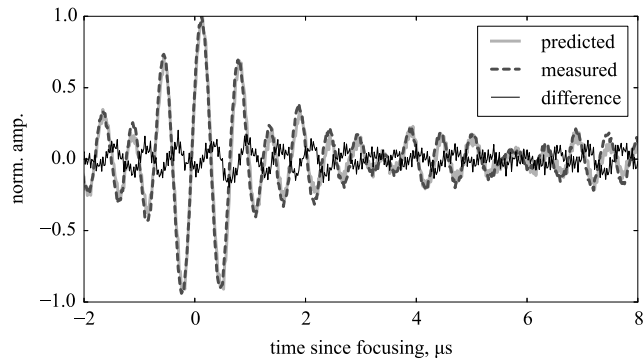


Fig. 12. Prediction from delayed TR-NEWS signal processing ($\Delta\tau = 0.25 \mu\text{s}$) versus the results from actual experiment in bi-layered aluminium sample.

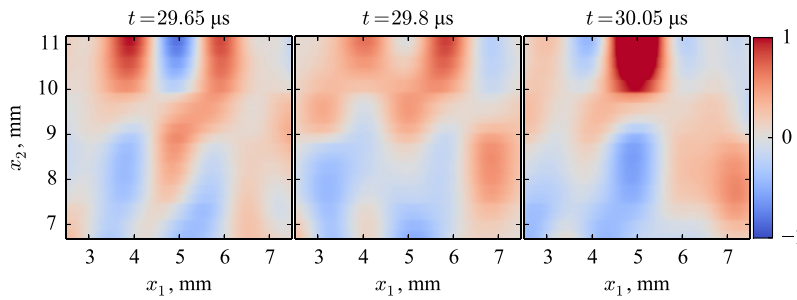


Fig. 13. Several separate waves arriving and interacting in CFRP simulation of the focusing.

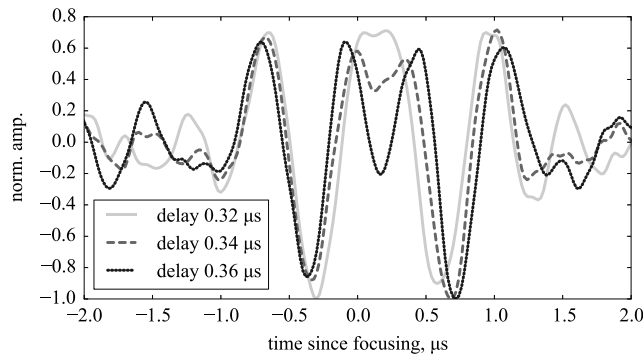


Fig. 14. Delayed TR-NEWS focusing manipulations in CFRP experiment with three different delay values, showing different moments of converging wave interaction at the focusing moment.

use time delays to slightly offset the focusing to investigate the interaction of the waves near the receiver. For an experiment of undamaged CFRP material such delayed signals are shown in Fig. 14. It could be possible to detect nonlinear effects (which can be caused by material defects [26]) in the focusing region by comparing the measured results to the prediction that is based on linear superposition assumption (Eq. (7)). Interaction of solitons (instead of linear waves) could also be detected, for example, by phase difference due to nonlinear interaction [27].

4.4. Arbitrary wave envelope generation

Experiments with bi-layered aluminium sample [22] and CFRP sample show that delayed TR-NEWS method can be used to generate an arbitrary wave envelope at the focusing point by taking the individual delta signal $y_{TR} \sim \delta(t - T)$ as a basis for amplitude modulation (Fig. 15). Such amplitude modulation could be used in a material to generate a low-frequency component in the focusing point (receiver) of the test setup.

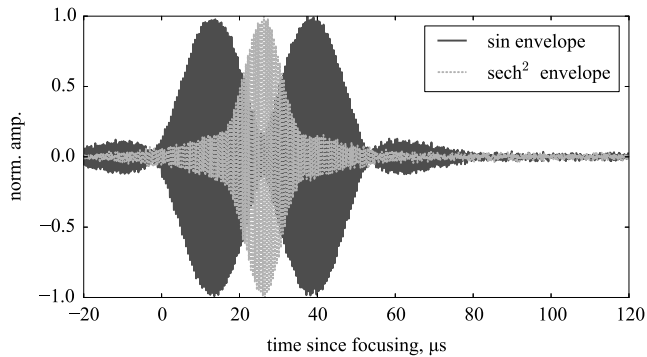


Fig. 15. Delayed TR-NEWS in CFRP for creating an envelope of special shape at the focusing.

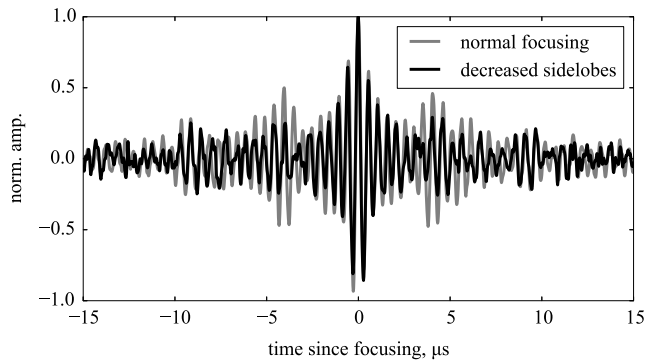


Fig. 16. Results of a delayed TR-NEWS focusing experiment with the CFRP sample: due to using of two time-delayed and scaled copies of the original signal the size of the side lobes can be reduced significantly compared to normal focusing.

4.5. Side lobe reduction

The side lobe reduction by using two delayed peaks of $a_i = \{1, 1\}$ and $\Delta\tau = 0.25 \mu\text{s}$ is effective in bi-layered aluminium. In CFRP experiment, the side lobe reduction is most effective when performed directly by using delayed TR-NEWS on the side lobes according to scheme in Fig. 6. The process is as follows: the time difference between the side lobe and the main peak of the original focused signal is taken as delay τ_i and the amplitude of the side lobe as negative amplitude $-a_i$. This process is repeated for the other side lobe. Thereafter Eq. (6) is used to sum these signals together to reduce the side lobes. In physical experiments the side lobe reduction is effective because the frequency content of the peak and the side lobes matches well (Fig. 16).

5. Conclusions

It has been shown that the results of simulations and experiments match well. Therefore one can conclude that the simulation shows the nature of the wave field at the focusing point inside the material. By using the simulations and the experiments together it is possible to conclude several findings about the delayed TR-NEWS signal processing optimization method which can be important in NDT, especially if the focusing takes place in a region where the nonlinear properties of the material enable emergence of solitary waves above some threshold of wave energy.

It was shown that the delayed TR-NEWS can be used to modify and widen the focusing peak y_{TR} . This could be used to enlarge the region affected by the focusing. Solitary waves are evolution waves, which need to propagate in the nonlinear environment for some length to have an appreciable change of wave shape. Using the delayed TR-NEWS method, the high-amplitude focusing area could be widened to an extent necessary to see a wave shape change thanks to the propagation of the signal through a region of the material with nonlinear effects or a region of a defect. In bi-layered aluminium, the widening of the focusing was conducted by a two-pulse delay $\Delta\tau = 0.25 \mu\text{s}$ with equal amplitudes $a_i = \{1, 1\}$, which also decreased the side lobes. In case of CFRP the effect of decreasing the side lobes by this particular time-delay was smaller. It was found that the reduction of the side lobes in CFRP is more effective by applying the delayed TR-NEWS impulses directly on the side lobes by using additional smaller waves tailored to arrive at the focusing point at the same time and magnitude as the side lobes but with an opposite amplitude sign.

It was shown in simulations that the focusing is the result of an interaction between several waves. It was also shown in the experiments that the delayed TR-NEWS method allows to slightly offset these interactions to capture different wave interaction moments. In case of linear waves there is little difference between linear superposition prediction and actual interactions. However, in the presence of nonlinear effects at the focusing point, the actual focusing shape should differ from the linear superposition. Any differences could then be used to detect local sources of nonlinearities at the focusing point. Alternatively, pulse inversion could be used for detection of nonlinear effects.

The delayed TR-NEWS method allows to use the single focused peak as a basis of amplitude modulation to create wave envelopes of arbitrary shapes in the focusing region. This could be used to introduce a low-frequency component into the material by using a high-frequency transmitter.

Future studies will include the analysis of local nonlinear effects in the focusing region using the proposed delayed TR-NEWS signal processing method and performing corresponding FEM simulations. The latter can be used for prediction of the size of defects in the material.

Acknowledgements

This research has been conducted within the *co-tutelle* Ph.D. studies of Martin Lints, between the Institute of Cybernetics at Tallinn University of Technology in Estonia and the Institut National des Sciences Appliquées Centre Val de Loire at Blois, France. The laboratory visits have been funded by European Social Funds via Estonian Ministry of Education and Research and Archimedes Foundation (30.1-9.3/287, 30.1-9.3/1137 and 16-3.4/1390) through DoRa and Kristjan Jaak Scholarship programmes. This research is partly supported by Estonian Research Council (project IUT33-24).

Appendix A. Supplementary material

Supplementary material related to this article can be found online at <http://dx.doi.org/10.1016/j.wavemoti.2016.07.001>.

References

- [1] S. Dos Santos, S. Vejvodova, Z. Prevorovsky, Nonlinear signal processing for ultrasonic imaging of material complexity, *Proc. Est. Acad. Sci.* 59 (2) (2010) 108–117.
- [2] D. Givoli, Time reversal as a computational tool in acoustics and elastodynamics, *J. Comput. Acoust.* 22 (03) (2014) 1430001.
- [3] S. Dos Santos, M. Lints, N. Poirot, A. Salupere, Optimized excitation for nonlinear wave propagation in complex media: From biomedical acoustic imaging to nondestructive testing of cultural heritage, *J. Acoust. Soc. Am.* 138 (3) (2015) 1796–1796.
- [4] M. Frazier, B. Taddese, T. Antonsen, S.M. Anlage, Nonlinear time reversal in a wave chaotic system, *Phys. Rev. Lett.* 110 (2013) 063902.
- [5] K. Hajek, J. Sikula, New possibilities to increase sensitivity of the ultrasound non-linear modulation methods, *Int. J. Microstruct. Mater. Prop.* 6 (3–4) (2011) 283–292.
- [6] F. Ciampa, G. Scarselli, M. Meo, Nonlinear imaging method using second order phase symmetry analysis and inverse filtering, *J. Nondestruct. Eval.* 34 (2) (2015) 1–6.
- [7] P.R. Armitage, C.D. Wright, Design, development and testing of multi-functional non-linear ultrasonic instrumentation for the detection of defects and damage in CFRP materials and structures, *Compos. Sci. Technol.* 87 (2013) 149–156.
- [8] D.H. Simpson, C.T. Chin, P.N. Burns, Pulse inversion doppler: a new method for detecting nonlinear echoes from microbubble contrast agents, *IEEE Trans. Ferr.* 46 (2) (1999) 372–382.
- [9] M. Scalerandi, Power laws and elastic nonlinearity in materials with complex microstructure, *Phys. Lett. A* 380 (3) (2016) 413–421.
- [10] S. Dos Santos, C. Plag, Excitation symmetry analysis method (ESAM) for calculation of higher order nonlinearities, *Int. J. Non-Linear Mech.* 43 (2008) 164–169.
- [11] A. Glozzi, M. Scalerandi, Modeling dynamic acousto-elastic testing experiments: Validation and perspectives, *J. Acoust. Soc. Am.* 136 (4) (2014) 1530–1541.
- [12] T. Goursolle, S. Callé, S. Dos Santos, O.B. Matar, A two-dimensional pseudospectral model for time reversal and nonlinear elastic wave spectroscopy, *J. Acoust. Soc. Am.* 122 (6) (2007) 3220–3229.
- [13] T. Ulrich, A. Sutin, R. Guyer, P. Johnson, Time reversal and non-linear elastic wave spectroscopy (TR-NEWS) techniques, *Int. J. Non-Linear Mech.* 43 (3) (2008) 209–216.
- [14] M. Meo, G. Zumpano, A new nonlinear elastic time reversal acoustic method for the identification and localisation of stress corrosion cracking in welded plate-like structures – a simulation study, *Int. J. Solids Struct.* 44 (2007) 3666.
- [15] M. Pernot, G. Montaldo, M. Tanter, M. Fink, “Ultrasonic stars” for time-reversal focusing using induced cavitation bubbles, *Appl. Phys. Lett.* 88 (3) (2006) 034102.
- [16] S. Delrue, K. Van Den Abeele, O.B. Matar, Simulation study of a chaotic cavity transducer based virtual phased array used for focusing in the bulk of a solid material, *Ultrasonics* 67 (2016) 151–159.
- [17] T.J. Ulrich, P.A. Johnson, R.A. Guyer, Interaction dynamics of elastic waves with a complex nonlinear scatterer through the use of a time reversal mirror, *Phys. Rev. Lett.* 98 (2007) 104301–104304.
- [18] M. Lints, A. Salupere, S. Dos Santos, Simulation of solitary wave propagation in carbon fibre reinforced polymer, *Proc. Est. Acad. Sci.* 64 (3) (2015) 297–303.
- [19] A. Salupere, K. Tamm, On the influence of material properties on the wave propagation in mindlin-type microstructured solids, *Wave Motion* 50 (7) (2013) 1127–1139.
- [20] A. Berezovski, M. Berezovski, J. Engelbrecht, Numerical simulation of nonlinear elastic wave propagation in piecewise homogeneous media, *Mater. Sci. Eng.* 418 (2006) 364–369.
- [21] R.J. LeVeque, D.H. Yong, Solitary waves in layered nonlinear media, *SIAM J. Appl. Math.* 63 (5) (2003) 1539–1560.
- [22] M. Lints, S. Dos Santos, A. Salupere, Delayed time reversal in non destructive testing for ultrasound focusing, in: T. Hobza (Ed.), *Proceedings of the SPMS 2015*, Czech Technical University, Prague, 2015, pp. 115–124.
- [23] Mechanical properties of carbon fibre composite materials, http://www.performance-composites.com/carbonfibre/mechanicalproperties_2.asp, accessed: 2016/02/29.
- [24] J.N. Reddy, *An Introduction to the Finite Element Method*, McGraw-Hill, New York, 2006.
- [25] A. Logg, K.-A. Mardal, G. Wells (Eds.), *Automated Solution of Differential Equations by the Finite Element Method: The FEniCS Book*, in: *Lecture Notes in Computational Science and Engineering*, Springer, 2012.
- [26] I.Y. Solodov, N. Krohn, G. Busse, CAN: an example of nonclassical acoustic nonlinearity in solids, *Ultrasonics* 40 (1) (2002) 621–625.
- [27] P.L. Bhatnagar, *Nonlinear Waves in One-dimensional Dispersive Systems*, Oxford University Press, Oxford, 1979.

Publication III

S. Dos Santos, M. Lints, N. Poirot, Z. Farová, A. Salupere, M. Caliez, and Z. Převorovský. Nonlinear Time Reversal for Non Destructive Testing of complex medium : a review based on multi-physics experiments and signal processing strategies. In P. Mazal, editor, *NDT in Progress 2015 - 8th International Workshop of NDT Experts, Proceedings*, pages 31–40. Brno University of Technology, October 2015

Nonlinear Time Reversal for Non Destructive Testing of complex medium : a review based on multi-physics experiments and signal processing strategies

Serge DOS SANTOS¹, Martin LINTS^{1,2}, Nathalie POIROT³, Zuzana FAROVA^{1,4},
Andrus SALUPERE², Michael CALIEZ⁵ and Zdenek PREVOROVSKY⁴

¹ INSA Centre Val de Loire, Unité Mixte de Recherche "Imagerie et Cerveau", Inserm U930, 3 Rue de la Chocolaterie, CS 23410, 41034 Blois cedex, France, serge.dossantos@insa-cvl.fr

² CENS, Institute of Cybernetics at Tallinn University of Technology, Akadeemia tee 21, 12618 Tallinn, Estonia

³ GREMAN CNRS, IUT de Blois, 15 rue de la chocolaterie 41000 Blois, France

⁴ Institute of Thermomechanics AS CR, v.v.i., Dolejskova 5, CZ-18200, Prague 8, Czech Republic

⁵ INSA Centre Val de Loire, Blois Campus; Laboratoire de Mécanique et Rhéologie, 3 rue de la Chocolaterie, CS23410, 41034 Blois, France

Abstract The interaction between an acoustic wave and a complex media has an increase interest for nondestructive testing (NDT) applications. For specific applications using nonlinear imaging, inversion procedure needs specific signal processing techniques and new coding schemes. This paper tends to show how symmetry analysis can help us to define new methodologies and new experimental set-up involving modern nonlinear signal processing tools. Generalized TR (Time Reversal) based NEWS (Nonlinear Elastic Wave Spectroscopy) methods and their associate symmetry skeleton will be taken as an example with some new spatio-temporal signal processing tools. The purpose of this paper is to present the extension of TR-NEWS for skin ageing characterization. Hysteresis behavior coming from the complex loading of the skin has been identified with PM-space statistical approach, usually associate to aging process in NDT. Phenomenological hysteretic parameters extracted will be presented and associated to standard parameters used for skin characterization. As another application of mixing properties in a wide frequency range, new broadband techniques are needed in the domain of the preservation of cultural heritage. The use of TR-NEWS based analysis (10 MHz) combined with a FTIR-based system (wavenumber range from 3650-650 cm⁻¹) has shown a specific property of the tuffeau limestone which is a mix of calcite, SiO₂ and CaSO₄·2H₂O whereas other damaged sample is calcite.

Key words: Ultrasonic Testing (UT), Other Methods, signal processing, TR-NEWS, nonlinear ultrasonic imaging, nonlinear acoustic testing, nonlinear time reversal

1 Introduction

Nondestructive Testing (NDT) of complex media is of increasing importance, not only in aeronautic industry, but also in various areas of industry also including modern biomedical media. A general definition of NDT is a examination, test, or evaluation performed on any type of test object without changing or altering that object in any way, in order to determine the absence or presence of conditions or defects that may have an effect on the usefulness or serviceability of that object[1].

Nondestructive tests are usually conducted in order to measure various characteristics such as size, dimension, configuration or structure, including alloy content, hardness and grain size. NDT, as a technology, has seen significant growth over the past 30 years and is considered today to be one of the fastest growing technologies from the standpoint of uniqueness and innovation.

With the increase of modern signal processing tools observed during the last 20 years, the area of interest of NDT based innovations can be explored in such domain like old or new materials for biomedical, or within the increasing demand of inspection of ancient materials in the domain of cultural heritage. Among these modern signal processing tools, nonlinear signal processing is a new field of research with the aim to optimize the excitation of information coming from nonlinear effects[2, 3]. Within the wide range of possibilities of signal processing methods, those using symmetry properties seems to be more efficient for extraction of a specific information. Various nonlinear methods have been investigated in recent years for the detection of faults and fatigue in carbon-fibre reinforced composite materials and structures. However, there is no universally-agreed rationale for which technique is best suited to the detection of which type of defect. Furthermore, even if such a rationale were to exist, real-world samples potentially contain a variety of defects (e.g. micro-cracking, delamination and disbonding) induced by various damage mechanisms (stress, impact, heat) such that no single nonlinear testing technique can offer the optimum inspection choice in all circumstances[4, 5].

Various nonlinear methods have been developed in recent years for defect detection in complex materials[6, 7]. The most common include harmonic and overtone generation, inter-modulation product generation and resonant frequency shift, also known as Nonlinear Elastic Wave Spectroscopy (NEWS) methods. Consequently, new optimized excitations are needed and, thanks to the analysis of symmetry properties of the system such as reciprocity, nonlinear time reversal[8] and other pulse-inverted (PI) techniques, a wide range of innovation can be proposed[9]. This is the case of TR-NEWS methods that use pulse-inversion and chirp-coded coding schemes[10, 11]. The interaction between an acoustic wave and a complex media has an increase interest for NDT applications, but also for biomedical ultrasound. For specific applications using nonlinear imaging, inversion procedure needs specific signal processing techniques and new coding schemes[12]. Nonlinear techniques use the fact that microcracks and delaminations generate harmonic and/or subharmonic tones of the frequency at which they are excited. As an example, intermodulation product generation which is based on the monitoring of nonlinear wave mixing in the material[7] is an alternative and a potentially more sensitive nonlinear method for defect detection in composites. In order to confirm these results, this paper tends to show how symmetry analysis can help us to define new methodologies and new experimental set-up involving modern nonlinear signal processing tools[13].

There is, however, still a need for applying NEWS in a complex medium where an adequate knowledge of the initial excitation and the geometry of the medium should be known precisely in order to predict the ultrasonic propagation with high efficiency. Consequently, using symmetry invariance, TR-NEWS methods are supplemented and improved by new excitations having the intrinsic property of enlarging frequency analysis bandwidth and time domain scales, with now both medical

acoustics and electromagnetic applications[12]. Among the family of pulse coded excitation, solitonic coding constitutes a new scheme in the sense that solitary waves are the best candidates for pulse propagation in nonlinear and dispersive media[14]. Such spatio-temporal focusing may enable efficient delivery of solitonic optimized excitations to a specific target location within a complex enclosure. This method has the potential to be applied in many real-world contexts where the wish to focus acoustic energy at a location is impractical or impossible. Their robustness during propagation could inform aeronautic end-users during monitoring process of layered; granular, lightweight or functionally graded materials.

The purpose of this paper is also to present the extension of TR-NEWS for skin aging characterization using the nonlinear time reversal signal processing tool known to localize, in a complex medium, sources of nonlinearity potentially responsible of complex material aging. One other aspect related to the problem of complex medium aging is the multiscale aspect of the nonlinear signature which can be studied using PM-space. Since the validation of nonlinear time reversal methods within the NDT community[15], another fields of applications have been investigated recently. One can cite landmine detection, composite and echodentography[16]. The NEWS methods have been shown to improve cracks detection and might, therefore, also be advantageous in medical diagnostic ultrasound applied to echodentography. All of these applications concern aging characterization or degradation in a complex medium. Linear and nonlinear behavior of skin elasticity is measured locally thanks to an acousto-mechanical loading of the skin conducted with INSTRON loading machines specifically optimized for biomaterials. Hysteretic behavior coming from the complex loading of the skin is identified with PM-space statistical approach, usually associate to ageing process in NDT. Phenomenological hysteretic parameters extracted is presented and associated to standard parameters used for skin characterization.

Finally as another application of mixing properties in a wide frequency range, new broadband techniques are needed in the domain of the preservation of cultural heritage. This is an interdisciplinary challenge which needs the expertise of many scientific disciplines as well as chemistry, physic, optics, etc. Advanced signal and image processing for art and cultural heritage investigation is a topic of major interest in order to provide a quantitative source of information to art historians. The Loire Valley in France has a diversified cultural heritage, including monuments where the mainly construction units is stone. Most castles were built with two French highly porous limestone called Richemont and tuffeau limestones. The objective of this paper is to investigate TR-NEWS for skin aging[17] and for tuffeau limestone characterization (Fig.3) which are both subjected to a growing area of research.

2 The Strategy of Symmetry Analysis

Invariance with respect to time is one of the properties of a more general algebraic approach that is applied in physics which uses intrinsic symmetries for the simplification and the analysis of complex systems. Symmetry analysis is a framework of the bases of a systemic approach aimed at using absolute symmetries like Time Re-

versal (TR), reciprocity between emitters and receivers, and others. These methods are highly strategic in the sense that they conduct improvement of the measurements so as to optimize the determination of nonlinear properties extracted with coded excitations (e.g. pulse-inversion PI or chirp-coded processes, etc.) with the virtual increase of the effective bandwidth of the excitation. Coded excitations and signal processing is now considered as an efficient way for imaging the complexity in bio-materials with hierarchical properties[18]. Accurate analysis of nonlinear time reversal systems needs the use of new methods of signal processing[19]. Most of systems used in engineering presents a level of nonlinearity that was considered negligible and included in the small stochastic part of the noise. Modern engineering is developed now by considering this stochastic part of the nonlinear signature as a new vector of information coming from the complex system under study[9]. The huge variety of information extracted from this small stochastic part of the response coming from a complex system induces an increase of uncertainty associate to the linear part. This linear part, with its underlying hypothesis of stationarity and determinism, should be consequently associated to a grater uncertainty if the system under study presents intrinsically a complex structure with mesoscopic properties, memory effects, preconditioning, and aging. Of course, these properties are breaking now the stationarity hypothesis implicitly assumed in any linear signal processing, since linear systems theory dominates the field of engineering. This consequence completely justifies this strategy to use nonlinear signal processing tools.

3 Generalized TR based NEWS multimodal instrumentation

Recent years there has been a considerable development of TR based NEWS methods using invariance with respect to TR and reciprocity, both in numerical and experimental aspects. These methods were practically elaborated as the well-known TR-NEWS methods[20]. Chirp-coded pulse excitation[10, 11] is proposed for improving the SNR of ultrasound imaging. Nevertheless, the chirp-coded pulse elongated that the axial resolution of an ultrasound image. Thus, pulse compression technique is utilized to improve the axial resolution of the images. However, it is still lacking the information about the effects of chirp-coded pulse, which was modulated with different window functions, in conjunction with different strain analysis algorithms upon the qualities of imaging. The aim of this study is development of advanced TR-NEWS methods with chirp-coded excitation for assessing biomechanical properties of porcine skin and for NDT of limestones studied within cultural heritage applications. Improvement of TR-NEWS has been conducted with coded excitation using chirp frequency excitation and the concept was presented and validated in the context of NDE imaging[9]. The chirp-coded TR-NEWS method uses TR for the focusing of the broadband acoustic chirp-coded excitation. The method consist in the successive steps :

- emission of a linear frequency sweep signal (the chirp-coded excitation)
- recording of the response to the emitted signal (the chirp-coded coda)
- computation of the pseudo-impulse response which is the correlation between the chirp-coded excitation and its response

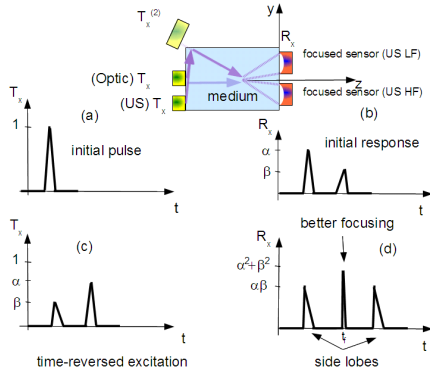


Figure 1: *The four elementary steps of the multi-modal TR-NEWS method : (a) after the excitation of a broadband initial excitation (a short pulse here), the recorded initial response (b) is averaged, filtered, time reversed (c) and rebroadcasted as a time-reversed excitation with the same experimental conditions. The optimized excitation based on this TR-NEWS approach is used for extraction of the local nonlinear signature located in the time domain with respect to the maximum and the side lobes of the crosscorrelation function given by the focused signal (d). The multimodal property come from the fact that the focusing is increase thanks to the use of a broadband multi-physics modality (US LF and HF, optics, etc.).*

- recording of the response to the time-reversed emitted pseudo-impulse excitation (chirp-coded TR-NEWS coda)

In order to describe chirp-coded TR-NEWS process in terms of a time-invariant system, we consider a chirp excitation $c(t)$ send in a medium with impulse response $h_{21}(t)$. As described schematically for a simple medium (Fig.1), side lobes could be interpreted with cross-correlations functions and present a symmetry property with respect to the focusing time t_f . The chirp-coded TR-NEWS method uses TR for the focusing of the broadband acoustic chirp-coded excitation. In order to describe chirp-coded TR-NEWS process in terms of a time-invariant system, we consider a chirp excitation $c(t) = A \cos(2\pi f(t)t)$ where $f(t) = At + f_0$ send in a medium with impulse response $h_{21}(t)$. The chirp-coded coda response $y(t, T)$ recorded for a finite time duration T is given by $y(t, T) = h_{21}(t) * c(t) = \int_{\mathbb{R}} h(t - t', T)c(t')dt'$, where $h(t - t', T)$ is an approximation of the (linear) Green's function that satisfy the linear wave equation. The correlation $\Gamma(t)$, computed during Δt , is given by

$$\Gamma(t) = \int_{\Delta t} y(t - t', T)c(t')dt' \simeq h(t) * c(t) * c(T - t, T), \quad (1)$$

and is called the pseudo-impulse response. $\Gamma(t)$ is also proportional to the impulse response $h(t)$ if $\Gamma_c(t) = c(t) * c(-t) = \delta(t)$. Under these hypothesis, $\Gamma(t)$ can be considered proportional to the impulse response (referred as the coda) of the medium and used for enhancing the TR-NEWS focusing. If $\Gamma(t)$ is time reversed and used as a new excitation, the response $y_{TR}(t)$ of the medium (called chirp-coded TR-NEWS

coda) is then given by

$$y_{TR}(t, T) = \Gamma(T - t) * h_{21}(t) = \Gamma_h(T - t, T), \quad (2)$$

and provides the linear autocorrelation of the system which peaks at $t = T$ and induces a spatial focusing at the receiver. All this theory is valid under linear behavior of the medium represented by its impulse response $h_{21}(t)$. Any source of nonlinearity in the system will result to a perturbation of this method, and will induce additional terms in Eqs.(1-2). When focusing is performed inside a reverberating medium, like the skin or the Tuffeau limestone, the effective aperture of the TR-NEWS process becomes virtually infinite. Indeed, the impulse response computed using previous equations become sharp. This corresponds to an infinite aperture (sources surrounding the focus) producing a focal area used for analyzing the medium.

4 TR-NEWS for skin imaging monitoring

The measurement of skin's mechanical properties (nonlinearity, anisotropy, and viscoelasticity) is important in several fields, including medicine and cosmetics, and present a huge dispersion depending on age, gender, physical size of individual and location on the body (forearms, face, etc). Small changes in the mechanical properties are very sensitively reflecting many diseases. Their influence on the appearance of aging, and their role indicating disease and pathologies is also a societal goal of biomechanical research[17, and ref. therein]. Hysteresis is a phenomenon that occurs in ferromagnetic and ferroelectric materials, as well as in the deformation of some mesoscopic materials, which are flexible or compressible. For example, sand rock[21], which is one of the example of nonclassical nonlinear materials, for which hysteresis behavior is one of the key properties. In electronics, hysteresis is produced by positive feedback to avoid an oscillation. Today hysteresis and memory based modeling is one of the most interesting and challenging fields of innovation in many engineering applications such as actuators. It seems to be a promising way to understand mesoscopic properties of biomechanical materials. Like porous materials characterized by anisotropy, nonlinearity, hysteresis and susceptibility to fluid sorption, we propose in this paper to study human skin with a multiscale model where each state is defined by a set of internal parameters acting on the element. The other consequence is a pragmatic analysis swarming by phenomenological approaches in the family of PM models. The accurate extracted information coming from such systems needs to be associated to the symmetry hypothesis of the underlying mesoscopic structure with respect to scaling effects responses.

The behavior of PM space responses with respect to the optimized various types of signals with the PM space theory was studied. The PM space model has a prominent future in the modeling of viscoelastic behavior of complex materials. It has been recently proposed for understanding physical mechanism including porosity, amorphous or crystalline bonding material and pre-existing cracks, magnetics, magnetostrictive and shape memory, and smart structure components. With this representation and its identification and classification, the physical response (electrical for electromagnetic relays, or acousto-mechanical biomaterial like the skin) can

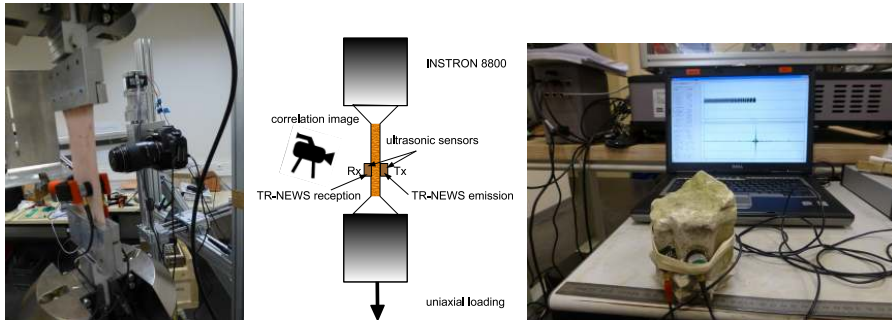


Figure 2: *TR-NEWS experimental set-up for acousto-mechanical imaging of the porcine skin aging (a,b) and for the aging characterization of Tuffeau limestones*

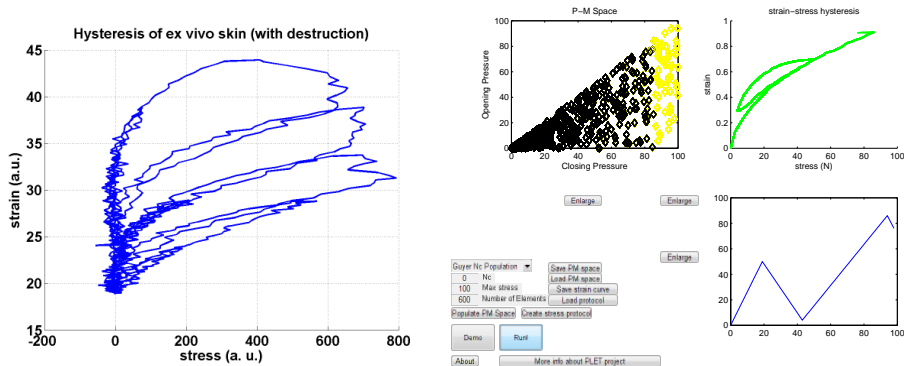


Figure 3: *Skin PM space for memory analysis extracted from hysteretic strain-stress measurements conducted on ex vivo porcine skin. Optimization of the strain-stress curve induces a PM space with 600 hysterons distributed along a Guyer distribution[17]. This original result constitutes the first PM-space identification of viscoelastic and/or hysteretic properties of the skin under uniaxial loading.*

be predicted. Since the strain-stress characteristic of porcine skin under increasing loading is characterized by hysteretic behavior, the preconditioning signature will be investigated with the objective of extracting the memory of the skin[18].

5 Cultural heritage and new NDT multimodal imaging

Electromagnetic waves with Terahertz (THz) frequencies or corresponding sub-millimeter wavelength are associated to the range between infrared and microwaves. These properties give to the THz frequency range an interesting future for new applications in NDT. Besides security applications, THz technologies for NDT are about to enter markets as pharmaceuticals and the composite industries[22], but also for studying NDT on historical heritage. Structural maintenance of historical buildings requires knowledge based strategies to keep under control all parameters governing the structural integrity of these historical buildings, and particularly a robust mon-

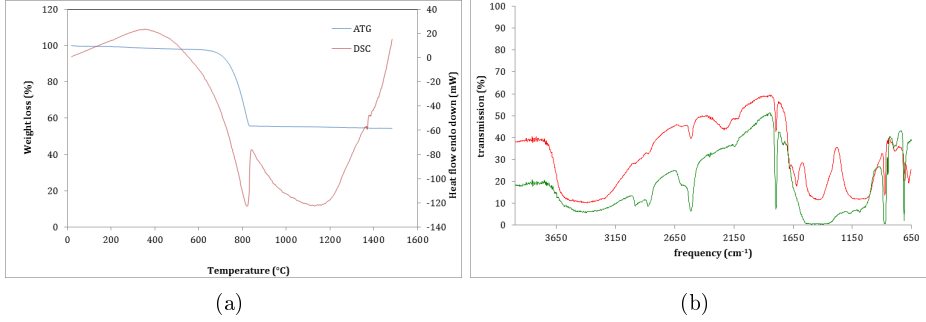


Figure 4: (a): ATD/DSC analysis of the Tuffeau limestone. The slope temperature was chosen to 10°C/mn. The transition observed at 800°C corresponds to the CaCO₃ decomposition. (b): FTIR analysis performed in the frequency range [3650:650]cm⁻¹ where CaCO₃ vibration modes are identified.

itoring. In order to test TR-NEWS approach for NDT of the fine art objects and the cultural and historical heritage, some preliminary tests have been conducted on Tuffeau limestones. The objective is to confirm the interest of using multi-physics laser based imaging methods for low-cost ultrasound sensor for the detection of defects[23].

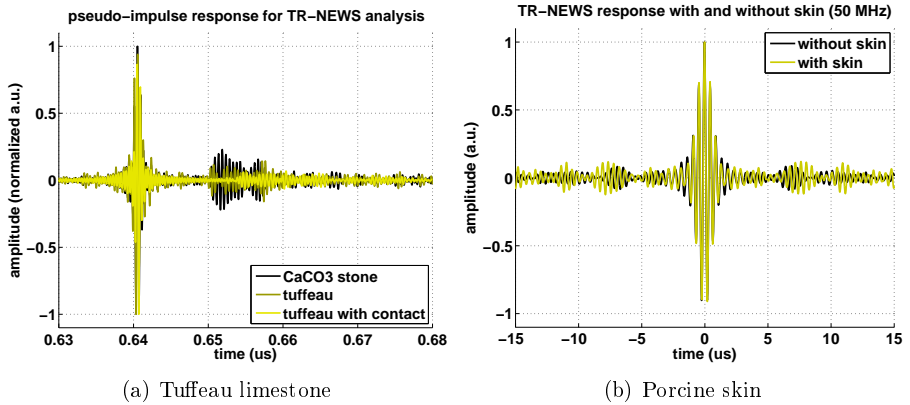


Figure 5: TR-NEWS pseudo impulse response (a) and cross correlation function (b). The skin signature is located near the maximum of the crosscorrelation function.

As seen in Fig.5, the chirp-coded excitation $c(t)$ with $\Delta f \in [0.1 : 1.5]$ MHz is plotted in the time domain with $\Delta t = \frac{N}{f_c} = \frac{64000}{50e6} = 1.28$ ms. The pseudo-impulse response given by Eq.1 is plotted in the time domain after filtering with a 20.75 MHz low-pass filter and $N_a = 148$ averages. The pseudo-impulse properties has been compared in the time and the frequency domains. The reverberant properties (in the time domain) of the skin and the Tuffeau limestone have been reached as observed in (a).

6 Conclusions and perspectives

The use of TR-NEWS based analysis (50 MHz) combined with a FTIR-based system (wavenumber range from 2000-800 cm^{-1}) has shown a specific property of the tuffeau limestone which is a mix of calcite, SiO_2 and $\text{CaSO}_4 \cdot 2\text{H}_2\text{O}$ whereas other damaged sample is calcite. In the future, the ultrasound nonlinear imaging system should be used on human subjects to demonstrate the feasibility of collecting *in vivo* data. The objective to extend this modern approach to skin and human brain, from whose memory effects are currently admitted, gives to this approach a promising future for modern engineering, and medical biomechanical imaging. Concerning cultural heritage applications, we believe that TR-NEWS and its multi-modal aspect including US and FTIR techniques will benefit art collection community as a whole, and further emphasize scientist's contribution to the cultural heritage as well.

7 Acknowledgments

This work is supported by the Région Centre-Val de Loire under the PLET project.

References

- [1] C. Hellier, *Handbook of Nondestructive Evaluation, Second Edition*. McGraw-Hill Professional, 2012.
- [2] E. N. Janssen *et al* , “Dual energy time reversed elastic wave propagation and nonlinear signal processing for localisation and depth-profiling of near-surface defects: A simulation study,” *Ultrasonics*, vol. 51, no. 8, pp. 1036 – 1043, 2011.
- [3] S. Park, *et al* , “Evaluation of residual tensile strength of fire-damaged concrete using a nonlinear resonance vibration method,” *Magazine of Concrete Research*, vol. 67, pp. 235–246, 2014.
- [4] J. Jingpin, *et al* , “Micro-crack detection using a collinear wave mixing technique,” *NDT & E International*, vol. 62, p. 122, 2014.
- [5] J. Jiao, *et al* , “Evaluation of the intergranular corrosion in austenitic stainless steel using collinear wave mixing method,” *NDT & E International*, vol. 69, pp. 1–8, 2015.
- [6] K. Van Den Abeele, *et al* , “Quantification of material nonlinearity in relation to microdamage density using nonlinear reverberation spectroscopy: Experimental and theoretical study,” *The Journal of the Acoustical Society of America*, vol. 126, no. 3, pp. 963–972, 2009.
- [7] P. Armitage and C. D. Wright, “Design, development and testing of multi-functional non-linear ultrasonic instrumentation for the detection of defects and damage in CFRP materials and structures,” *Composites Science and Technology*, vol. 87, pp. 149 – 156, 2013.
- [8] M. Frazier, *et al* , “Nonlinear time reversal in a wave chaotic system,” *Phys. Rev. Letters*, vol. 110, p. 063902, 2013.

- [9] S. Dos Santos, *et al* , “Nonlinear signal processing for ultrasonic imaging of material complexity,” *Proc. of the Estonian Academy of Sciences*, vol. 59, pp. 301–311, 2010.
- [10] J. Liu and M. F. Insana, “Coded pulse excitation for ultrasonic strain imaging,” *Ultrasonics, Ferroelectrics, and Frequency Control, IEEE Transactions on*, vol. 52, pp. 231–240, 2005.
- [11] H. Peng and D. C. Liu, “Enhanced ultrasound strain imaging using chirp-coded pulse excitation,” *Biomedical Signal Processing and Control*, vol. 8, pp. 130–141, 2013.
- [12] S. Dos Santos, *et al* , “Time reversal based new methods for localization and classification of nonlinear vibrations in bio-mechanical media,” in *20th International Congress on Sound & Vibration : ICSV20, Bangkok : International Institute of Acoustics and Vibration*, M. Crocker and M. Pawelczyk, Eds., 2013.
- [13] V. Sanchez-Morcillo, *et al* , “Spatio-temporal dynamics in a ring of coupled pendula: Analogy with bubbles,” in *Localized Excitations in Nonlinear Complex Systems*, Springer International Publishing, 2014, vol. 7, pp. 251–262.
- [14] M. Lints, *et al* , “Simulation of solitary wave propagation in carbon fibre reinforced polymer,” *Proc. of the Estonian Academy of Sciences*, vol. 64, pp. 297–303, 2015.
- [15] X. Guo, *et al* , “Detection of fatigue-induced micro-cracks in a pipe by using time-reversed nonlinear guided waves: A three-dimensional model study,” *Ultrasonics*, vol. 52, p. 912, 2012.
- [16] S. Dos Santos and Z. Prevorsevsky, “Imaging of human tooth using ultrasound based chirp-coded nonlinear time reversal acoustics,” *Ultrasonics*, vol. 51, no. 6, pp. 667 – 674, 2011.
- [17] S. Dos Santos, *et al* , “Skin hysteretic behavior using acousto mechanical imaging and nonlinear time reversal signal processing,” in *Proceedings of the 22nd International Congress on Sound and Vibration, Malcolm J. Crocker Marek Pawelczyk, Francesca Pedrielli, Eleonora Carletti, Sergio Luzzi*, Eds., 2015.
- [18] S. Dos Santos and J. Chaline, “Symmetry analysis for nonlinear time reversal methods applied to nonlinear acoustic imaging,” in *to be published in proc. of the 20th International Symposium on Nonlinear Acoustics*, A. C. Proceedings, Ed., 2015.
- [19] E. N. Janssen and K. Van den Abeele, “Dual energy time reversed elastic wave propagation and nonlinear signal processing for localisation and depth-profiling of near-surface defects: A simulation study,” *Ultrasonics*, vol. 51, pp. 1036 – 1043, 2011.
- [20] T. Ulrich, *et al* , “Time reversal and non-linear elastic wave spectroscopy (TR-NEWS) techniques,” *International Journal of Non-Linear Mechanics*, vol. 43, no. 3, pp. 209 – 216, 2008.
- [21] R. A. Guyer, *et al* , “Hysteresis, discrete memory, and nonlinear wave propagation in rock: A new paradigm,” *Phys. Rev. Lett.*, vol. 74, pp. 3491–3494, 1995.
- [22] P. U. Jepsen, *et al* , “Thz spectroscopy and imaging – modern techniques and applications,” *Laser Photonics Rev.*, vol. 5, pp. 124–166, 2011.
- [23] F.-J. García-Diego, *et al* , “Development of a low-cost airborne ultrasound sensor for the detection of brick joints behind a wall painting,” *Sensors*, vol. 12, pp. 1299–1311, 2012.

Publication IV

M. Lints, S. Dos Santos, C. Kožená, V. Kůs, and A. Salupere. Fully synchronized acoustomechanical testing of skin: biomechanical measurements of nonclassical nonlinear parameters. In *24th International Congress on Sound and Vibration, 23–27 July, 2017, London*, number 867. ICSV, International Institute of Acoustics and Vibrations, 2017

FULLY SYNCHRONIZED ACOUSTOMECHANICAL TESTING OF SKIN: BIOMECHANICAL MEASUREMENTS OF NONCLASSICAL NONLINEAR PARAMETERS

Martin Lints

INSA Centre Val de Loire, Blois Campus; COMUE "Léonard de Vinci", U930 "Imagerie et Cerveau" Inserm, 3 rue de la Chocolaterie, CS23410, 41034 Blois, France

*Institute of Cybernetics at Tallinn University of Technology, Akadeemia tee 21, 12618, Tallinn, Estonia
email: martin.lints@cens.ioc.ee*

Serge Dos Santos

INSA Centre Val de Loire, Blois Campus; COMUE "Léonard de Vinci", U930 "Imagerie et Cerveau" Inserm, 3 rue de la Chocolaterie, CS23410, 41034 Blois, France

Colette Kozena, Vaclav Kus

Czech Technical University in Prague, FNSPE, Brehova 7, CZ-11519, Prague, Czech Republic

Andrus Salupere

Institute of Cybernetics at Tallinn University of Technology, Akadeemia tee 21, 12618, Tallinn, Estonia

An accurate description of soft biomechanical tissues is an open problem in many fields, with applications ranging from medical imaging and characterisation of tissue aging to medical simulations. Skin is one of these highly complex tissues which is difficult to model due to its non-classically nonlinear effects such as hysteresis, memory effects and viscoelasticity. A promising model for describing the mechanical behaviour of skin is the Preisach–Mayergoyz model.

The goal of this paper is to present a fully synchronised acoustomechanical method for finding the elasticity and hysteresis parameters of an *ex vivo* skin sample. The coupled test equipment enables to measure nonclassical nonlinearity of porcine skin using a novel setup for mechanically loading a test object and conducting ultrasonic measurements in a synchronised fashion. The skin sample is uniaxially loaded into quasistatic tension with a sinusoidal load path of increasing amplitude and offset. Ultrasonic tests up to 5 MHz range are conducted along the thickness of the sample. The mechanical extension forms the hysteresis loops in the strain-stress plane while the ultrasonic testing equipment with the Time Reversal – Nonlinear Elastic Wave Spectroscopy signal processing method focuses the high intensity acoustic energy to measure the hysteresis and elasticity parameters of skin under various mechanical loadings. The multiscale properties of the skin are revealed from the hysteresis measurements from both synchronised data sets. This test setup could also be used for other kinds of nonclassically nonlinear materials.

Keywords: skin, acoustomechanical testing, hysteresis, nonlinearity

1. Introduction

A novel testing method is developed for measuring the parameters for a mechanical model for the skin using modern ultrasonic Non-Destructive Testing (NDT) methods coupled with mechanical excitations. Skin is a multiscale material with complex properties, including memory effects, hysteresis, creep, and nonlinearity [1, 2]. Its mechanical behaviour is here modelled by Preisach–Mayergoyz

(PM) hysteresis model [3], for which finding parameters can be difficult due to the number of model parameters and large variance between material samples [4].

Accurate characterization of the properties of the skin tissue could be valuable for surgery simulation, medical ultrasonic imaging, disease diagnostics, research on skin aging and skin damage and many other problems in medicine and cosmetics. Skin properties can have large variance between people or even location on the body of a person and in time, making measurements complex [5].

Several approaches have been used to measure the biomechanical properties of the skin and its accurate description remains to be an open research problem. In previous studies it has been found that using computer optimization routines, it is possible to find good parameter estimates for the PM hysteresis model to describe the mechanical parameters of skin under tension test. The works preceding this paper have discussed biomechanical properties, memory and aging effects of skin and statistical determination of PM parameters for various statistical distributions [6, 7].

In this paper a novel testing apparatus is presented which can be used to measure the nonlinear and hysteresis properties of the skin tissue *ex vivo*. The mechanical and acoustical excitations of a skin sample are coupled to probe the nonlinear mechanical effects of skin. The synchronization of different measurement devices allows an even further optimization of the mechanical parameter search. The automatic coupling between the different devices enables to speed up the testing process, to have finer control over complex relaxation and viscoelasticity effects. The automation of the measuring process allows to measure statistical distribution of the mechanical properties of the test objects, which can additionally depend on the loading, extension, their history or time properties. The acoustical measurement of the test object for this setup prototype utilizes the Time Reversal – Nonlinear Elastic Wave Spectroscopy (TR-NEWS) ultrasonic testing method [8, 9].

2. Experimental setup and theory

The acoustomechanical test setup (Fig. 1) consists of Camera IDS, 1:2.8 50mm \varnothing 30.5 TAMRON lens and an Electromechanical Load Frame MTS Criterion model C43, with a load cell MTS model LPB.502, max 500N, sensitivity 2.055 mV/V. The TR-NEWS Data Acquisition (DAQ) system is designed by Juvitek TRA-02 (0.02 – 5 MHz). For synchronization and amplification, amplifier ENI model A150 (55 dB at 0.3–35 MHz), pulse generator GPG-8018G as pulse extender. Chosen sensors were shear wave transducer Technisonic ABFP-0202-70 (2.25 MHz) for emission and longitudinal wave transducer Panametrics V155 (5 MHz) for reception.

In the test setup prototype, the timestamps of the ultrasonic tests are used as synchronization points. The load frame, camera and load cell are controlled by one computer, the TRA-2 DAQ by another. Amplifier is used to amplify the signals from the TRA-2 to the transmitting shear wave transducer. For the synchronization, the TRA-2 emits a short sync pulse whenever it is in transmission, which is extended and amplified by a signal generator and then fed into the load frame digital input. The software controlling the load frame reads this input signal to write the synchronization points (as date time group and time vector point) into the experiment file. On the TRA-2 side (acoustic measurement), the synchronization is conducted similarly: the experiment output files have the current date time group in the filename. In post-processing, the strain from video is calculated and all the signals, including acoustic measurement points, are synchronized.

Since the TR-NEWS procedure relies on two transmissions for one measurement, then two synchronization pulses are sent by TRA-2 per one full TR-NEWS measurement, which is counted accordingly by the load frame controlling software. In future, a more optimal solution would be to control all of the experiment by a single computer and solve the synchronization purely in software or establish a two-way communication between the controlling computers. For the prototype, the TRA-2 controlling computer is acting as the master and the one controlling the load frame acts as the slave. The prototype setup has room for improvement on procedural aspects, but this does not affect the outcome of the experiments.

To start the experiment, the extension load path is imported into the load frame controller. Arbitrary load paths, within physical limits, are possible. The load frame starts moving when the first full TR-NEWS test is completed. After that it follows the prescribed path, stopping for the duration of each new TR-NEWS test. Since the TR-NEWS test is automated and can be conducted fully by a single click of a button, then this results in only short (~ 8 s) plateaus in the extension for the duration of ultrasonic test. The possibility of arbitrary load path enables to investigate the influence of loading speed, which can be important in analysing the energy dissipation mechanism of skin [7]. In this study, a quasistatic loading is used.

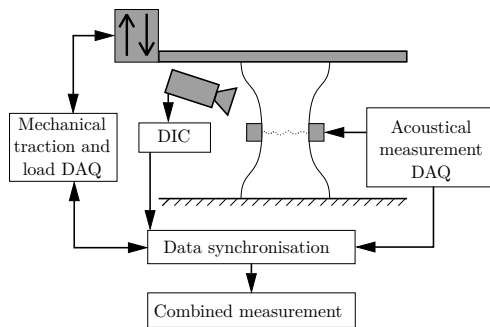


Figure 1: Coupling of the mechanical and acoustical measurements (DIC – Digital Image Correlation)

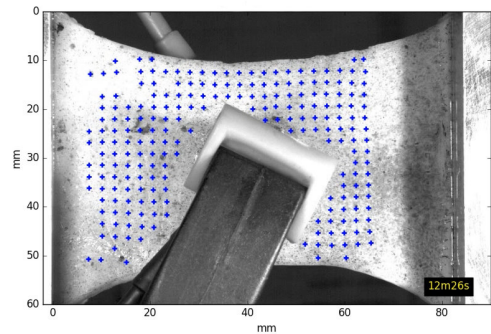


Figure 2: DIC frame with displacement markers added in post-processing. The extension is toward right (video available at [10]).

2.1 Digital image correlation

It is difficult to extend the skin sample in the load frame to result in uniform strain in the sample. This is because skin is not homogeneous, it has varying mechanical properties and the clamps used to grip the skin can damage it near the clamp or it can slip out. For these reasons, a more accurate way of measuring the displacement field is needed. Here the Digital Image Correlation (DIC) method is used [11]. Therefore, the extension is filmed, and the images are processed to reveal the displacement field of the region of interest, frame by frame. Although commercial and open-source solutions exist for DIC, a new prototype code was developed in Python for flexibility reasons, making use of packages *scipy* [12] and *scikit-image* [13] for the data and image processing (Fig. 2). Video is available at [10].

2.2 Preisach–Mayergoyz model for hysteresis in skin

The PM hysteresis model was originally developed for ferromagnetic and ferroelectric materials, but later found use in nonequilibrium dynamics of mesoscopic materials [6, 14, 15] and from there to various applications concerning distributed microdamage in materials [16]. In addition to hysteresis itself, this model allows to describe the properties of elasticity and nonlinearity in the material [17]. When microdamage is present in biological materials, high levels of nonlinearity, including hysteresis, is found.

The PM hysteresis model assumes that the material is composed of a large number of small elastic particles (units, cracks, elementary cells etc.). These elementary cells, or hysterions, are Preisach's operators $\hat{\gamma}_{P_c, P_o}$. The hysterions can be in closed or open state and parameters P_c and P_o represent the

hysterions' closing and opening values ($P_o \leq P_c$). The hysteron can be expressed as follows:

$$\hat{\gamma}_{P_c, P_o}(u(t)) = \begin{cases} -1, & u(t) \leq P_o, \\ 1, & u(t) \geq P_c, \\ k, & u(t) \in (P_o, P_c), \end{cases} \quad (1)$$

where $u(t)$ is an input signal and

$$k = \begin{cases} 1, & \text{if } \exists t^* : u(t^*) > P_c \text{ and } \forall \tau \in (t^*, t), u(\tau) \in (P_o, P_c), \\ -1, & \text{if } \exists t^* : u(t^*) < P_o \text{ and } \forall \tau \in (t^*, t), u(\tau) \in (P_o, P_c). \end{cases} \quad (2)$$

Applying the input signal $u(t)$, the PM space output $y(t)$ is described and results the integrated stress contribution from the skin, which is composed of a large number of hysterons, which is then expressed as a linear combination of final number of hysterons in the discrete case, $y(t) = \sum_{i=1}^N \mu(P_{c_i}, P_{o_i}) \hat{\gamma}_{P_{c_i}, P_{o_i}}(u(t))$, or in the continuous case $y(t) = \int \int_{P_o \leq P_c} \mu(P_c, P_o) \hat{\gamma}_{P_c, P_o}(u(t)) dP_c dP_o$, where $\mu(P_c, P_o)$ is probability function and $u(t)$ is the input signal, and N is the number of hysterons of the PM space. The distribution μ of PM space could be one of the following: random distribution, normal random, Guyer distribution used for PM space characterisation of rocks [18], or von Mises distribution of fibers [7]. Main task in the field of elasticity PM space modeling is the identification of probability density function $\mu(P_c, P_o)$. The primary goal is to determine the density of hysterons in PM space only from the knowledge of hysteresis curve and the input signal corresponding to the loading protocol.

For the purposes of this study, PM space model can be used to describe the multiscale properties of the porcine skin test object: i) large amplitude, quasistatic deformation is induced by the load frame; and ii) small amplitude, high-frequency wideband deformation is induced by the TR-NEWS ultrasonic testing. In the simplest theory, the hysteresis loops should be self-similar regardless of their amplitude. Supposing that an ultrasonic testing is conducted inside the large-scale quasistatic hysteresis loop, then the corresponding hysteresis loops should look like in Fig. 3. The small scale hysteresis (from ultrasonic measurement) should indicate the density of hysterions near that particular small region (region inside the small hysteresis loop) of the current quasistatic strain and stress.

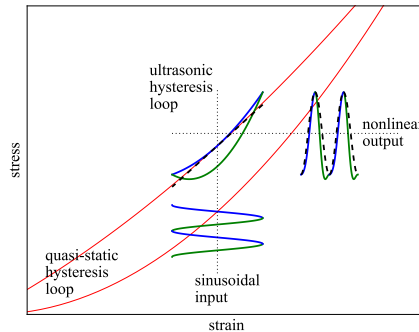


Figure 3: Illustration of acoustomechanical measurement of multiscale hysteresis properties. The material nonlinearity and hysteresis is measured using ultrasonic small amplitude input at the stress and strain level reached with quasistatic large amplitude excitation.

2.3 TR-NEWS signal processing

There has been recent active research on modeling nonclassically nonlinear effects in biomaterials using memory-based phenomenological approaches. Nonclassically nonlinear effects can show

aging and degradation in mesoscopic materials and biomaterials (such as teeth [19], skin and bone). TR-NEWS testing method can take advantage of multimodal ultrasonic imaging to study the mechanical properties of materials under the PM model. Nonlinear time reversal methods provide the means to detect, localize and image the structural damage in a complex medium, thanks to the use of advanced signal processing techniques based on multiscale analysis and multimodal imaging. In TR-NEWS the reverberant properties of a test object are advantageous for the signal-processing induced ultrasonic focusing, due to the method relying on internal reflections for the wave focusing process. Consequently it is suitable for use in multiscale skin mechanical properties' characterisation.

The first step of the TR-NEWS signal processing is the transmission and reception of a chirp (or broadband) signal in the test object. In this work, the chirp signal span from 0 to 5 MHz linearly. The cross-correlation function between the sent and received signals contains the information of the internal reflections, due to orthogonality of the changing harmonic component of the chirp signal. Thereafter the cross-correlation is time-reversed and resent in the same direction as the chirp. The time-reversal of the cross-correlation (information of internal reflections) produces a wave focusing at the receiving transducer, containing the main signal and its sidelobes. Additional optimization possibilities of the TR-NEWS method are available using delayed TR-NEWS method [9].

In presence of nonlinear effects in the test object, the symmetry breaking of TR-NEWS signal could be measured by the "loss of symmetries". In other words, the sidelobes of the TR-NEWS focused signal could contain the information about the nonlinearities, including hysteresis, in the material properties.

3. Results

Figure 4 compares the strain calculated from extension, strain from image processing and the loading. The test sample is excited with sinusoidal excitation with increasing amplitude and base value. In random times during the test, the extension is stopped for 8 seconds to conduct the TR-NEWS measurement. These measurement points are shown by the plateaus in extension data and also by points in Fig. 5. During each measurement, a precise and discrete time moment is captured by acoustic and mechanical test setups which is later used to synchronize the measurement data.

The strain calculated from the video follows closely the features in the load frame extension data and matches well with load frame loading data. Moreover, the strain from the image correlation shows physical features of the test sample which the load frame extension cannot capture, such as viscoelasticity and relaxation under load. At around 500 seconds of the testing time (Fig. 4), the skin reaches its elastic limit and starts to slip out of the load frame clamps.

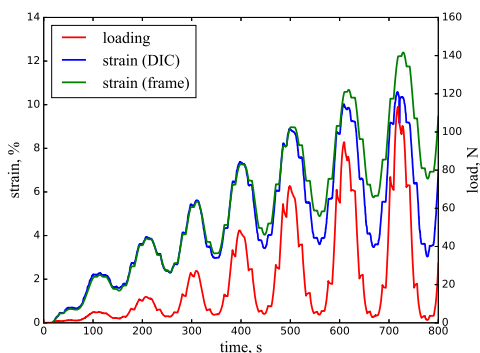


Figure 4: Strain calculated from load frame extension versus strain from DIC and loading of the material

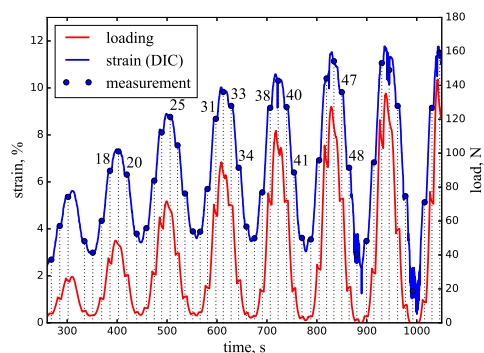


Figure 5: Strain and load at a selection of measurement points

3.1 Hysteresis curves

The test setup allows to compute successfully the true strain and the actual hysteresis curves. Fig. 6 shows the hysteresis curves computed with the strain calculated from the load frame extension versus strain calculated from the video by DIC. It is apparent that the true strain, calculated from the video, contains noise but makes more physical sense. The TR-NEWS measurement points, where extension is stopped, show the relaxation effects in the true strain (from video), while the load frame strain cannot show that (Fig. 7). This results in smaller true hysteresis curve area, accuracy of which is very important for parameter fitting with PM space theory. Additionally, when the loading is resumed, the true strain hysteresis curves continue along the old path. Therefore the true strain is what should be mainly used for hysteresis analysis. The noise of the true strain can be optimized by better lightning conditions and camera setup and by taking care in selecting the region of interest in the video file to be analysed. Additionally, a low pass filter could be experimented with for smoothing the noise in the DIC data. The nonclassically nonlinear model can be improved to take into account the viscoelastic effects, such as the relaxation visible in these results. The TR-NEWS measurement points are shown by round markers in Fig. 7. These markers indicate at which load and strain values the multiscale measurements (Section 2.2) are conducted.

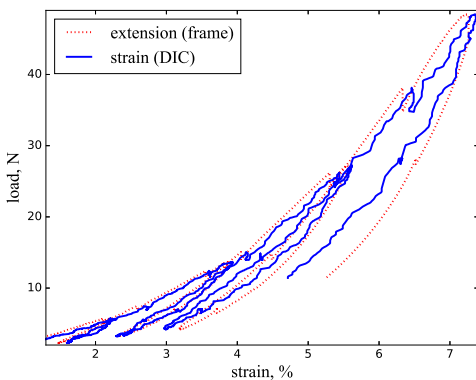


Figure 6: Hysteresis loops using the true strain calculated by DIC, compared with hysteresis from load frame data

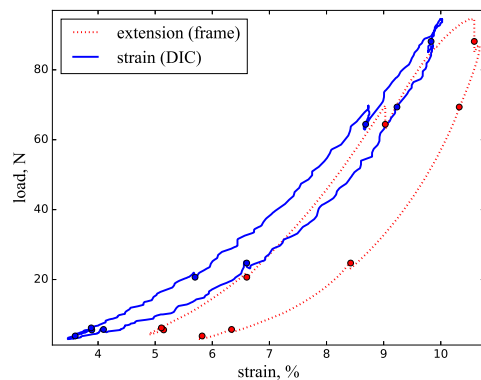


Figure 7: A single hysteresis loop in the test in the timespan from 550 s until 675 s, with round markers showing the synchronization points of TR-NEWS measurements

3.2 TR-NEWS measurements of nonlinearity

In the experiment shown here, 73 TR-NEWS measurements were captured, at various strains and stresses. Fig. 5 shows a selection of these points. Comparing some TR-NEWS measurements taken at approximately the same strain levels (points 18, 20, 34, 41 and 48 in Fig. 5), it can be seen from their TR-NEWS focusing sidelobes in Fig. 8 that as the cycle count of the skin sample increases, the sidelobe part of the TR-NEWS signal increases, which can indicate damage in the material.

Although previous measurements were taken at the same strain, their stresses were different (Fig. 5). Nevertheless the changing stress at constant strain is not what changes the sidelobe amplitude: comparing the TR-NEWS measurements for approximately constant stress (points 25, 31, 33, 38, 40 and 47 in Fig. 5), then again as time and damage increase, the amplitude of the sidelobe part of the TR-NEWS measurements rise (Fig. 9), indicating the increase of nonlinearities.

The increase of sidelobe amplitude with increasing damage to the skin sample is small but sure. In the future experiments, larger sample size needs to be analysed and the nonlinearity linked to some measure of hysteresis in the loops. It would also be possible to use different methods of investigating

the nonlinearity using advanced optimization techniques of TR-NEWS signal processing, such as pulse inversion or delayed TR-NEWS [9].

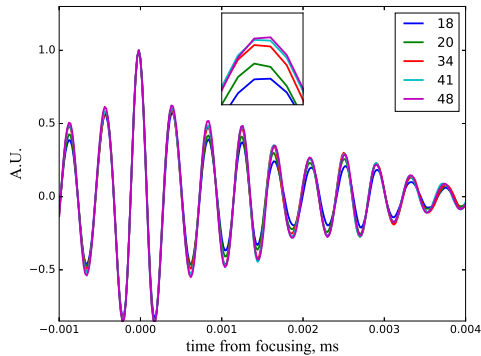


Figure 8: TR-NEWS focusing measurements at roughly the same strain, showing differences

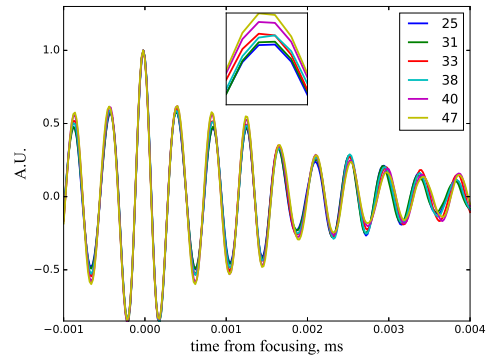


Figure 9: TR-NEWS focusing measurements at roughly the same stress, showing differences

4. Conclusion

A novel fully synchronized acoustomechanical testing setup has been presented here, which links together a load frame with arbitrary extension load path, load measurement, video extension measurement for determining true strain field for the soft test object, and modern ultrasonic nonlinear testing method. This setup allows to measure the nonlinearity, hysteresis, creep and other complex multiscale mechanical properties of the test object in an automated way. The automation of the measurement is useful for the future use of high-speed measurements for determining the statistical distributions of the mechanical properties of the test object. This measurement setup is promising for wide variety of test objects, including but not limited to skin, and enables to also use other modern ultrasonic testing methods.

The purpose of this work was to present the acoustomechanical measurement system. The full analysis of the measurement results for skin or other complex materials using this system is left for the future. Therefore the results presented here have not yet been optimized and instead serve as demonstration for the multiscale hysteresis experiments which can be conducted on a complex nonclassically nonlinear material, such as skin. A more focused experimental work is needed to analyse the nonlinearities in the skin sample and characterize the skin tissue fully using statistical PM hysteresis theory.

Possible improvements to the measurement system presented here include controlling all of the measurement equipment by a single computer and solving the synchronization in software, having an option of preselecting the load frame extension or load values at which the TR-NEWS measurements are conducted, and improving the TR-NEWS measurement software to speed up the measurement process to minimize the relaxation effects.

5. Acknowledgments

This research is supported by European Social Funds via Estonian Ministry of Education and Research and Archimedes Foundation through DoRa and Kristjan Jaak Scholarship programmes, Estonian Research Council (project IUT33-24), and by the Région Centre Val de Loire (France) under the PLET project 2013-00083147.

REFERENCES

1. Fung, Y. C., *Biomechanics: Biomechanical properties of living tissues*, Springer-Verlag (1993).
2. Pan, L., Zan, L. and Foster, F. S. Ultrasonic and viscoelastic properties of skin under transverse mechanical stress in vitro, *Ultrasound in Med. & Biol.*, **24**, 995–1007, (1998).
3. Mayergoyz, I. D., *Mathematical Models of Hysteresis and Their Applications*, Elsevier (2003).
4. Hauptert, S., Renaud, G., Rivière, J., Talmant, M., Johnson, P. A. and Laugier, P. High-accuracy acoustic detection of nonclassical component of material nonlinearity, *J. Acoust. Soc. Am.*, **130**, 2654–2661, (2011).
5. Daly, C. Biomechanical properties of dermis, *Journal of Investigative Dermatology*, **79** (Suppl. 1), (1982).
6. Kozena, C., Kus, V. and Dos Santos, S. Hysteresis and memory effects in skin aging using PM space density identification, *2016 15th Biennial Baltic Electronics Conference (BEC)*, pp. 179–182, (2016).
7. Dos Santos, S., Kus, V., Remache, D., Pittet, J., Gratton, M. and Caliez, M. Memory effects in the biomechanical behavior of ex vivo skin under acoustomechanical testings: a multiscale preisach modeling of aging, *Proceedings of the 23rd International Congress on Sound & Vibration*, (2016).
8. Lints, M., Salupere, A. and Dos Santos, S. Simulation of solitary wave propagation in carbon fibre reinforced polymer, *Proc. Estonian Acad. Sci.*, **64** (3), 297–303, (2015).
9. Lints, M., Dos Santos, S. and Salupere, A. Solitary waves for Non-Destructive Testing applications: Delayed nonlinear time reversal signal processing optimization, *Wave Motion*, <http://dx.doi.org/10.1016/j.wavemoti.2016.07.001>, (2016).
10. Lints, M. *Digital Image Correlation video of porcine skin during acoustomechanical testing*. http://homes.ioc.ee/lints/files/MLints2017_skin_ext_DIC.mp4, Accessed: 2017/01/31.
11. Hild, F. and Roux, S. Digital Image Correlation: from Displacement Measurement to Identification of Elastic Properties – a Review, *Strain*, **42** (2), 69–80, (2006).
12. Jones, E., Oliphant, T., Peterson, P., et al., (2001–), *SciPy: Open source scientific tools for Python*. <http://www.scipy.org/>, [Online; accessed 2014-12-08].
13. van der Walt, S., Schönberger, J. L., Nunez-Iglesias, J., Boulogne, F., Warner, J. D., Yager, N., Gouillart, E., Yu, T. and the scikit-image contributors. scikit-image: image processing in Python, *PeerJ*, **2**, e453, (2014).
14. Guyer, R. A., McCall, K. R. and Boitnott, G. N. Hysteresis, discrete memory, and nonlinear wave propagation in rock: A new paradigm, *Phys. Rev. Lett.*, **74**, 3491–3494, (1995).
15. Guyer, R. A. and Johnson, P. A., *Nonlinear Mesoscopic Elasticity: The Complex Behaviour of Granular Media including Rocks and Soil*, WILEY-VCH (2009).
16. Aleshin, V. and Van Den Abeele, K. Micro-potential model for acoustical hysteresis, *Proceedings of the 18th International Congress on Acoustics*, vol. 3, pp. 1859–1862, (2004).
17. Helbig, K. and Rasolofosaon, P. N. J. A Theoretical Paradigm for Describing Hysteresis and Nonlinear Elasticity in Arbitrary Anisotropic Rocks, *Anisotropy 2000*, pp. 383–398, Society of Exploration Geophysicists, (2001).
18. Guyer, R. A. and Johnson, P. A. Nonlinear mesoscopic elasticity: Evidence for a new class of materials, *Physics today*, **52** (4), 30–36, (1999).
19. Dos Santos, S. and Prevorovsky, Z. Imaging of human tooth using ultrasound based chirp-coded nonlinear time reversal acoustics, *Ultrasonics*, **51** (6), 667–674, (2011).

Publication V

M. Lints, A. Salupere, and S. Dos Santos. Simulation of detecting contact nonlinearity in carbon fibre polymer using ultrasonic nonlinear delayed time reversal. *Acta Acust. united Ac.*, 2017. (accepted)

Simulation of detecting contact nonlinearity in carbon fibre polymer using ultrasonic nonlinear delayed time reversal

Martin Lints^{1),2)}, Andrus Salupere¹⁾, Serge Dos Santos²⁾

¹⁾ Tallinn University of Technology, Department of Cybernetics, Akadeemia tee 21, 12618 Tallinn, Estonia. martin.lints@cens.ioc.ee

²⁾ INSA Centre Val de Loire, Blois Campus; COMUE "Léonard de Vinci", U930 "Imagerie et Cerveau" Inserm, 3 rue de la Chocolaterie, CS23410, 41034 Blois, France.

Abstract

A finite element method simulation of a carbon fibre reinforced polymer block is used to analyse the nonlinearities arising from a contacting delamination gap inside the material. The ultrasonic signal is amplified and nonlinearities are analysed using delayed Time Reversal – Nonlinear Elastic Wave Spectroscopy signal processing method. This signal processing method allows to focus the wave energy onto the receiving transducer and to modify the focused wave shape, allowing to use several different methods, including pulse inversion, for detecting the nonlinear signature of the damage. It is found that the small crack with contacting acoustic nonlinearity produces a noticeable nonlinear signature when using pulse inversion signal processing, and even higher signature with delayed time reversal, without requiring any baseline information from an undamaged medium.

1 Introduction

In the past, the use of carbon fibre reinforced polymer (CFRP) has been limited to non-structural parts of high-tech aeronautical products. In recent times, due to the effort of weight reduction and product lifetime enhancement, the application areas of CFRP have widened to the load-bearing parts of the aeronautical, automotive and civil engineering products. Due to the increased demands on the strength of the CFRP products and possible complex failure mechanisms, the Non-Destructive Testing (NDT) methods of CFRP have been an important applied and academic problem.

The complex failure mechanisms of CFRP include microcracking and delamination. Microcracking can occur at lower loads or due to aging and can be difficult to examine using ultrasonic NDT. With increased loading, the damage can evolve to delaminations, a very fine cracking between the layers of the CFRP. These damages are difficult to detect using ultrasonic

methods due to their small thicknesses. The damage can exhibit itself as a contact acoustical nonlinearity (CAN) [1]. A statistical distribution of microcracks or delamination damage in the material could also be described by hysteresis in a continuum material model [2, 3, 4]. This can also be applicable for other materials than CFRP, for example biological tissues [5, 6].

Nonlinear ultrasonic methods known as Nonlinear Elastic Wave Spectroscopy (NEWS) methods, have been in development for detecting and localizing fatigue and micro-crack damage by their nonlinear effects [7, 8]. The detection of harmonic overtones is one of the simplest measures of nonlinearities [9]. Many nonlinear analysis methods not requiring filtering have been developed, for example scaling subtraction method [10, 11] or Pulse Inversion (PI) with its generalizations [12, 13], and applications of Time Reversal (TR) using scattering as new sources.

In this paper we demonstrate how to apply the delayed TR-NEWS signal processing method [14] for detecting the nonlinear signature of a single small crack in CFRP as CAN. In the Finite Element Method (FEM) simulation, the CFRP is modelled as anisotropic, layered medium. The ultrasonic signal is focused by TR-NEWS to the region of the material with the defect. The nonlinear signature of the crack is detected by PI and compared with the delayed TR-NEWS method, which allows to create arbitrary wave envelope at the focusing region of TR-NEWS. It is used here to create an interaction of waves near the damage. The signature of the damage appears as the nonlinear effect of the wave interaction on the contacting crack. This signal processing requires only one transmitting and one receiving transducer. The effectiveness of the delayed TR-NEWS method has been shown in the previous work by physical experiments and simulations in undamaged and linear materials [14]. In this paper, the FEM simulation model is advanced further by including absorbing boundary conditions and the contacting crack defect in the material.

2 Mathematical and simulation model

This section describes the simulation which is based on a physical experiment. It shows some important points about the mathematical model, the delayed TR-NEWS signal processing and the FEM simulation. Detailed information about the delayed TR-NEWS method is available at [14]. The derivation of mathematical and FEM model is discussed more in detail in [15], including the implementation of the absorbing boundary conditions, CAN and comparison of the FEM code used here with linear material code based on FEniCS library.

2.1 Mathematical model

The test object is a CFRP block consisting of 144 layers (Fig. 1). It is composed of fabric woven from yarns of fibre and impregnated with epoxy. The cross-section of the yarns have elliptical shape (Fig. 2) and the material has inclusions of pure epoxy, so a wave propagating through the material will encounter yarns (fibres with epoxy) and areas of pure epoxy.



Figure 1: (Colour online) CFRP block in the test configuration with transmitting transducer on side and receiving on top

The simulation is in time domain, since the TR-NEWS procedure relies on transient echoes and complex wave motion for the wave energy focusing process. Due to the heavy computational cost of time domain simulation, a simple laminate model is used where: i) the material consists of homogeneous layers, ii) each layer has its own elasticity properties, and iii) dispersion arises due to the periodical discontinuity of the material properties. It consists of CFRP layers with $90^\circ/0^\circ$ weave, $45^\circ/45^\circ$ weave and epoxy layer. The thicknesses of the layers are given by random variable functions which reflect the actual structure of the material. The random variable distribution, describing the CFRP structure, is measured from a close-up image of the CFRP test object [15]. This links the distribution of the microstructure inside the actual material with the thicknesses of the layers in the laminate model. It should enable a more realistic simulated material having dispersion effects due to discontinuities.

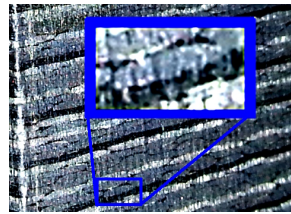


Figure 2: The layered structure of the CFRP with the fabric yarns in tight packing and epoxy in the voids

The three different kind of layers have the following mechanical properties: i) isotropic pure epoxy: $E = 3.7$ GPa, $\nu = 0.4$, $\rho = 1200$ kg/m³; ii) transversely isotropic composite with $0/90^\circ$ weave: $E_1 = E_2 = 70$ GPa, $G_{12} = 5$ GPa, $\nu_{12} = 0.1$, $\rho = 1600$ kg/m³; and iii) transversely isotropic composite with $45^\circ/45^\circ$ weave: $E_1 = E_2 = 20$ GPa, $G_{12} = 30$ GPa, $\nu_{12} = 0.74$, $\rho = 1600$ kg/m³. For the simulation, a laminate model was constructed using 50 pairs of epoxy and carbon fibre layers, where carbon fibre weave direction alternated between each pair.

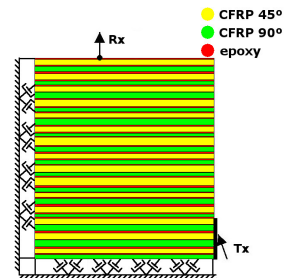


Figure 3: (Colour online) The laminate material model with layers of stochastic thicknesses and absorbing boundary conditions on bottom and left boundaries and four fixed degrees of freedom

The model (Fig. 3) includes Lysmer-Kuhlemeyer absorbing boundary conditions [16] so the wave energy would pass through the simulation region. The absorbing boundary conditions model more closely the corresponding physical experiments, conducted on the corner of a CFRP block. Additionally, the absorbing boundary conditions inhibit the TR-NEWS focusing, since it relies on the internal reflections. Four degrees of freedom are fixed, the rest are free. The simulation model includes a contacting delamination defect in the material near the receiving transducer (Fig. 4). In the simulation, the transmitting shear wave transducer can send maximum 50 kPa pulse at 70° degree angle.

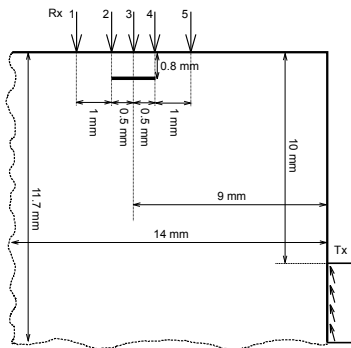


Figure 4: Schematic (not to scale) of the simulation geometry, location of crack, transmitter and receiver points without the layers

2.2 Signal processing

In the physical experiments, on which the simulation is based on, the CFRP block (Fig. 1) was studied using TR-NEWS NDT equipment and signal processing methods [14]. The 2D FEM simulations here reflect it as closely as possible in terms of transducer placement, frequencies and signal processing. The linear chirp excitation ranges from 0 to 2 MHz during 30 μ s, followed by 30 μ s of silence.

The TR-NEWS signal processing method creates a TR focusing by using a reciprocal type of TR [17] in conjunction with linear chirp pulse compression, utilized widely in RADAR and SONAR technology. The reciprocal TR is a two-pass method where for both passes the signal is sent from the same source, enabling to use non-contact measurement equipment on the receiving side. The use of linear chirp as initial excitation and the pulse compression of signal in TR-NEWS results in amplification of the wave energy to a single focused impulse wave. In this sense, the “Time Reversal” used here relies on the internal reflections as virtual transducers for the focusing and describes the signal processing method, which accounts for them accordingly, to create the impulse signal focusing. In the course of the two-pass single TR-NEWS focusing, the *a priori* knowledge of the medium geometry is not needed and the transducer placement can be arbitrary since the signal processing method generates the impulse focusing without any additional information. However, the complete test configuration must remain fixed during both transmission passes of the TR-NEWS procedure.

In short, the TR-NEWS signal processing steps consist of firstly propagating a linear chirp signal $c(t)$ and receiving a response $y(t)$. Then the correlation between sent and received signals Γ is time reversed and re-propagated from the original source in the same configuration. The resulting response $y_{TR}(t)$ is an impulse-signal, which is focused spatio-temporally.

The complete explanation of TR-NEWS steps is available in [14].

PI is an established method for detecting nonlinearities. It has been studied widely and is under constant development [12] and is used here as a comparison with delayed TR-NEWS. The procedure used here involves conducting TR-NEWS measurements with chirps $c(t)$ of positive and negative signs for amplitude (or 180° phase shift) and comparing the focused signals. Differences between the corresponding received TR-NEWS focused signals could indicate the presence of nonlinearities.

Delayed TR-NEWS signal processing is a further development of the TR-NEWS signal processing, which considers a single TR-NEWS focused impulse wave y_{TR} as a new basis which can be used to build arbitrary wave shapes at the focusing by assuming linear superposition principle. This is done by time-delaying and superimposing n time-reversed correlation $\Gamma(T - t)$ signals (Fig. 5 left column)

$$\Gamma_s(T-t) = \sum_{i=0}^n a_i \Gamma(T-t+\tau_i) = \sum_{i=0}^n a_i \Gamma(T-t+i\Delta\tau), \quad (1)$$

where a_i is the i -th amplitude coefficient and τ_i the i -th time delay. In case of uniform time delay the $\Delta\tau$ is the time delay between samples. Upon propagating this $\Gamma_s(t-T)$ through the media according to the last step of TR-NEWS, a delayed and scaled shape of signal at the focusing point can be created. The delayed TR-NEWS signal processing optimization can be used for amplitude modulation, signal improvement and sidelobe reduction [14].

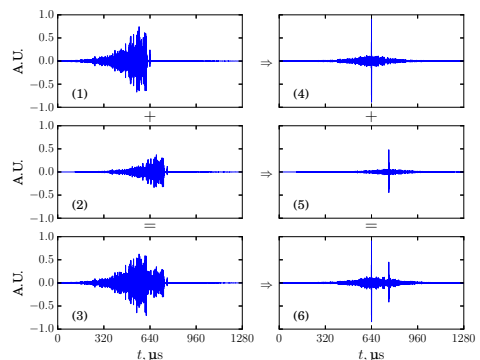


Figure 5: Delayed TR-NEWS signal processing steps starting from the cross-correlation step (left column) and prediction of linear superposition of waves (right column): (1) time reversed cross-correlation, (2) delayed and scaled cross-correlation, (3) linear superposition of two cross-correlations which becomes the new excitation, (4) TR-NEWS focused impulse, (5) delayed and scaled focusing, (6) linear superposition of the two impulse peaks.

It is possible to predict what the delayed TR-NEWS focusing output would be in a linear material (Fig. 5 right column):

$$\begin{aligned} y_{dTR}(t) &= \left[\sum_i a_i \Gamma_c(T - t + \tau_i) \right] * h(t) \stackrel{\text{linearity}}{=} \\ &= \sum_i a_i \Gamma_c(T - t + \tau_i) * h(t) = \sum_i a_i y_{TR}(t - \tau_i). \end{aligned} \quad (2)$$

The purpose of the prediction is twofold. Firstly it can be used to figure out optimal delay and amplitude parameters a_i and τ_i beforehand for the delayed TR-NEWS experiment, using the original focusing peak y_{TR} . Secondly, it could be possible to analyse the differences between the measured delayed TR-NEWS result and its prediction, which acts as a baseline for comparison. The difference could indicate the magnitude of nonlinearity, because the prediction relies on the applicability of linear superposition and is found to be accurate in experiments with linear material [14].

In this work, delayed TR-NEWS is used to create an interaction of focused waves under the receiving transducer. It is proposed that if it happens in a region with a defect or other nonlinearities, then there will be a difference between the recorded and predicted signals. This difference might be used as a new indicator for detecting nonlinear effects near the focusing region [14]. The goal of this work is to test this idea in simulations.

2.3 The FEM simulation model

The simulation program considers 2D wave propagation in a solid material with linear elasticity. The nonlinearity comes from an internal defect, a crack in the computational region (Fig. 4) which can come into contact with itself. This contact nonlinearity has asymmetric stiffness and is therefore nonclassically nonlinear. Since the CFRP is a complex material, then in this work it is modelled as a laminate with anisotropic layers arranged in a periodic manner, described in Section 2.1. Because the physical experiment was conducted on the corner of a large CFRP block, the simulation is also in a semi-infinite quarter-space. The region has two free surfaces for reflection and two absorbing boundaries for the wave energy to escape, which should make the TR-NEWS focusing process more difficult, but realistic.

The constitutive equation of the material itself is linear (although anisotropic). The linear plane strain elastodynamics problem is solved

$$\rho \ddot{u}_i - \sigma_{ij,j} = b_i, \quad (3)$$

where ρ is material density, u_i is displacement component, σ_{ij} is stress component and, b_i is body force

component [18]. Einstein summation convention is used and comma in index denotes spatial derivative. The constitutive equation in the variational formulation is

$$0 = \int_{\Omega} (\sigma_{ij} \delta \varepsilon_{ij} + \rho \ddot{u}_i \delta u_i) dx dy - \int_{\Omega} b_i \delta u_i dx dy - \int_{\Gamma} t_i \delta u_i ds \quad (4)$$

where ε_{ij} is strain and t_i is traction component on boundary. In our case the region Ω is a 2D space and boundary Γ surrounding it a 1D line. The body forces are zero in this simulation. Strain is assumed to be small.

The matrix formulation of the finite element model with damping is

$$M \ddot{\Delta} + C \dot{\Delta} + K \Delta = F, \quad (5)$$

where M is mass matrix, K is stiffness matrix, F is external forcing and Δ is displacement vector [15]. The damping matrix C contains the Lysmer-Kuhlemeyer absorbing boundary conditions [16] as a diagonal matrix, allowing to take advantage of the explicit solution scheme.

Equation (5) is solved for each timestep $\Delta t = 5 \cdot 10^{-10}$ s by explicit central difference scheme

$$\begin{aligned} \left(\frac{M}{\Delta t^2} + \frac{C}{2\Delta t} \right) u_{n+1} &= F_n - \\ \left(K - \frac{2M}{\Delta t^2} \right) u_n &- \left(\frac{M}{\Delta t^2} - \frac{C}{2\Delta t} \right) u_{n-1}. \end{aligned} \quad (6)$$

Each simulation considers a 60 μ s time window. This simulation code was developed in Fortran and Python using f2py [19] and scipy [20] packages. Full details of the FEM simulation model are available in [15].

2.3.1 Contact gap treatment

The goal of this work is to verify if delayed TR-NEWS is able to give information about nonlinear effects in material. For this, one simple CAN defect is introduced near the surface in the region where the TR-NEWS wave is focused (Fig. 4). The crack is straight, with no preload or initial gap. This results in a simple localised nonclassical nonlinearity. Coulomb friction is also applied.

Frictional contact problems can be sensitive to timestep length and loading path [23]. Therefore an explicit solution scheme Eq. (6) is used, which enables to keep timestep and applied contacting forces small [24]. This enables to have a simple contact gap treatment logic. A more precise solution could be expected from an implicit scheme, but that requires also further development of the contact gap treatment and is left for the future. Future refinements could also include thermoelastic contribution to the constitutive equation at the frictional contact gap [3].

Node-to-node contact model is used in FEM analysis [25]. It was chosen because of its simplicity, since we assume small deformations. Moreover, the choice of master and slave surfaces is unimportant for this scheme, unlike the more complex node-to-surface method. Since the defect is horizontal and fully known in advance, the calculation of normal and tangential gap between the nodes is simple. If the position of a node on a slave (lower) surface is (n_x^s, n_y^s) and on master (higher) (n_x^m, n_y^m) , then the normal contact gap is $g_N = n_y^s - n_y^m$ and the tangential gap (offset) is $g_T = n_x^s - n_x^m$. In case of normal penetration of one surface into another, then $g_N > 0$. If there is no penetration, then $g_N \leq 0$. The coefficient of friction is $\mu = 0.6$. The contact gap treatment has to satisfy the Kuhn-Tucker conditions on the crack surface:

$$\begin{cases} g_N \leq 0, \\ \lambda_N = \sigma \cdot n \leq 0, \\ g_N \cdot \lambda_N = 0, \end{cases} \quad (7)$$

where λ_N is the normal force on crack, σ is stress and n is the normal vector of the surface. The normal contact conditions are satisfied using the penalty plus Lagrange multiplier method [26] for the normal forcing. A simpler penalty method is used to satisfy Coulomb friction, which is activated from the second timestep since the beginning of non-slip contact [15]

The contact logic for the node pairs can be summarized by following steps.

- The initial contact forces are zeroed: normal $\lambda_N = 0$ and tangential $\lambda_T = 0$.
- System in Eq. (6) is solved.
- Vector gap functions are found: $g_N = n_y^s - n_y^m$ and $g_T = n_x^s - n_x^m$.
- Normal forcing is updated $\lambda_N = \lambda_N + g_N b$ where b is some big penalty value and $\lambda_N \geq 0$.
- Logic diverges to 3 paths:

No force is applied in case of no contact.

Only normal force is applied if preceding step had no contact or had contact with tangential slip.

Normal and tangential forces are applied if previous iteration had non-slip contact.

- The normal contact condition is verified by setting the penetration value $g_P = g_N$ where $g_N \geq 0$. Then the L^2 -norm of penetration is evaluated $\langle g_P | g_P \rangle < \varepsilon$ where ε is the limiting value for the error due to contact penetration. If the condition is not fulfilled, the iteration is repeated, otherwise new timestep is taken.

3 Results

The signal analysis of the time domain simulation results of the damaged and undamaged medium are compared, describing some analysis measures which could allow to detect the presence of damage as nonlinearity. The simulation follows ultrasonic TR-NEWS NDT procedures where the transducer data is available as time-series, measured at some specific location. The signals are low-pass filtered to keep only the ultrasonic component. Five measurement points are analysed at various distances from the 1 mm crack damage and transmitting transducer (Fig. 4). This simulates an ultrasonic NDT when searching for a nonlinear defect with both PI and delayed TR-NEWS. A video of the displacement fields for TR-NEWS focusing to point 3 in cracked medium is available at [27]. The simulations were also ran for a range of defect sizes from 1 mm downwards. The measurement point 3 was utilized (near the middle of the crack). These simulations compare the sensitivity of PI and delayed TR-NEWS in case of smaller crack sizes.

3.1 TR-NEWS with pulse inversion

Figure 6 shows the TR-NEWS focusing in undamaged CFRP for the receiver positions 1 to 5 (Fig. 4). It is an ordinary TR-NEWS focusing where at the middle of the signal ($t = 30 \mu\text{s}$) is the focusing, surrounded by the sidelobes. There are two aspects to note about this figure. Firstly, the sidelobes shift toward the main focusing and comparatively decrease in amplitude as the receiving transducer position shifts toward the transmitting transducer (from position 1 to position 5), indicating lower noise as the signal gets stronger. Secondly, the sidelobes are symmetrical with respect to the main lobe. This does not happen in nonlinear (damaged) material. The PI results indicate zero nonlinearity and are not shown here.

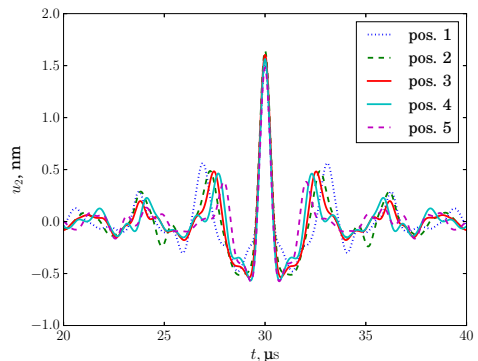


Figure 6: (Colour online) Unnormalized TR-NEWS focusing in simulation of undamaged CFRP

Figure 7 shows the TR-NEWS results of the cracked

CFRP simulation for the receiving transducer positions 1 to 5 (Fig. 4). Here the PI signal processing shows the nonlinearity as difference between TR-NEWS results from initial chirp signals with positive and negative sign. This nonlinear simulation with 1 mm crack exhibits nonlinearity particularly strongly in receiving position 3 (near the middle of the defect). Also, the sidelobes are unsymmetrical with respect to the main lobe. The comparison between left and right side of TR-NEWS focusing has been successfully applied since 2006 [5, 28, 29] to localize sources of nonlinearities.

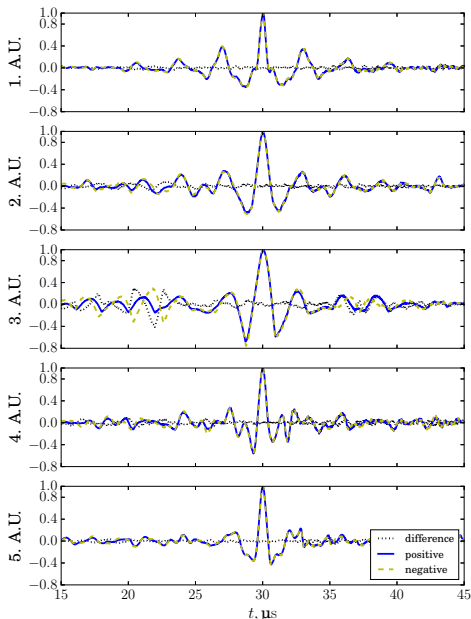


Figure 7: (Colour online) Normalized TR-NEWS focusing of damaged CFRP simulation with PI applied to detect nonlinearities as difference between negative and positive excitations

Figure 8 shows the envelopes of the PI measure of nonlinearity across the five measuring points. The nonlinearity magnitude depends on the measuring point location with respect to the crack: point 3 near the middle of the crack shows strongest nonlinearity, points 2 and 4 show less, and points 1 and 5 show the least.

Figure 9 shows the unnormalized focusing signal for the damaged medium, which can be compared with corresponding undamaged result in Fig. 6. The focused signals have some interesting properties:

1. The highest signal amplitude comes from the receiver position closest to the crack midpoint (pos. 3), not from the position closest to the transmitter (pos. 5).

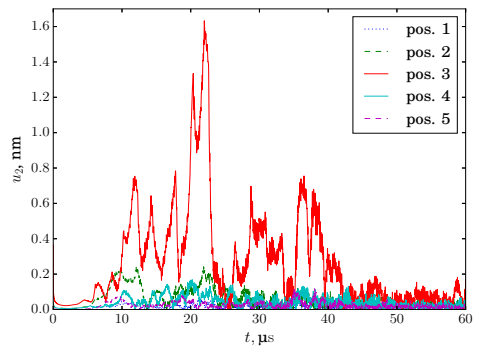


Figure 8: (Colour online) Nonlinearity magnitudes of PI signal processing from different measuring locations of 1 mm defect

2. Comparing the amplitudes of the positions 2 and 4, at far and near side of the crack end respective to transmitter: the farther position has larger focusing amplitude than the nearer position. Since the simulation region has two absorbing boundaries, the wave propagation is mostly in one direction, therefore the defect between pos. 2 and 4 must be capturing the wave energy and the TR-NEWS signal processing is using that energy as a new “virtual transducer” for the pos. 2 focusing. This could be further analysed in future works from the correlation signal which should indicate the contribution from additional reflections.
3. Amplitudes from the measurement positions 1 and 5 are “right way” around: the nearer measurement point has larger focusing amplitude than the farther.
4. Comparing just the TR-NEWS focusing amplitudes of undamaged (Fig. 6) and damaged (Fig. 9) CFRP, we see that indeed the additional reflection from the defect aids in amplifying the focused signal, increasing the focused wave amplitude. This is a known property of the reciprocal TR-NEWS signal processing.

Figure 10 shows a snapshot of the simulation u_2 displacement at a time moment $t = 32.6 \mu\text{s}$, just after the focusing. The defect in the material is acting as a source of new excitation after TR-NEWS focusing. Wave energy is captured between the damage and outside wall of the material and emitted as a wave. This behaviour is not visible in simulation with undamaged medium.

3.2 Delayed TR-NEWS analysis

The main point of this work is testing the nonlinearity measure of delayed TR-NEWS in simulation

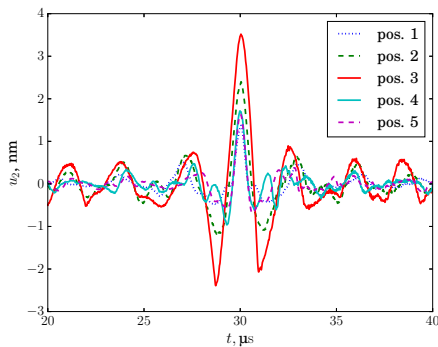


Figure 9: (Colour online) TR-NEWS focused wave in different measuring locations of damaged CFRP defect

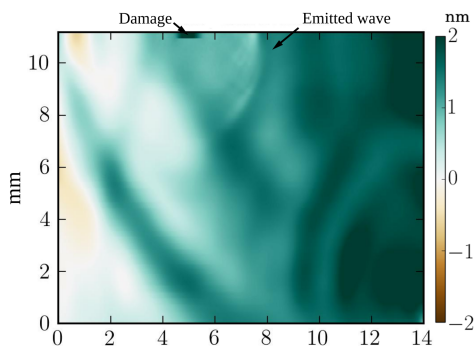


Figure 10: (Colour online) TR-NEWS focusing to pos. 3 at time $t = 32.6 \mu\text{s}$, showing displacement u_2 wave emission coming from the damaged region. Video available at [27]

of CFRP with a CAN type of nonlinearity. Section 2.2 describes the delayed TR-NEWS signal processing method which allows to create arbitrary envelope wave at the focusing (Eq. (1)), instead of the simple peak of the TR-NEWS. Equation (2) shows that in linear material, the outcome of the delayed TR-NEWS process can be predicted. Since the prediction works very well in physical NDT measurements of linear materials [14], it is now tested in simulation with the nonlinearity, supposing that the difference between the simulation result and the linear prediction (Eq. (2)) is due to nonlinear interaction of waves in the presence of nonlinearities or damage. Figure 11 shows the comparison between the linear superposition prediction and the simulation result of a simple delayed TR-NEWS process where two focusing peaks are at superposition with $1 \mu\text{s}$ time delay. The difference between the prediction and the simulation is large and obvious, indicating the presence of nonlinearity. This measure of nonlinearity seems to be

at least as strong as the measure calculated from PI (Fig. 7, pos. 3), so it is now investigated further.

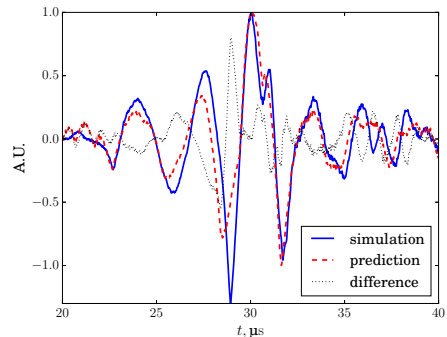


Figure 11: (Colour online) Delayed TR-NEWS nonlinearity measure between predicted and simulated values from position 3 on 1 mm damage with delayed peak amplitude $a_i = 1$ and delay value $\tau = 1 \mu\text{s}$ (Eq. (2))

Secondly, the effect of the crack size on the strength of the measured nonlinear effect is analysed. Simulations were ran with PI and delayed TR-NEWS nonlinearity analysis on medium with defect size between 0 and 1 mm. These are sub-wavelength for the used signal. The spatial focusing region was in the centre of the defect, in Rx position 3 in Fig. 4. Figure 12 shows the comparison of the envelopes of the nonlinearity measures. It can be seen that the nonlinearity measure of the delayed TR-NEWS is easily locatable in the temporal focusing region (near $t = 30 \mu\text{s}$), conversely the PI nonlinearity is located in the sidelobe region, potentially making it more difficult to analyse in applications. The magnitudes of the two nonlinearity measures are comparable. With 1 mm defect, the delayed TR-NEWS nonlinearity measure has larger maximum amplitude than PI but in case of smaller defects the advantage disappears. The PI seems to work slightly better at smaller defect sizes, but the delay $\tau = 1 \mu\text{s}$ in delayed TR-NEWS could be optimized further. Both methods work well for detecting sub-wavelength defects at the focusing region in the damaged material.

The delayed TR-NEWS signal processing could also be used for activating the contacting gap as the energy pocket. This could be done by creating a new focusing wave envelope which would have the resonant frequency of the defect, permitting higher amplitude waves near the damaged region, which would enhance the extraction of the nonlinear signature. This study is left for the future.

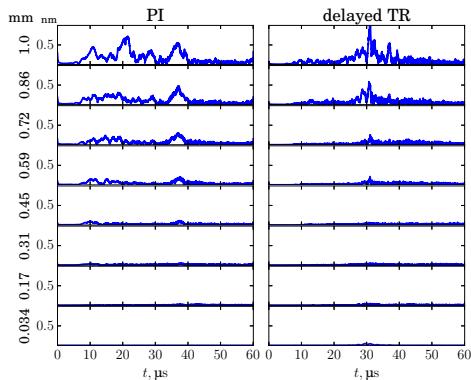


Figure 12: Comparison of the PI and delayed TR-NEWS nonlinearity measure envelopes (deformation u_2 difference in nm) depending on the size of the defect (in mm)

4 Conclusion

This paper investigated nonlinear NDT by using a simple FEM simulation model for a crack nonlinearity in CFRP. In the laminate model, the damage is a simple horizontal contacting crack near the receiving transducer. The signal processing uses TR-NEWS method for focusing the available wave energy near the receiving transducer. The magnitude of nonlinearity due to the damage is measured firstly with PI, secondly with the proposed delayed TR-NEWS signal processing procedure and compared. Both measures have comparable magnitude, with difference being that for PI it is mostly in the sidelobe region, but in delayed TR-NEWS in the focusing peak region.

The advantage of the delayed TR-NEWS nonlinearity analysis, compared to the established PI method, is that it only requires three wave transmissions (chirp transmission, TR-NEWS focusing, delayed TR-NEWS focusing), not four like PI. This can be important in applications where the measurement time needs to be minimized. The disadvantage is that it requires specifying at least the time delay parameter τ to create an interaction of waves, while in PI no such parameter needs to be specified. This makes PI more robust and easy to apply, but delayed TR-NEWS more flexible (for example in activating a defect resonance). Neither method requires any *a priori* baseline measurement knowledge.

Since the delayed TR-NEWS procedure allows to generate a wave at the focusing with arbitrary envelope, it could be used in the future to excite the crack damage by its resonance frequencies, using the damage as an energy pocket. Other perspectives include a more detailed simulation model for the CFRP in order to take more of its microstructure geometry into account to have stronger focusing. Additionally,

the damage could be modelled either by a collection of various cracks at various angles or by hysteresis. Moreover, heating from the frictional forces at the damage could be in future considered for a more precise simulation model.

Acknowledgement

This research has been conducted within the *co-tutelle* PhD studies of Martin Lints, between the Tallinn University of Technology, Department of Cybernetics in Estonia and the Institut National des Sciences Appliquées Centre Val de Loire at Blois, France. The research is supported by Estonian Research Council (project IUT33-24).

References

- [1] I. Y. Solodov, N. Krohn, G. Busse, CAN: an example of nonclassical acoustic nonlinearity in solids, *Ultrasonics* 40 (1) (2002) 621–625.
- [2] V. Aleshin, K. Van Den Abeele, Micro-potential model for acoustical hysteresis, in: *Proceedings of the 18th International Congress on Acoustics*, Vol. 3, 2004, pp. 1859–1862.
- [3] I. Y. Solodov, B. A. Korshak, Instability, Chaos, and “Memory” in Acoustic-Wave – Crack Interaction, *Phys. Rev. Lett.* 88 (1).
- [4] I. Y. Solodov, N. Krohn, G. Busse, Nonlinear ultrasonic NDT for early defect recognition and imaging, in: *Proceedings of European conf. on NDT (ECNDT)*, 2010, pp. 734–758.
- [5] S. Dos Santos, Z. Prevorovsky, Imaging of human tooth using ultrasound based chirp-coded nonlinear time reversal acoustics, *Ultrasonics* 51 (6) (2011) 667–674.
- [6] J. Riviere, S. Hauptert, P. Laugier, T. Ulrich, P.-Y. Le Bas, P. A. Johnson, Time reversed elastic nonlinearity diagnostic applied to mock osseointegration monitoring applying two experimental models, *The Journal of the Acoustical Society of America* 131 (3) (2012) 1922–1927.
- [7] X. Guo, D. Zhang, J. Zhang, Detection of fatigue-induced micro-cracks in a pipe by using time-reversed nonlinear guided waves: A three-dimensional model study, *Ultrasonics* 52 (7) (2012) 912–919.
- [8] J. Kober, Z. Prevorovsky, Theoretical investigation of nonlinear ultrasonic wave modulation spectroscopy at crack interface, *NDT & E International* 61 (2014) 10–15.

- [9] P. Blanloeuil, L. Rose, J. Guinto, M. Veidt, C. Wang, Closed crack imaging using time reversal method based on fundamental and second harmonic scattering, *Wave Motion* 66 (2016) 156–176.
- [10] C. Bruno, A. Gliozzi, M. Scalerandi, P. Antonaci, Analysis of elastic nonlinearity using the scaling subtraction method, *Physical Review B* 79 (6) (2009) 064108.
- [11] M. Scalerandi, A. S. Gliozzi, C. L. Bruno, K. Van Den Abeele, Nonlinear acoustic time reversal imaging using the scaling subtraction method, *Journal of Physics D: Applied Physics* 41 (21) (2008) 215404.
- [12] S. Dos Santos, C. Plag, Excitation symmetry analysis method (ESAM) for calculation of higher order non-linearities, *Int. J. Nonlinear Mech.* 43 (2008) 164 – 169.
- [13] F. Ciampa, M. Meo, Nonlinear elastic imaging using reciprocal time reversal and third order symmetry analysis, *The Journal of the Acoustical Society of America* 131 (6) (2012) 4316–4323.
- [14] M. Lints, S. Dos Santos, A. Salupere, Solitary waves for Non-Destructive Testing applications: Delayed nonlinear time reversal signal processing optimization, *Wave Motion* 71 (2017) 101–112.
- [15] M. Lints, A. Salupere, S. Dos Santos, Simulation of defects in CFRP and delayed TR-NEWS analysis, *Research Report Mech 320/17*, Tallinn University of Technology, Department of Cybernetics (2017).
- [16] A. H. Nielsen, Absorbing boundary conditions for seismic analysis in ABAQUS, in: *Proc. of the 2006 ABAQUS Users' Conference*, Cambridge, Massachusetts, 2006, pp. 23–25.
- [17] A. M. Sutin, J. A. TenCate, P. A. Johnson, Single-channel time reversal in elastic solids, *The Journal of the Acoustical Society of America* 116 (5) (2004) 2779–2784.
- [18] J. N. Reddy, *An Introduction to the Finite Element Method*, McGraw-Hill, New York, 2006.
- [19] P. Peterson, F2PY: a tool for connecting Fortran and Python programs, *Int. J. Computational Science and Engineering* 4 (4) (2009) 296–305.
- [20] E. Jones, T. Oliphant, P. Peterson, et al., SciPy: Open source scientific tools for Python, <http://www.scipy.org/>, (2001–), <http://www.scipy.org/>, accessed: 2014/12/08.
- [21] O. C. Zienkiewicz, R. L. Taylor, *The Finite Element Method Fifth edition Volume 1: The Basis*, Butterworth-Heinemann, 2000.
- [22] Ultrasonic Velocity Table, http://www.advanced-ndt.co.uk/index_htm_files/Reference%20Chart%20-%20Velocity%20Chart.pdf, accessed: 2016/09/24.
- [23] A. R. Mijar, J. S. Arora, Return Mapping Procedure for Frictional Force Calculation: Some Insights, *Journal of Engineering Mechanics* 131 (10) (2005) 1004–1012.
- [24] A. Schutte, J. F. Dannenberg, Y. H. Wijnant, A. de Boer, An implicit and explicit solver for contact problems, in: *Proceedings of ISMA2010 including USD2010*, 2010, pp. 4081–4094.
- [25] O. C. Zienkiewicz, R. L. Taylor, *The Finite Element Method Fifth edition Volume 2: Solid mechanics*, Butterworth-Heinemann, 2000.
- [26] A. R. Mijar, J. S. Arora, An augmented Lagrangian optimization method for contact analysis problems, 1: formulation and algorithm, *Struct Multidisc Optim* 28 (2004) 99–112.
- [27] M. Lints, FEM simulation video of TR-NEWS focusing on crack in CFRP, http://homes.ioc.ee/lints/files/cracked_CF_TR-NEWS_foc3.mp4, Accessed: 2017/02/01.
- [28] S. Dos Santos, B. Choi, A. Sutin, A. Sarvazyan, Nonlinear imaging based on time reversal acoustic focusing, *proc. of the 8ème Congrès Français d'Acoustique*, 359-362
- [29] T. J. Ulrich, M. Griffa, B. E. Anderson, Symmetry-based imaging condition in time reversed acoustics, *Journal of Applied Physics* 104, 064912 (2008)

Appendix B: CV

CURRICULUM VITAE

1. Personal data

Name	Martin Lints
Date and place of birth	1 April 1988, Kambja, Estonia
Nationality	Estonian

2. Contact information

Address	Tallinn University of Technology, School of Science, Department of Cybernetics, Akadeemia tee 21, 12618 Tallinn, Estonia
Phone	+372 620 4227
E-mail	martin.lints@cens.ioc.ee

3. Education

2014–...	INSA Centre Val de Loire, Inserm U930, Sciences & Technologie Industrielle, PhD studies
2013–...	Tallinn University of Technology, School of Science, Engineering Physics, PhD studies
2011–2013	Tallinn University of Technology, Faculty of Science, Engineering Physics, MSc <i>cum laude</i>
2008–2011	Tallinn University of Technology, Faculty of Science, Engineering Physics, BSc

4. Language competence

Estonian	native
English	fluent
French	beginner
Russian	beginner

5. Professional employment

2017– ...	Tallinn University of Technology, School of Science, Department of Cybernetics, Early Stage Researcher
2013–2016	Tallinn University of Technology, Institute of Cybernetics, Early Stage Researcher
2011–2013	Tallinn University of Technology, Institute of Cybernetics, Technician
2011–2011	Vertex Estonia AS, Project Manager

6. Voluntary work

2008–...	Estonian Defence League
----------	-------------------------

7. Computer skills

- Operating systems: Linux, Windows
- Document preparation: LaTeX, Inkscape, LibreOffice
- Mostly familiar with Python programming language
- Have also used Fortran, C, C++, Matlab, Bash, Java, VBA
- Scientific packages: SciPy, FEniCS, OpenCV, Maxima, Mathematica

8. Honours and awards

- 2013, Martin Lints, Students' research prize by Estonian Academy of Sciences

9. Defended theses

- 2013, Formation and detection of hidden solitons in the hierarchical Korteweg-de Vries system, MSc, supervisor Prof. Andrus Salupere, Tallinn University of Technology, Institute of Cybernetics
- 2011, Reflection and transmission of ultrasound waves from a layer of finite thickness, BSc, supervisor Dr. Andres Braunbrück, Tallinn University of Technology, Institute of Cybernetics

10. Field of research

- Wave propagation in complex media and applications

11. Scientific work

Papers

1. M. Lints, A. Salupere, and S. Dos Santos. Simulation of detecting contact nonlinearity in carbon fibre polymer using ultrasonic nonlinear delayed time reversal. *Acta Acust. united Ac.*, 2017. (accepted)
2. M. Lints, S. Dos Santos, C. Kožená, V. Kůs, and A. Salupere. Fully synchronized acoustomechanical testing of skin: biomechanical measurements of nonclassical nonlinear parameters. In *24th International Congress on Sound and Vibration, 23–27 July, 2017, London*, number 867. ICSV, International Institute of Acoustics and Vibrations, 2017
3. M. Lints, S. Dos Santos, and A. Salupere. Solitary Waves for Non-Destructive Testing Applications: Delayed Nonlinear Time Reversal Signal Processing Optimization. *Wave Motion*, 71:101–112, 2017.
<http://dx.doi.org/10.1016/j.wavemoti.2016.07.001>
4. M. Lints, S. Dos Santos, and A. Salupere. Focusing aspects of delayed Time Reversal based Nonlinear Elastic Wave Spectroscopy methods. *IEEE International Ultrasonics Symposium, IUS*, 7728831, 2016
5. M. Lints, A. Salupere, and S. Dos Santos. Simulation of solitary wave propagation in carbon fibre reinforced polymer. *Proc. Estonian Acad. Sci.*, 64(3):297–303, 2015
6. S. Dos Santos, M. Lints, N. Poirot, Z. Farová, A. Salupere, M. Caliez, and Z. Převorovský. Nonlinear Time Reversal for Non Destructive Testing of complex medium : a review based on multi-physics experiments and signal processing strategies. In P. Mazal, editor, *NDT in Progress 2015 - 8th International Workshop of NDT Experts, Proceedings*, pages 31–40. Brno University of Technology, October 2015
7. M. Lints, S. Dos Santos, and A. Salupere. Delayed time reversal in non destructive testing for ultrasound focusing. In T. Hobza, editor, *SPMS 2015: Stochastic and Physical Monitoring Systems, Proceedings of the International Conference, June 22–June 27, 2015, Drhleny, Czech Republic*. pages 115–124. Czech Technical University, 2015
8. S. Dos Santos, M. Lints, N. Poirot, and A. Salupere. Optimized excitation for nonlinear wave propagation in complex media: from biomedical acoustic imaging to nondestructive testing of cultural heritage. *J. Acoust. Soc. Am.*, 138(3, pt 2):1796, 2015

9. A. Salupere, M. Lints, and J. Engelbrecht. On solitons in media modelled by the hierarchical KdV equation. *Arch. Appl. Mech.*, 84:1583–1593, 2014
10. M. Lints, A. Salupere, and S. Dos Santos. Simulation of nonlinear time reversal wave propagation in carbon fibre reinforced polymer. In *11th European Conference on Non-Destructive Testing (ECNDT 2014): October 6–10, 2014, Prague, Czech Republic, Proceedings*. Prague: Brno University of Technology, 1–10, 2014
11. M. Lints, A. Salupere, and S. Dos Santos. Formation and detection of solitonic waves in dilatant granular materials: potential application for nonlinear NDT. In *7th International Workshop NDT in Progress: NDT of Lightweight Materials, Fraunhofer Institute for Nondestructive Testing, Dresden, Germany, 7-8 November*. Dresden: Fraunhofer IZFP, 2013
12. L. Kurik, V. Sinivee, M. Lints, and U. Kallavus. Method for data collection and integration into 3D architectural model. In E. Khaled and T. Sobh, editors *Innovations and Advances in Computer, Information, Systems Sciences, and Engineering*. Springer, pages 707–717. (Lecture Notes in Electrical Engineering; 152), 2013

Conference presentations

1. M. Lints, S. Dos Santos, C. Kožená, V. Kůs, and A. Salupere. *Fully synchronized acoustomechanical testing of skin: biomechanical measurements of nonclassical nonlinear parameters*, 24th International Congress on Sound and Vibration (ICSV 24), 23–27 July 2017, London, United Kingdom
2. M. Lints, A. Salupere, and S. Dos Santos. *Dispersion simulations in layered CFRP*, 28th Nordic Seminar on Computational Mechanics (NSCM 28), 22–23 October 2015, Tallinn, Estonia
3. S. Dos Santos, M. Lints, and A. Salupere. *Solitary Waves for Non-Destructive Testing Applications: Delayed Nonlinear Time Reversal Signal Processing Optimization*, Application of Mathematics in Technical and Natural Sciences (AMiTaNS), 28 June–3 July 2015, Albena, Bulgaria
4. M. Lints, S. Dos Santos, and A. Salupere. *Delayed time reversal for ultrasound focusing in non destructive testing*, Stochastic and Physical Monitoring Systems (SPMS), 22–27 June 2015, Drhleny, Czech Republic

5. M. Lints, A. Salupere, and S. Dos Santos. *Simulation of nonlinear time reversal wave propagation in carbon fibre reinforced polymer*, 11th European Conference on Non-Destructive Testing (ECNDT 2014), 6–10 October 2014, Prague, Czech Republic
6. M. Lints, A. Salupere, and S. Dos Santos. *Simulation of solitary wave propagation in carbon fibre reinforced polymer*, IUTAM Symposium on Complexity of Nonlinear Waves: 8–12 September 2014, Tallinn
7. S. Dos Santos, Z. Dvořáková, J. Chaline, M. Lints, and D. Remache. *Imageurs du non-linéaire : de l'imagerie ultrasonore médicale au contrôle non destructif industriel*, Rencontre du non-linéaire, 18–20 March 2014, Lille, France
8. S. Dos Santos, M. Lints, J. Chaline, and A. Salupere. *Nonlinear time reversal using solitonic waves in dispersive media: potential application for nonlinear NDT*, XX All-Russian Scientific and Technical Conference on Non-Destructive Control and Technical Diagnostics, 3–6 March 2014, Moscow, Russian Federation.

ELULOOKIRJELDUS

1. Isikuandmed

Nimi	Martin Lints
Sünniaeg ja -koht	01.04.1988, Kambja, Eesti
Kodakondsus	Eesti

2. Kontaktandmed

Aadress	TTÜ Küberneetika Instituut, Akadeemia tee 21, 12618 Tallinn
Telefon	+372 620 4227
E-post	martin.lints@cens.ioc.ee

3. Haridus

2014–...	INSA Centre Val de Loire, Inserm U930, Sciences & Technologie Industrielle, doktoriõpe
2013–...	Tallinna Tehnikaülikool, Matemaatika-loodusteaduskond, tehniline füüsika, doktoriõpe
2011–2013	Tallinna Tehnikaülikool, Matemaatika-loodusteaduskond, tehniline füüsika, MSc <i>cum laude</i>
2008–2011	Tallinna Tehnikaülikool, Matemaatika-loodusteaduskond, tehniline füüsika, BSc

4. Keelteoskus

eesti keel	emakeel
inglise keel	kõrgtase
prantsuse keel	algtase
vene keel	algtase

5. Teenistuskäik

2017– ...	Tallinna Tehnikaülikool, Loodusteaduskond, Küberneetika instituut, Nooremteadur,
2013–2016	Tallinna Tehnikaülikooli Küberneetika Instituut, Nooremteadur,
2011–2013	Tallinna Tehnikaülikooli Küberneetika Instituut, Tehnik,
2011–2011	Vertex Estonia AS, projektijuht

6. Vabatahtlik töö

2008–...	Kaitseliit
----------	------------

7. Computer skills

- Operatsioonisüsteemid: Linux, Windows
- Kontoritarkvara: LaTeX, Inkscape, LibreOffice
- Enamjaolt kasutan Pythoni programmeerimiskeelt
- Samuti tuttav: Fortran, C, C++, Matlab, Bash, Java, VBA
- Teadustarkvara paketid: SciPy, FEniCS, OpenCV, Maxima, Mathematica

8. Autasud

- 2013, Martin Lints, Eesti Teaduste Akadeemia üliõpilaste parimate teadustööde auhind

9. Kaitstud lõputööd

- 2013, Peidetud solitonide formeerumine ja tuvastamine hierarhilises Kortewegi-de Vriesi süsteemis, MSc, juhendaja Prof. Andrus Salupere, Tallinna Tehnikaülikool, Küberneetika Instituut
- 2011, Ultrahelilainete peegelduvus ja läbivus lõpliku paksusega kihilt, BSc, Juhendaja Dr. Andres Braunbrück, Tallinna Tehnikaülikool, Küberneetika Instituut

10. Teadustöö põhisuunad

- Lainelevi komplekssetes keskkondades ja rakendused

11. Teadustegevus

Teadusartiklite, konverentsiteeside ja konverentsiettekannete loetelu on toodud ingliskeelse elulookirjelduse juures.

DISSERTATIONS DEFENDED AT
TALLINN UNIVERSITY OF TECHNOLOGY ON
NATURAL AND EXACT SCIENCES

1. **Olav Kongas.** Nonlinear dynamics in modeling cardiac arrhythmias. 1998.
2. **Kalju Vanatalu.** Optimization of processes of microbial biosynthesis of isotopically labeled biomolecules and their complexes. 1999.
3. **Ahto Buldas.** An algebraic approach to the structure of graphs. 1999.
4. **Monika Drews.** A metabolic study of insect cells in batch and continuous culture: application of chemostat and turbidostat to the production of recombinant proteins. 1999.
5. **Eola Valdre.** Endothelial-specific regulation of vessel formation: role of receptor tyrosine kinases. 2000.
6. **Kalju Lott.** Doping and defect thermodynamic equilibrium in ZnS. 2000.
7. **Reet Koljak.** Novel fatty acid dioxygenases from the corals *Plexaura homomalla* and *Gersemia fruticosa*. 2001.
8. **Anne Paju.** Asymmetric oxidation of prochiral and racemic ketones by using sharpless catalyst. 2001.
9. **Marko Vendelin.** Cardiac mechanoenergetics *in silico*. 2001.
10. **Pearu Peterson.** Multi-soliton interactions and the inverse problem of wave crest. 2001.
11. **Anne Menert.** Microcalorimetry of anaerobic digestion. 2001.
12. **Toomas Tiivel.** The role of the mitochondrial outer membrane in *in vivo* regulation of respiration in normal heart and skeletal muscle cell. 2002.
13. **Olle Hints.** Ordovician scolecodonts of Estonia and neighbouring areas: taxonomy, distribution, palaeoecology, and application. 2002.
14. **Jaak Nõlvak.** Chitinozoan biostratigraphy in the Ordovician of Baltoscandia. 2002.
15. **Liivi Kluge.** On algebraic structure of pre-operad. 2002.
16. **Jaanus Lass.** Biosignal interpretation: Study of cardiac arrhythmias and electromagnetic field effects on human nervous system. 2002.
17. **Janek Peterson.** Synthesis, structural characterization and modification of PAMAM dendrimers. 2002.
18. **Merike Vaher.** Room temperature ionic liquids as background electrolyte additives in capillary electrophoresis. 2002.
19. **Valdek Mikli.** Electron microscopy and image analysis study of powdered hardmetal materials and optoelectronic thin films. 2003.
20. **Mart Viljus.** The microstructure and properties of fine-grained cermets. 2003.

21. **Signe Kask.** Identification and characterization of dairy-related *Lactobacillus*. 2003.
22. **Tiiu-Mai Laht.** Influence of microstructure of the curd on enzymatic and microbiological processes in Swiss-type cheese. 2003.
23. **Anne Kuusksalu.** 2–5A synthetase in the marine sponge *Geodia cydonium*. 2003.
24. **Sergei Bereznev.** Solar cells based on polycrystalline copper-indium chalcogenides and conductive polymers. 2003.
25. **Kadri Kriis.** Asymmetric synthesis of C2-symmetric bimorpholines and their application as chiral ligands in the transfer hydrogenation of aromatic ketones. 2004.
26. **Jekaterina Reut.** Polypyrrole coatings on conducting and insulating substrates. 2004.
27. **Sven Nõmm.** Realization and identification of discrete-time nonlinear systems. 2004.
28. **Olga Kijatkina.** Deposition of copper indium disulphide films by chemical spray pyrolysis. 2004.
29. **Gert Tamberg.** On sampling operators defined by Rogosinski, Hann and Blackman windows. 2004.
30. **Monika Übner.** Interaction of humic substances with metal cations. 2004.
31. **Kaarel Adamberg.** Growth characteristics of non-starter lactic acid bacteria from cheese. 2004.
32. **Imre Vallikivi.** Lipase-catalysed reactions of prostaglandins. 2004.
33. **Merike Peld.** Substituted apatites as sorbents for heavy metals. 2005.
34. **Vitali Syritski.** Study of synthesis and redox switching of polypyrrole and poly(3,4-ethylenedioxythiophene) by using *in-situ* techniques. 2004.
35. **Lee Põllumaa.** Evaluation of ecotoxicological effects related to oil shale industry. 2004.
36. **Riina Aav.** Synthesis of 9,11-secosterols intermediates. 2005.
37. **Andres Braunbrück.** Wave interaction in weakly inhomogeneous materials. 2005.
38. **Robert Kitt.** Generalised scale-invariance in financial time series. 2005.
39. **Juss Pavelson.** Mesoscale physical processes and the related impact on the summer nutrient fields and phytoplankton blooms in the western Gulf of Finland. 2005.
40. **Olari Ilison.** Solitons and solitary waves in media with higher order dispersive and nonlinear effects. 2005.
41. **Maksim Säkki.** Intermittency and long-range structurization of heart

- rate. 2005.
42. **Enli Kiipli.** Modelling seawater chemistry of the East Baltic Basin in the late Ordovician–Early Silurian. 2005.
 43. **Igor Golovtsov.** Modification of conductive properties and processability of polyparaphenylene, polypyrrole and polyaniline. 2005.
 44. **Katrin Laos.** Interaction between furcellaran and the globular proteins (bovine serum albumin beta-lactoglobulin). 2005.
 45. **Arvo Mere.** Structural and electrical properties of spray deposited copper indium disulphide films for solar cells. 2006.
 46. **Sille Ehala.** Development and application of various on- and off-line analytical methods for the analysis of bioactive compounds. 2006.
 47. **Maria Kulp.** Capillary electrophoretic monitoring of biochemical reaction kinetics. 2006.
 48. **Anu Aaspõllu.** Proteinases from *Vipera lebetina* snake venom affecting hemostasis. 2006.
 49. **Lyudmila Chekulayeva.** Photosensitized inactivation of tumor cells by porphyrins and chlorins. 2006.
 50. **Merle Uudsemaa.** Quantum-chemical modeling of solvated first row transition metal ions. 2006.
 51. **Tagli Pitsi.** Nutrition situation of pre-school children in Estonia from 1995 to 2004. 2006.
 52. **Angela Ivask.** Luminescent recombinant sensor bacteria for the analysis of bioavailable heavy metals. 2006.
 53. **Tiina Lõugas.** Study on physico-chemical properties and some bioactive compounds of sea buckthorn (*Hippophae rhamnoides* L.). 2006.
 54. **Kaja Kasemets.** Effect of changing environmental conditions on the fermentative growth of *Saccharomyces cerevisiae* S288C: auxo-accelerostat study. 2006.
 55. **Ildar Nisamedtinov.** Application of ^{13}C and fluorescence labeling in metabolic studies of *Saccharomyces* spp. 2006.
 56. **Alar Leibak.** On additive generalisation of Voronoï's theory of perfect forms over algebraic number fields. 2006.
 57. **Andri Jagomägi.** Photoluminescence of chalcopyrite tellurides. 2006.
 58. **Tõnu Martma.** Application of carbon isotopes to the study of the Ordovician and Silurian of the Baltic. 2006.
 59. **Marit Kauk.** Chemical composition of CuInSe₂ monograin powders for solar cell application. 2006.
 60. **Julia Kois.** Electrochemical deposition of CuInSe₂ thin films for photovoltaic applications. 2006.
 61. **Ilona Oja Acik.** Sol-gel deposition of titanium dioxide films. 2007.

62. **Tiia Anmann.** Integrated and organized cellular bioenergetic systems in heart and brain. 2007.
63. **Katrin Trummal.** Purification, characterization and specificity studies of metalloproteinases from *Vipera lebetina* snake venom. 2007.
64. **Gennadi Lessin.** Biochemical definition of coastal zone using numerical modeling and measurement data. 2007.
65. **Enno Pais.** Inverse problems to determine non-homogeneous degenerate memory kernels in heat flow. 2007.
66. **Maria Borissova.** Capillary electrophoresis on alkyylimidazolium salts. 2007.
67. **Karin Valmsen.** Prostaglandin synthesis in the coral *Plexaura homomalla*: control of prostaglandin stereochemistry at carbon 15 by cyclooxygenases. 2007.
68. **Kristjan Piirimäe.** Long-term changes of nutrient fluxes in the drainage basin of the gulf of Finland – application of the PolFlow model. 2007.
69. **Tatjana Dedova.** Chemical spray pyrolysis deposition of zinc sulfide thin films and zinc oxide nanostructured layers. 2007.
70. **Katrin Tomson.** Production of labelled recombinant proteins in fed-batch systems in *Escherichia coli*. 2007.
71. **Cecilia Sarmiento.** Suppressors of RNA silencing in plants. 2008.
72. **Vilja Mardla.** Inhibition of platelet aggregation with combination of antiplatelet agents. 2008.
73. **Maie Bachmann.** Effect of Modulated microwave radiation on human resting electroencephalographic signal. 2008.
74. **Dan Hüvonen.** Terahertz spectroscopy of low-dimensional spin systems. 2008.
75. **Ly Villo.** Stereoselective chemoenzymatic synthesis of deoxy sugar esters involving *Candida antarctica* lipase B. 2008.
76. **Johan Anton.** Technology of integrated photoelasticity for residual stress measurement in glass articles of axisymmetric shape. 2008.
77. **Olga Volobujeva.** SEM study of selenization of different thin metallic films. 2008.
78. **Artur Jõgi.** Synthesis of 4'-substituted 2,3'-dideoxynucleoside analogues. 2008.
79. **Mario Kadastik.** Doubly charged Higgs boson decays and implications on neutrino physics. 2008.
80. **Fernando Pérez-Caballero.** Carbon aerogels from 5-methylresorcinol-formaldehyde gels. 2008.
81. **Sirje Vaask.** The comparability, reproducibility and validity of Estonian food consumption surveys. 2008.

82. **Anna Menaker.** Electrosynthesized conducting polymers, polypyrrole and poly(3,4-ethylenedioxythiophene), for molecular imprinting. 2009.
83. **Lauri Ilison.** Solitons and solitary waves in hierarchical Korteweg-de Vries type systems. 2009.
84. **Kaia Ernits.** Study of In₂S₃ and ZnS thin films deposited by ultrasonic spray pyrolysis and chemical deposition. 2009.
85. **Veljo Sinivee.** Portable spectrometer for ionizing radiation “Gammamapper”. 2009.
86. **Jüri Virkepu.** On Lagrange formalism for Lie theory and operadic harmonic oscillator in low dimensions. 2009.
87. **Marko Piirsoo.** Deciphering molecular basis of Schwann cell development. 2009.
88. **Kati Helmja.** Determination of phenolic compounds and their antioxidative capability in plant extracts. 2010.
89. **Merike Sõmera.** Sobemoviruses: genomic organization, potential for recombination and necessity of P1 in systemic infection. 2010.
90. **Kristjan Laes.** Preparation and impedance spectroscopy of hybrid structures based on CuIn₃Se₅ photoabsorber. 2010.
91. **Kristin Lippur.** Asymmetric synthesis of 2,2'-bimorpholine and its 5,5'-substituted derivatives. 2010.
92. **Merike Luman.** Dialysis dose and nutrition assessment by an optical method. 2010.
93. **Mihhail Berezovski.** Numerical simulation of wave propagation in heterogeneous and microstructured materials. 2010.
94. **Tamara Aid-Pavlidis.** Structure and regulation of BDNF gene. 2010.
95. **Olga Bragina.** The role of Sonic Hedgehog pathway in neuro- and tumorigenesis. 2010.
96. **Merle Randrüüt.** Wave propagation in microstructured solids: solitary and periodic waves. 2010.
97. **Marju Laars.** Asymmetric organocatalytic Michael and aldol reactions mediated by cyclic amines. 2010.
98. **Maarja Grossberg.** Optical properties of multinary semiconductor compounds for photovoltaic applications. 2010.
99. **Alla Maloverjan.** Vertebrate homologues of Drosophila fused kinase and their role in Sonic Hedgehog signalling pathway. 2010.
100. **Priit Pruunsild.** Neuronal Activity-Dependent Transcription Factors and Regulation of Human BDNF Gene. 2010.
101. **Tatjana Knazeva.** New Approaches in Capillary Electrophoresis for Separation and Study of Proteins. 2011.
102. **Atanas Katerski.** Chemical Composition of Sprayed Copper Indium

- Disulfide Films for Nanostructured Solar Cells. 2011.
103. **Kristi Timmo.** Formation of Properties of CuInSe₂ and Cu₂ZnSn(S,Se)₄ Monograin Powders Synthesized in Molten KI. 2011.
 104. **Kert Tamm.** Wave Propagation and Interaction in Mindlin-Type Microstructured Solids: Numerical Simulation. 2011.
 105. **Adrian Popp.** Ordovician Proetid Trilobites in Baltoscandia and Germany. 2011.
 106. **Ove Pärn.** Sea Ice Deformation Events in the Gulf of Finland and This Impact on Shipping. 2011.
 107. **Germo Väli.** Numerical Experiments on Matter Transport in the Baltic Sea. 2011.
 108. **Andrus Seiman.** Point-of-Care Analyser Based on Capillary Electrophoresis. 2011.
 109. **Olga Katargina.** Tick-Borne Pathogens Circulating in Estonia (Tick-Borne Encephalitis Virus, *Anaplasma phagocytophilum*, *Babesia* Species): Their Prevalence and Genetic Characterization. 2011.
 110. **Ingrid Sumeri.** The Study of Probiotic Bacteria in Human Gastrointestinal Tract Simulator. 2011.
 111. **Kairit Zovo.** Functional Characterization of Cellular Copper Proteome. 2011.
 112. **Natalja Makarytsheva.** Analysis of Organic Species in Sediments and Soil by High Performance Separation Methods. 2011.
 113. **Monika Mortimer.** Evaluation of the Biological Effects of Engineered Nanoparticles on Unicellular Pro- and Eukaryotic Organisms. 2011.
 114. **Kersti Tepp.** Molecular System Bioenergetics of Cardiac Cells: Quantitative Analysis of Structure-Function Relationship. 2011.
 115. **Anna-Liisa Peikolainen.** Organic Aerogels Based on 5-Methylresorcinol. 2011.
 116. **Leeli Amon.** Palaeoecological Reconstruction of Late-Glacial Vegetation Dynamics in Eastern Baltic Area: A View Based on Plant Macrofossil Analysis. 2011.
 117. **Tanel Peets.** Dispersion Analysis of Wave Motion in Microstructured Solids. 2011.
 118. **Liina Kaupmees.** Selenization of Molybdenum as Contact Material in Solar Cells. 2011.
 119. **Allan Olsper.** Properties of VPg and Coat Protein of Sobemoviruses. 2011.
 120. **Kadri Koppel.** Food Category Appraisal Using Sensory Methods. 2011.
 121. **Jelena Gorbatšova.** Development of Methods for CE Analysis of Plant Phenolics and Vitamins. 2011.

122. **Karin Viipsi.** Impact of EDTA and Humic Substances on the Removal of Cd and Zn from Aqueous Solutions by Apatite. 2012.
123. **David Schryer.** Metabolic Flux Analysis of Compartmentalized Systems Using Dynamic Isotopologue Modeling. 2012.
124. **Ardo Illaste.** Analysis of Molecular Movements in Cardiac Myocytes. 2012.
125. **Indrek Reile.** 3-Alkylcyclopentane-1,2-Diones in Asymmetric Oxidation and Alkylation Reactions. 2012.
126. **Tatjana Tamberg.** Some Classes of Finite 2-Groups and Their Endomorphism Semigroups. 2012.
127. **Taavi Liblik.** Variability of Thermohaline Structure in the Gulf of Finland in Summer. 2012.
128. **Priidik Lagemaa.** Operational Forecasting in Estonian Marine Waters. 2012.
129. **Andrei Errapart.** Photoelastic Tomography in Linear and Non-linear Approximation. 2012.
130. **Külliki Krabbi.** Biochemical Diagnosis of Classical Galactosemia and Mucopolysaccharidoses in Estonia. 2012.
131. **Kristel Kaseleht.** Identification of Aroma Compounds in Food using SPME-GC/MS and GC-Olfactometry. 2012.
132. **Kristel Kodar.** Immunoglobulin G Glycosylation Profiling in Patients with Gastric Cancer. 2012.
133. **Kai Rosin.** Solar Radiation and Wind as Agents of the Formation of the Radiation Regime in Water Bodies. 2012.
134. **Ann Tiiman.** Interactions of Alzheimer's Amyloid-Beta Peptides with Zn(II) and Cu(II) Ions. 2012.
135. **Olga Gavrilova.** Application and Elaboration of Accounting Approaches for Sustainable Development. 2012.
136. **Olesja Bondarenko.** Development of Bacterial Biosensors and Human Stem Cell-Based *In Vitro* Assays for the Toxicological Profiling of Synthetic Nanoparticles. 2012.
137. **Katri Muska.** Study of Composition and Thermal Treatments of Quaternary Compounds for Monograin Layer Solar Cells. 2012.
138. **Ranno Nahku.** Validation of Critical Factors for the Quantitative Characterization of Bacterial Physiology in Accelerostat Cultures. 2012.
139. **Petri-Jaan Lahtvee.** Quantitative Omics-level Analysis of Growth Rate Dependent Energy Metabolism in *Lactococcus lactis*. 2012.
140. **Kerti Orumets.** Molecular Mechanisms Controlling Intracellular Glutathione Levels in Baker's Yeast *Saccharomyces cerevisiae* and its Random Mutagenized Glutathione Over-Accumulating Isolate. 2012.

141. **Loreida Timberg.** Spice-Cured Sprats Ripening, Sensory Parameters Development, and Quality Indicators. 2012.
142. **Anna Mihhalevski.** Rye Sourdough Fermentation and Bread Stability. 2012.
143. **Liisa Arike.** Quantitative Proteomics of *Escherichia coli*: From Relative to Absolute Scale. 2012.
144. **Kairi Otto.** Deposition of In₂S₃ Thin Films by Chemical Spray Pyrolysis. 2012.
145. **Mari Sepp.** Functions of the Basic Helix-Loop-Helix Transcription Factor TCF4 in Health and Disease. 2012.
146. **Anna Suhhova.** Detection of the Effect of Weak Stressors on Human Resting Electroencephalographic Signal. 2012.
147. **Aram Kazarjan.** Development and Production of Extruded Food and Feed Products Containing Probiotic Microorganisms. 2012.
148. **Rivo Uiboupin.** Application of Remote Sensing Methods for the Investigation of Spatio-Temporal Variability of Sea Surface Temperature and Chlorophyll Fields in the Gulf of Finland. 2013.
149. **Tiina Kriščiunaite.** A Study of Milk Coagulability. 2013.
150. **Tuuli Levandi.** Comparative Study of Cereal Varieties by Analytical Separation Methods and Chemometrics. 2013.
151. **Natalja Kabanova.** Development of a Microcalorimetric Method for the Study of Fermentation Processes. 2013.
152. **Himani Khanduri.** Magnetic Properties of Functional Oxides. 2013.
153. **Julia Smirnova.** Investigation of Properties and Reaction Mechanisms of Redox-Active Proteins by ESI MS. 2013.
154. **Mervi Sepp.** Estimation of Diffusion Restrictions in Cardiomyocytes Using Kinetic Measurements. 2013.
155. **Kersti Jääger.** Differentiation and Heterogeneity of Mesenchymal Stem Cells. 2013.
156. **Victor Alari.** Multi-Scale Wind Wave Modeling in the Baltic Sea. 2013.
157. **Taavi Päll.** Studies of CD44 Hyaluronan Binding Domain as Novel Angiogenesis Inhibitor. 2013.
158. **Allan Niidu.** Synthesis of Cyclopentane and Tetrahydrofuran Derivatives. 2013.
159. **Julia Geller.** Detection and Genetic Characterization of *Borrelia* Species Circulating in Tick Population in Estonia. 2013.
160. **Irina Stulova.** The Effects of Milk Composition and Treatment on the Growth of Lactic Acid Bacteria. 2013.
161. **Jana Holmar.** Optical Method for Uric Acid Removal Assessment Dur-

- ing Dialysis. 2013.
162. **Kerti Ausmees.** Synthesis of Heterobicyclo[3.2.0]heptane Derivatives via Multicomponent Cascade Reaction. 2013.
 163. **Minna Varikmaa.** Structural and Functional Studies of Mitochondrial Respiration Regulation in Muscle Cells. 2013.
 164. **Indrek Koppel.** Transcriptional Mechanisms of BDNF Gene Regulation. 2014.
 165. **Kristjan Pilt.** Optical Pulse Wave Signal Analysis for Determination of Early Arterial Ageing in Diabetic Patients. 2014.
 166. **Andres Anier.** Estimation of the Complexity of the Electroencephalogram for Brain Monitoring in Intensive Care. 2014.
 167. **Toivo Kallaste.** Pyroclastic Sanidine in the Lower Palaeozoic Bentonites – A Tool for Regional Geological Correlations. 2014.
 168. **Erki Kärber.** Properties of ZnO-nanorod/In₂S₃/CuInS₂ Solar Cell and the Constituent Layers Deposited by Chemical Spray Method. 2014.
 169. **Julia Lehner.** Formation of Cu₂ZnSnS₄ and Cu₂ZnSnSe₄ by Chalco-genisation of Electrochemically Deposited Precursor Layers. 2014.
 170. **Peep Pitk.** Protein- and Lipid-rich Solid Slaughterhouse Waste Anaerobic Co-digestion: Resource Analysis and Process Optimization. 2014.
 171. **Kaspar Valgepea.** Absolute Quantitative Multi-omics Characterization of Specific Growth Rate-dependent Metabolism of *Escherichia coli*. 2014.
 172. **Artur Noole.** Asymmetric Organocatalytic Synthesis of 3,3'-Disubstituted Oxindoles. 2014.
 173. **Robert Tsanev.** Identification and Structure-Functional Characterisation of the Gene Transcriptional Repressor Domain of Human Gli Proteins. 2014.
 174. **Dmitri Kartofelev.** Nonlinear Sound Generation Mechanisms in Musical Acoustic. 2014.
 175. **Sigrid Hade.** GIS Applications in the Studies of the Palaeozoic Graptolite Argillite and Landscape Change. 2014.
 176. **Agne Velthut-Meikas.** Ovarian Follicle as the Environment of Oocyte Maturation: The Role of Granulosa Cells and Follicular Fluid at Pre-Ovulatory Development. 2014.
 177. **Kristel Hälvin.** Determination of B-group Vitamins in Food Using an LC-MS Stable Isotope Dilution Assay. 2014.
 178. **Mailis Päre.** Characterization of the Oligoadenylate Synthetase Subgroup from Phylum Porifera. 2014.
 179. **Jekaterina Kazantseva.** Alternative Splicing of *TAF4*: A Dynamic Switch between Distinct Cell Functions. 2014.

180. **Jaanus Suurväli.** Regulator of G Protein Signalling 16 (RGS16): Functions in Immunity and Genomic Location in an Ancient MHC-Related Evolutionarily Conserved Synteny Group. 2014.
181. **Ene Viiard.** Diversity and Stability of Lactic Acid Bacteria During Rye Sourdough Propagation. 2014.
182. **Kristella Hansen.** Prostaglandin Synthesis in Marine Arthropods and Red Algae. 2014.
183. **Helike Lõhelaid.** Allene Oxide Synthase-lipoxygenase Pathway in Coral Stress Response. 2015.
184. **Normunds Stivrīnš.** Postglacial Environmental Conditions, Vegetation Succession and Human Impact in Latvia. 2015.
185. **Mary-Liis Kütt.** Identification and Characterization of Bioactive Peptides with Antimicrobial and Immunoregulating Properties Derived from Bovine Colostrum and Milk. 2015.
186. **Kazbulat Šogenov.** Petrophysical Models of the CO₂ Plume at Prospective Storage Sites in the Baltic Basin. 2015.
187. **Taavi Raadik.** Application of Modulation Spectroscopy Methods in Photovoltaic Materials Research. 2015.
188. **Reio Põder.** Study of Oxygen Vacancy Dynamics in Sc-doped Ceria with NMR Techniques. 2015.
189. **Sven Siir.** Internal Geochemical Stratification of Bentonites (Altered Volcanic Ash Beds) and its Interpretation. 2015.
190. **Kaur Jaanson.** Novel Transgenic Models Based on Bacterial Artificial Chromosomes for Studying BDNF Gene Regulation. 2015.
191. **Niina Karro.** Analysis of ADP Compartmentation in Cardiomyocytes and Its Role in Protection Against Mitochondrial Permeability Transition Pore Opening. 2015.
192. **Piret Laht.** B-plexins Regulate the Maturation of Neurons Through Microtubule Dynamics. 2015.
193. **Sergei Žari.** Organocatalytic Asymmetric Addition to Unsaturated 1,4-Dicarbonyl Compounds. 2015.
194. **Natalja Buhhalko.** Processes Influencing the Spatio-temporal Dynamics of Nutrients and Phytoplankton in Summer in the Gulf of Finland, Baltic Sea. 2015.
195. **Natalia Maticiuc.** Mechanism of Changes in the Properties of Chemically Deposited CdS Thin Films Induced by Thermal Annealing. 2015.
196. **Mario Öeren.** Computational Study of Cyclohexylhemicucurbiturils. 2015.
197. **Mari Kalda.** Mechanoenergetics of a Single Cardiomyocyte. 2015.
198. **Ieva Grudzinska.** Diatom Stratigraphy and Relative Sea Level Changes

- of the Eastern Baltic Sea over the Holocene. 2015.
199. **Anna Kazantseva.** Alternative Splicing in Health and Disease. 2015.
 200. **Jana Kazarjan.** Investigation of Endogenous Antioxidants and Their Synthetic Analogues by Capillary Electrophoresis. 2016.
 201. **Maria Safonova.** SnS Thin Films Deposition by Chemical Solution Method and Characterization. 2016.
 202. **Jekaterina Mazina.** Detection of Psycho- and Bioactive Drugs in Different Sample Matrices by Fluorescence Spectroscopy and Capillary Electrophoresis. 2016.
 203. **Karin Rosenstein.** Genes Regulated by Estrogen and Progesterone in Human Endometrium. 2016.
 204. **Aleksei Tretjakov.** A Macromolecular Imprinting Approach to Design Synthetic Receptors for Label-Free Biosensing Applications. 2016.
 205. **Mati Danilson.** Temperature Dependent Electrical Properties of Kesterite Monograin Layer Solar Cells. 2016.
 206. **Kaspar Kevvai.** Applications of ^{15}N -labeled Yeast Hydrolysates in Metabolic Studies of *Lactococcus lactis* and *Saccharomyces Cerevisiae*. 2016.
 207. **Kadri Aller.** Development and Applications of Chemically Defined Media for Lactic Acid Bacteria. 2016.
 208. **Gert Preegel.** Cyclopentane-1,2-dione and Cyclopent-2-en-1-one in Asymmetric Organocatalytic Reactions. 2016.
 209. **Jekaterina Služenikina.** Applications of Marine Scatterometer Winds and Quality Aspects of their Assimilation into Numerical Weather Prediction Model HIRLAM. 2016.
 210. **Erkki Kask.** Study of Kesterite Solar Cell Absorbers by Capacitance Spectroscopy Methods. 2016.
 211. **Jürgen Arund.** Major Chromophores and Fluorophores in the Spent Dialysate as Cornerstones for Optical Monitoring of Kidney Replacement Therapy. 2016.
 212. **Andrei Šamarin.** Hybrid PET/MR Imaging of Bone Metabolism and Morphology. 2016.
 213. **Kairi Kasemets.** Inverse Problems for Parabolic Integro-Differential Equations with Instant and Integral Conditions. 2016.
 214. **Edith Soosaar.** An Evolution of Freshwater Bulge in Laboratory Scale Experiments and Natural Conditions. 2016.
 215. **Peeter Laas.** Spatiotemporal Niche-Partitioning of Bacterioplankton Community across Environmental Gradients in the Baltic Sea. 2016.
 216. **Margus Voolma.** Geochemistry of Organic-Rich Metalliferous Oil Shale/Black Shale of Jordan and Estonia. 2016.

217. **Karin Ojamäe.** The Ecology and Photobiology of Mixotrophic Alveolates in the Baltic Sea. 2016.
218. **Anne Pink.** The Role of CD44 in the Control of Endothelial Cell Proliferation and Angiogenesis. 2016.
219. **Kristiina Kreek.** Metal-Doped Aerogels Based on Resorcinol Derivatives. 2016.
220. **Kaia Kukk.** Expression of Human Prostaglandin H Synthases in the Yeast *Pichia pastoris*. 2016.
221. **Martin Laasmaa.** Revealing Aspects of Cardiac Function from Fluorescence and Electrophysiological Recordings. 2016.
222. **Eeva-Gerda Kobrin.** Development of Point of Care Applications for Capillary Electrophoresis. 2016.
223. **Villu Kikas.** Physical Processes Controlling the Surface Layer Dynamics in the Stratified Gulf of Finland: An Application of Ferrybox Technology. 2016.
224. **Maris Skudra.** Features of Thermohaline Structure and Circulation in the Gulf of Riga. 2017.
225. **Sirje Sildever.** Influence of Physical-Chemical Factors on Community and Populations of the Baltic Sea Spring Bloom Microalgae. 2017.
226. **Nicolae Spalatu.** Development of CdTe Absorber Layer for Thin-Film Solar Cells. 2017.
227. **Kristi Luberg.** Human Tropomyosin-Related Kinase A and B: from Transcript Diversity to Novel Inhibitors. 2017.
228. **Andrus Kaldma.** Metabolic Remodeling of Human Colorectal Cancer: Alterations in Energy Fluxes. 2017.
229. **Irina Osadchuk.** Structures and Catalytic Properties of Titanium and Iridium Based Complexes. 2017.
230. **Roman Boroznjak.** A Computational Approach for Rational Monomer Selection in Molecularly Imprinted Polymer Synthesis. 2017.
231. **Sten Erm.** Use of Mother-Daughter Multi-Bioreactor Systems for Studies of Steady State Microbial Growth Space. 2017.
232. **Merike Kriisa.** Study of ZnO:In, Zn(O,S) and Sb₂S₃ Thin Films Deposited by Aerosol Methods. 2017.
233. **Marianna Surženko.** Selection of Functional Starter Bacteria for Type I Sourdough Process. 2017.
234. **Nkwusi God'swill Chimezie.** Formation and Growth of Cu₂ZnSnS₄ Monograin Powder in Molten CdI₂. 2017.